Ethiopian Meteorology Institute (EMI)

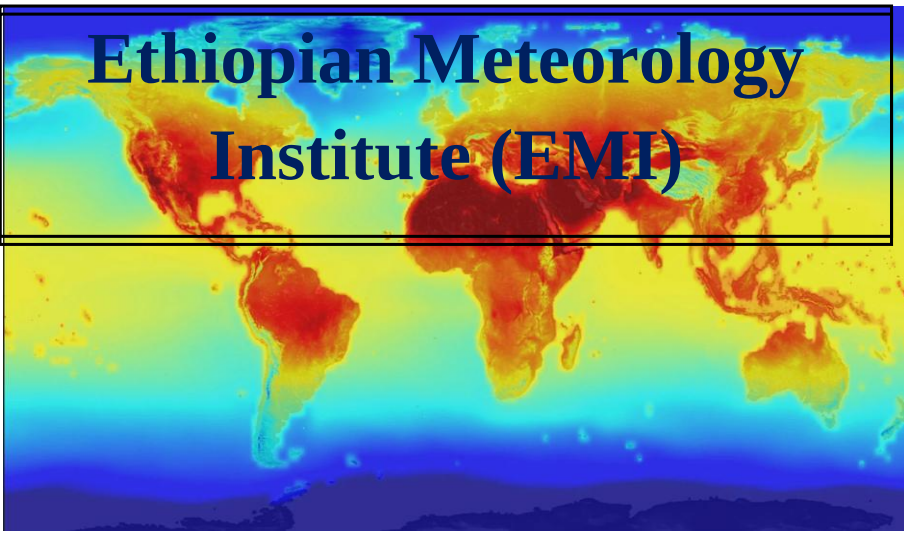

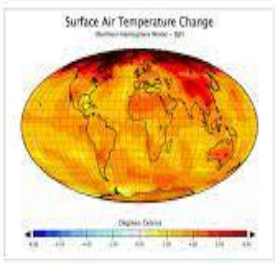

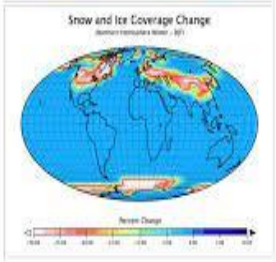

Ethiopian Climate Projection

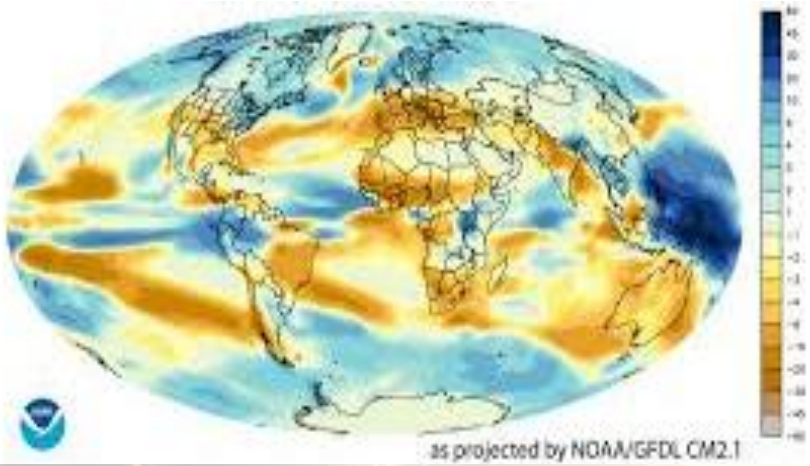

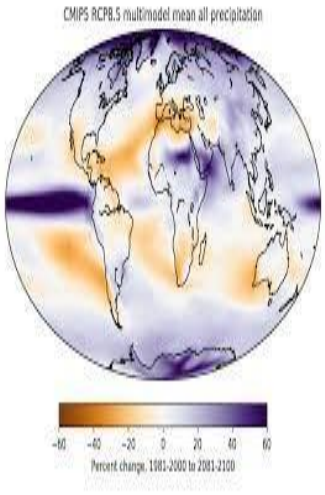

Ethiopian Meteorology Institute (EMI)

FUTURE PROJECTION OF RAINFALL AND TEMPERATURE IN MID AND LONG-TERM PERIODS OVER ETHIOPIA: Using multi-models CMIP6 ensemble data

Lead Authors: Mohammed Abera (MSc.), Ajebush Gochaw (MSc.) and Tofikk Redi (MSc.) and Chali Debele (MSc.)

Contribute Authors: Tesfaye Desu (Dr.), Rahel Yirdaw (MSc.) and Elias Fiseha (MSc)

Reviewers: Asaminew Teshome (Dr.), Fetene Teshome,

Editing & Design: Mohammed Abera and Tofikk Redi

December 2025

Content

Lists of Figures

Lists of Tables

Executive summary

This study evaluates future rainfall and temperature projections over Ethiopia under medium and worst shared socioeconomic pathways (SSPs) using CMIP6 climate models, integrating high-resolution ENACTS observational data for model validation. The study assesses climate model performance using statistical metrics such as RMSE, MAE, IOA, and CC against ENACTS observational data for Ethiopia from 1985-2014. CMIP6 models, particularly the top 10 best-performing models, are used for future rainfall and temperature projections under SSP2_4.5 and SSP5_8.5 scenarios. Model bias correction, including distribution mapping and variance scaling, enhances the accuracy of rainfall and temperature simulations. Ensemble modeling through simple arithmetic mean (SAM) effectively combines multiple GCM outputs, reducing uncertainty in projections. Temperature indicates clear and pervasive warming across all regions and seasons, with Tmax and Tmin rising more strongly under SSP5-8.5. Lowland and arid zones exhibit the largest Tmin increases, contributing to greater diurnal temperature ranges in some areas. Although rainfall shows spatially heterogeneous changes such as Kiremt (JJAS) rainfall generally increases, especially under higher emissions, while Belg (FMAM) and Bega (ONDJ) show more variable responses across zones. Expect amplified inter-annual variability and regional contrasts by 2041–2100. Bias correction (distribution mapping and variance scaling) with ENACTS validation improves model fidelity, but residual uncertainty remains at the zone level due to model spread and regional climate heterogeneity. The implications of this rainfall and temperature variability on agriculture were warming and shifting rainfall patterns could alter growing seasons, water demand, and crop suitability. Drought-resilient varieties and Climate smart agriculture (CSA) practices become critical in high-variability zones; on water and infrastructure also due to increased rainfall variability and higher temperatures necessitate enhanced storage, flood/drought risk management, and zone-tailored water allocation and on health and urban resilience results Rising Tmin and Tmax imply heightened heat exposure, especially in lowlands; urban heat mitigation and heat-health planning are warranted. Finally as recommendations based on the results are: Use zone-level adaptation plans with scenario comparison (SSP2-4.5 vs. SSP5-8.5) and time horizons, updating with new ENACTS/CMIP6 data; Invest in climate-smart agriculture, irrigation where feasible, and water storage with attention to shifting seasonal timing (notably Kiremt vs. Belg/Bega); Strengthen early warning systems for heat and extreme rainfall; integrate heat-health strategies for vulnerable populations and Augment analyses with climate extremes indices (heavy rainfall days, drought frequency) to complement mean changes.

1. Introduction

1.1. Background

Climate change is a disaster that will cause the frequency and severity of climatic extremes to increase. Sea level rise, warming oceans, increased rainfall unpredictability, global temperature increases, and extreme drought and flood events could all be directly impacted by this problem (Kandji et al., 2006). One of the main causes of the climate change issue is human activity (Oreskes, 2004). According to Kisakye et al., 2018, the issue of water scarcity is exacerbated by climate change, which has a detrimental impact on rainfall reliability and savings, with more disastrous outcomes during the dry season. Transportation safety is also impacted by the unpredictability of rainfall intensity and duration, which raises the incidence of accidents and congestion during peak hours (Koetse & Rietveld, 2009). Africa is among the continents most affected by climate change and is particularly susceptible to its effects, such as drought and floods brought on by rising air temperatures and shifting precipitation patterns, which threaten agriculture, water security, and socioeconomic development (Obsi Gemeda & Dafisa Sima, 2015).

The changing climate has manifested itself in higher climate extremes events (Madakumbura et al., 2021; Myhre et al., 2019). Extreme weather events typically have more catastrophic impacts than average climate change. Situations that could cost nations a great deal include droughts brought on by extended periods of exceptionally low precipitation or expected increases in flash flood events after more frequent and extreme precipitation events (Rettie et al., 2023).

Climate change and global warming have emerged as some of the world's most significant environmental issues. It has been demonstrated to searchers and scientists in recent decades that the weather patterns in many parts of the planet have changed (Solomon et al., 2007). Climate change has altered not only the overall magnitude of rainfall but also its seasonal distribution and inter-annual variability worldwide (Easterling et al., 2000). The frequency of extremes in temperature, precipitation, and/or wind speed on fine temporal and/or spatial scales has a significant impact on a number of sectors and risks, including agriculture, coastal flooding, drought, power distribution, public health, transportation, and urban planning (Huang et al., 2020; Macintyre & Heaviside, 2019).

The average global temperature is predicted to rise by 2 degrees Celsius above pre-industrial levels by 2050, according to scientists. The global maximum temperature has increased simultaneously since the beginning of the industrial revolution (Forster et al., 2023). This warming will result in more intense rainfall as well as more frequent and severe heat waves, droughts, floods, and other extreme weather events (Abbasnia, 2016; Dokken, n.d.).

Africa, like many parts of the world, is highly vulnerable to the growing impacts of extreme high temperature events. The continent has witnessed a noticeable increase in the frequency and intensity of climate extremes, particularly in recent decades (Dosio et al., 2022; Iyakaremye et al., 2021). In East Africa, where the economy is predominantly reliant on rain-fed agriculture and water-sensitive sectors, countries like Ethiopia are experiencing more frequent and severe droughts and floods, significantly affecting food security, water availability, and energy production (Hamed et al., 2022; Tegegne et al., 2021).

Ethiopia's economy is heavily dependent on rainy season agriculture, which is extremely susceptible to the impact of climate change, particularly variations in precipitation trends (Sinore & Wang, 2024). Future climate projections further indicate a likely intensification of EHT events in East Africa under continued global warming (Das et al., 2023).

Future climate projections further indicate a likely intensification of extreme high temperature events in East Africa under continued global warming (Ayugi et al., 2022; Babaousmail et al., 2022)(Ayugi et al., 2022; Babaousmail et al., 2022). However, despite these alarming trends, there remains a critical research gap in understanding the historical and projected characteristics of EHT events in this region, particularly in relation to large-scale atmospheric circulation mechanisms such as the Intertropical Convergence Zone (ITCZ) (Akinsanola et al., 2021; El Kenawy et al., 2020).

The year 2017 demonstrates up-to-date evidence for climate change as it was the warmest year on record for the global ocean (Cheng & Zhu, 2018). It is well accepted that climate change will have a far more detrimental effect on developing countries compared to developed countries, mainly because the capacity to respond to such changes is lower in developing countries (G. Feyissa et al., 2018). Studies show that the effects of climate change are severely affecting people in East African nations including Burundi, Kenya, Sudan, and Tanzania (Hassaan et al., 2017; Mwangi & Mutua, 2015).

The ensemble's models are generally consistent, showing that "heavy" occurrences result in higher total precipitation as well as larger one-day and five-day rainfall maxima (McSweeney et al., 2008). In Kenya, Ethiopia, and Somalia, climate-related extremes have been the dominant trigger of natural disasters (Wilby & Dawson, 2013). Overall, warm days and nights are projected to become more frequent in the entire Great Horn of Africa, while the occurrence of cold nights is likely to decrease (Omondi et al., 2014).

Climate projections are vital for planning adaptation in Ethiopia, guiding intervention in agriculture, water, disaster risk management, and infrastructure (Gebrechorkos et al., 2019). CMIP6 models form a reliable basis for policy development (Debela et al., 2015), while climate zone studies strengthen regional risk

estimation. Globally, Climate projections like CMIP6 models help to predict future temperature, rainfall, and extreme weather under different emission scenarios (Eyring et al., 2016). They guide climate policy and adaptation at global, regional, and national levels.

Agriculture, energy, and water are the main sectors that derive developing country's economy. The precipitation and temperature are the two major hydrologic variables used to measure the extent and magnitude of climate change in these sectors (Jaweso et al., 2019). Consequently, the alteration of magnitude, timing, and intensity of rainfall causes a significant negative impact on developing countries' economies. Therefore, analyzing the spatiotemporal trend of precipitation and temperature is crucial for efficient natural resources management.

Additionally; understanding and projecting changes in future precipitation and temperature patterns is important for informed assessment of climate change impacts and design of adaptation strategies. Knowledge on the magnitude of global (and large-scale regional) precipitation and temperature and how it varies on different time scales is important for many reasons, including understanding global and regional water and energy balances, answering questions related to water resources for humans and agriculture and in order to better understand how environmental changes can affect this critical parameter.

In conclusion, climate projections play a critical role in understanding and addressing climate change at global, regional, and national levels. Globally, they inform mitigation and adaptation efforts to limit temperature rise and manage climate risks. Regionally, they highlight Africa’s vulnerability to climate change, particularly in relation to food security, water resources, and extreme weather events. Nationally, Ethiopia's reliance on climate projections is crucial for policy planning, agriculture, and disaster management. As climate change impacts intensify, leveraging CMIP6 model data to analyze climate change, it may enhance Ethiopia’s capacity to develop targeted and effective adaptation and mitigation strategies.

This study examines historical, mid-term (2041–2070), and long-term (2071-2100) projections of rainfall, maximum and minimum temperature over Ethiopia under medium (SSP2-4.5) and worst-case (SSP5-8.5) scenarios. SSP2-4.5 represents a moderate mitigation pathway, while SSP5-8.5 reflects high emissions with limited climate policy, leading to substantial warming. By analyzing CMIP6 multi-model ensembles, we assess spatial and temporal patterns of rainfall and temperature change, regional disparities, and uncertainties in projections. The findings aim to inform adaptation and mitigation strategies, highlighting hotspots of extreme warming, seasonal shifting and periods of accelerated rainfall and temperature changes. Given Ethiopia’s rapid population growth and developmental challenges, understanding these climate trajectories is essential for policy formulation and resilience planning in a warming world.

1.2. Purpose of the study

The purpose of this study is to analyze and project future rainfall and temperature patterns in Ethiopia under different climate change scenarios, specifically focusing on regional and seasonal variations. By utilizing climate model projections, the study aims to assess potential changes in rainfall amounts, anomalies, and variability over the coming century and to identify and suggest best CMIP6 model for Ethiopia. The findings intend to inform policymakers, stakeholders, and vulnerable communities, guiding effective adaptation strategies and resource management to mitigate the impacts of climate variability and change on agriculture, water resources, and overall livelihood sustainability in Ethiopia.

2. Study areas and datasets

2.1. Study areas

Ethiopia is located in the eastern middle latitude of Africa between 3° North-15° North and 33° East-48° East and members of IGAD countries. Most of the country's annual production depends on the intensity and length of summer's primary rainy season. It has five traditional climatic zones (cold highlands, highlands, middle lands, lowlands, and hot lowlands). The country's agricultural practices (crop production, livestock, and mixed agriculture) are rain feed. According to Yigezu Wendimu, 2021, Ethiopia is characterized by high-input and resource-intensive farming systems that harmoniously cause losses of essential microorganisms, massive deforestation, freshwater shortages, soil nutrient reduction, and high levels of greenhouse gas emissions, and hindered agricultural production. Based on figure 1, most of the eastern parts of Ethiopia (Afar regional state, Somali Regional state), Southwestern Ethiopia (Welega), and some portions of Northwestern Tigray are lowlands, and western, central north, and southwest of Ethiopia are high lands. Most of the lowlands (Somali, wollega, and Afar) are vulnerable to climate change hazards, and there is seasonal migration between regions in search of water and food for cattle.

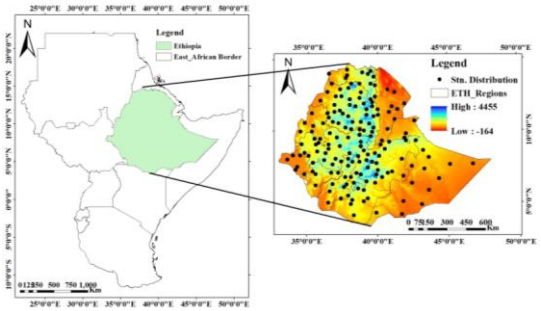

Figure 1: Study area with its digital elevation model and used station distribution

2.2. Climatological rainfall seasonality

There are two rainy seasons, namely, the minor rainy season, Belg (February–May), and the main rainy season, Kiremt (June-September), over the northern parts. The southern and southeastern parts of the country receive rainfall from February to May and September to November, known as East African long and short rains, respectively. The central part of the country is also known for its rainfall from February to May and June to September. According to Figure 2 from the results of ENACTs observed precipitation, July to September is the primary rain season for the whole country.

On the other hand; homogeneity zone one; that represents north-eastern parts of the country especially most parts afar and tip of northern Somali regions. In this homogeneity zone there are two rainy seasons, such as Belg (FMAM) and Kiremt (JJAS); homogeneity zone two: that represents eastern Tigray, most parts of eastern Amhara and borders of western Afar regions. In this homogeneity zone also two rainy seasons, that is similar from zone one; homogeneity zone three: that represents western tigray, most parts of Amhara and parts of western Oromia; in this zone mostly dominated mono-modal rainfall types and one long rainy season covers from May to September. Homogeneity zone four: represents tip parts of northern Afar, northern Somali and parts of eastern Oromia including Dire Dawa and Harari regions. This zone also have two rainy seasons; that is short rainy season known as Belg (FMAM) and long rainy season known as Kiremt (JJAS). Homogeneity zone Five: represents central parts of the country; such as tip parts of southern Amhara and Afar, central Oromia, northern parts of central and northern Ethiopia, tip parts of Sidama and Addis Ababa regions. Over this zone have two rainy season and mostly similar rainfall patterns from homogeneity zone four. Homogeneity zone Six: represents Benshangul gumuz, some parts of western Amhara, western Oromia, Gambella, northern parts of south western Ethiopia and central and western Ethiopia regions. Over this zone mostly dominated long rainy season from March to September and rainfall patterns are also similar from homogeneity zone three. Homogeneity zone Seven: represents parts of eastern Oromia and northern Somali regions. This homogeneity zone also two rainy seasons and the pattern also similar from homogeneity zone four. Homogeneity zone Eight: represents central and north eastern Somali region: Over this zone from February to May short rainy season known as Belg (FMAM) and from October to January long rainy season known as Bega (ONDJ). Homogeneity zones nine: represents Sidama, parts of central and southern Ethiopia and parts of western oromia regions. This zone also characterized by two rainy seasons such as Belg (FMAM) short rainy season and Kiremt (JJAS) long rainy season. Homogeneity zone ten: represents southern parts of south west Ethiopia and southern parts of

central and southern Ethiopia regions. This zone also one long rainy season and rainfall patterns are also similar with homogeneity zone six. Homogeneity zone eleven: represents south eastern parts of Somali region. Rainfall seasons and patterns are similar from homogeneity zone eight. Homogeneity zone twelve: represents southern parts of Oromia regions. This zone is also similar seasonality's and rainfall patterns from homogeneity zone eight and eleven (Figure 2).

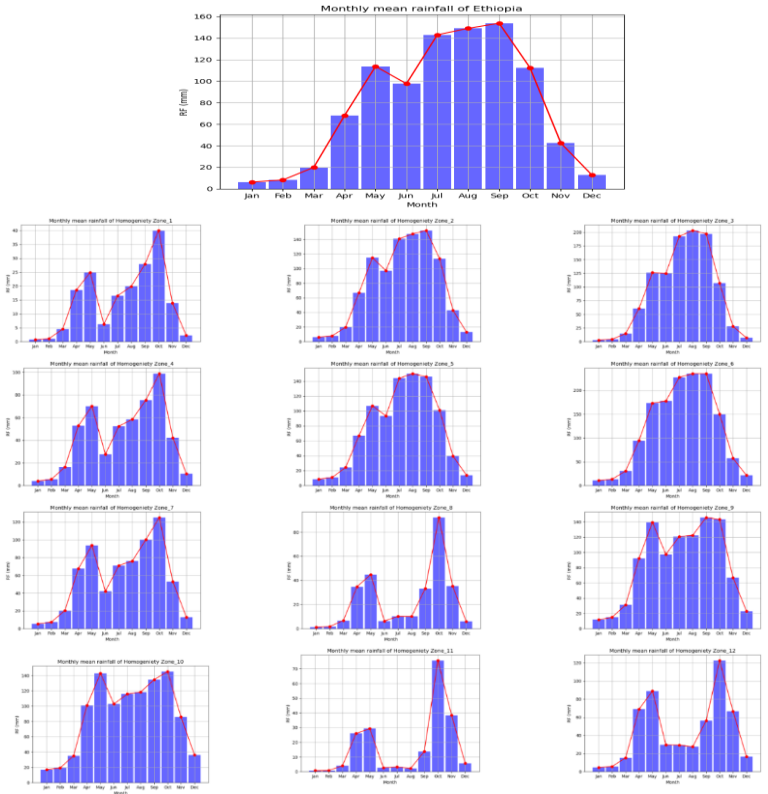

Figure 2: Monthly rainfall climatology from 1985-2014 over Ethiopia and twelve homogeneity zones

2.3. Data set and method

3.1.1. ENACTS data set

ENACTS was developed through collaboration between the Ethiopian Meteorology Institute (EMI), the International Research Institute for Climate and Society (IRI), and the University of Reading to generate high-resolution gridded climate time series for Ethiopia (Dinku et al., 2014). The ENACTS dataset integrates two main sources of information. Such as, the first is accurate rainfall and temperature data from more than 600 EMI monitored weather stations. The second is satellite-based rainfall and temperature estimates from EUMETSAT's and TAMSAT system, which were calibrated using the extensive station network to produce accurate spatially complete climate fields. Station observations were used to correct biases in the satellite products, while the satellite data filled spatial and temporal gaps in the station records, resulting in consistent daily or 10-day (dekadal) datasets with over 40 years of rainfall and temperature information at a nominal 0.0375° x 0.0375° resolution. Unlike most global satellite products that rely on about 17 GTS (Global Telecommunication System) synoptic stations, ENACTS incorporates over 600 stations, making it one of the most reliable long-term climate datasets available for Ethiopia (Dinku et al., 2014). ENACTS is widely regarded as a gold standard product due to its integration of accurate local observations with global satellite data and its sustainability for continuous updates (Dinku et al., 2018).

Thus, ENACTS data (0.0375° × 0.0375°, from 1981–2020) from 160 point stations across Ethiopia regions were used as the observational reference dataset to evaluate the performance of CMIP6 models in simulating rainfall and temperature for the period 1981–2014. Figure 1 shows the spatial distribution of the 160 rainfall, Tmax, and Tmin stations.

2.3.2. CMIP6 model data set

The study used monthly historical (1985–2014) and future (2015–2100) rainfall and temperature (Tmax and Tmin) datasets derived from CMIP6 climate model scenarios, including the historical, the medium-concentration scenario SSP2-4.5, and the high-concentration scenario SSP5-8.5 (O'Neill et al., 2016). Model outputs were obtained from the Copernicus Climate Data Store.

Accordingly, three analysis periods were considered: the historical baseline (1985–2014), the midterm future (2040-2070), and the far-term future (2071-2100). This study examined a total of 50 rainfall, 33 Tmax, and 24 Tmin historical CMIP6 models to identify the 10 best-performing models for each

parameter. Model performance was evaluated against the ENACTS observational dataset during the historical period (1985–2014). Based on this assessment, the top 10 models were selected for rainfall, Tmax, and Tmin. All selected models are available under both SSP2-4.5 and SSP5-8.5 scenarios. The detailed results of the best-performing models compared with ENACTS observations are presented in Tables 1, 2, and 3.

Table 1: Best 10 CMIP6 models used in rainfall study

No.	Models (under SSP2-4.5 and SSP5-8.5)	Country	Resolution (longitude x latitude)	Remarks
1	HadGEM3-GC31-LL	UK	1.9^0 x 1.3^0	
2	AWI-CM-1-1-MR	Germany	0.9^0 x 0.9^0	
3	UKESM1-0-LL	UK	1.88^0 x 1.25^0	
4	MPI-ESM1-2-LR	Germany	1.9^0 x 1.9^0	
5	KACE-1-0-G	Korea	1.25^0 x 1.87^0	
6	ACCESS-CM2	Australia	1.9^0 x 1.3^0	
7	CAMS-CSM1-0	China	1.13^0 x 1.13^0	
8	INM-CM5-0	Russia	2.0^0 x 1.5^0	
9	NESM3	China	1.9^0 x 1.9^0	
10	EC-Earth3-Veg-LR	Europe	1.1^0 x 1.1^0	

Table 2: Best 10 CMIP6 models used in Tmax study

No.	Models (under SSP2-4.5 and SSP5-8.5)	Country	Resolution(longitude x latitude)	Remark
1	ACCESS-CM2	Australia	1.9^0 x 1.3^0	
2	AWI-CM-1-1-MR	Germany	0.9^0 x 0.9^0	
3	Can ESM5-canOE	Canada	2.81^0 x 2.81^0	
4	EC-Earth3-Veg-LR	Europe	1.1^0 x 1.1^0	
5	EC-Earth3-CC	Europe	0.7^0 x 0.7^0	
6	FGOALS-g3	China	2.0^0 x 2.5^0	
7	HadGEM3-GC31-LL	UK	1.9^0 x 1.3^0	
8	INM-CM4-8	Russia	2.0^0 x 1.5^0	
9	INM-CM5-0	Russia	2.0^0 x 1.5^0	

10	MIROC-ES2L	Japan	2.8125 x 2.79	

Table 3: Best 10 CMIP6 models used in Tmin study

No	Model (under SSP2-4.5 and SSP5-8.5)	Country	Resolution(longitude x latitude)	Remark
1	FGOALS-g3	China	2.0^0 x 2.5^0	
2	NRM-ESM2-1	France	1.4° × 1.4°	
3	IPSL-CM6A-LR	France	2.5° × 1.3°	
4	CanESM5-CanOE	Canada	2.81^0 x 2.81^0	
5	MRI-ESM2-0	Japan	0.3°x0.5°	
6	EC-Earth3-CC	Europe	0.7^0 x 0.7^0	
7	GFDL-ESM4	USA	0.5°x1°	
8	CNRM-CM6-1	France	1.4° × 1.4°	
9	EC-Earth3-Veg-LR	Europe	1.1^0 x 1.1^0	
10	HadGEM3-GC31-LL	UK	1.9^0 x 1.3^0	

2.3.3. Model evaluation and selection method

The models evaluated by observing their ability to capture the annual rainfall and temperature cycle and mean seasonal climatology (ONDJ, FMAM and JJAS seasons). The study used two main performance analysis techniques, such as, the performance of CMIP6 rainfall, Tmax, and Tmin datasets under the SSP2-4.5 and SSP5-8.5 scenarios in reproducing the climate characteristics of the study area was evaluated through spatial comparisons against ENACTS rainfall, Tmax, and Tmin observations. Since the resolutions are different for most models and observations, all data were regridded to a common grid of ENACTS (0.0375° - 0.0375°) resolution using the bilinear interpolation method to confirm uniform resolution (Makula & Zhou, 2022).

And also, the statistical metrics used for this study included root-mean-squared error (RMSE), mean absolute error (MAE), index of agreement (IOA) mean bias (MB) and Pearson correlation coefficient (CC) for the period 1985–2014. These quantitative metrics have been employed in many studies in Africa (Akinsanola et al., 2021; Alaminie et al., 2021; Dyer et al., 2020; Ngoma et al., 2021) and are summarized in Table 4 along with their equations.

Table 4: Description of quantitative statistical measures

Statistics	Formula	Ranges	Best value
Root mean squared error	RMSE= $\sqrt{\frac{\sum_{i=1}^{n}(m-o)^2}{n}}$……..(eq.1)	0 to ∞	0
Mean absolute error	MAE= $\frac{\sum\|m-o\|}{n}$…….(eq.2)	0 to ∞	0
Index of agreement	IOA=1 − $[((o_i - m_i)^2/(o_i - \bar{o})^2)]$….(eq.3)	0 to 1	1
Correlation	CORR= $\frac{\sum(m_i-\bar{m})(o_i-\bar{o})}{\sqrt{\sum(m_i-\bar{m})(o_i-\bar{o})^2}}$…….....(eq.3)	-1 to 1	1
Mean bias	Bias= $\frac{\sum(m-o)}{n}$……..(eq.4)	$-\infty\ to\ \infty$	0

2.3.4. Model bias correction

Typical bias uncorrected Global Climate Models (GCMs), with spatial resolutions of about 50 km, often fail to represent local circulation patterns accurately (Christensen et al., 2008; Tong et al., 2021). So that, applying bias correction can improve the reliability of GCM outputs, although the effectiveness of each method depends on regional climate and topographic characteristics. GCM simulations commonly exhibit biases such as excessive low-intensity wet days, misrepresented hot or cold extremes, and inaccurate seasonal precipitation and temperature distributions (Jehanzaib et al., 2020).

Hence, because different bias correction techniques perform variably across regions, it is essential to evaluate multiple methods and select the best-performing approach (Tsegay et al., 2015).

In this study, three methods empirical quantile mapping, distribution mapping, and variance scaling were statistically assessed for correcting monthly rainfall and temperature biases. Based on error statistics, distribution mapping and variance scaling showed superior performance. Therefore, these two methods were applied for bias correction of monthly rainfall and temperature across the entire study area (Teng et al., 2015).

2.3.5. Multi Model Ensemble (MME)

In this study, future rainfall and temperature projections from multiple GCMs were used to analyze the spatiotemporal climate characteristics of the area. Relying on a single GCM introduces substantial uncertainty due to model structural limitations and algorithmic assumptions, which can propagate errors in climate projections (Tsegay et al., 2015). To reduce this uncertainty, ensemble climate data derived from

several models were used, as MMEs generally provide more robust and reliable outputs (Jehanzaib et al., 2020).

Projected monthly rainfall and temperature data were obtained from the Copernicus Climate Data Store (C3S). The ensemble was generated using one widely applied MME method using Simple Arithmetic Mean (SAM), which averages outputs from all selected models under the assumption that each model is equally likely to represent future climate conditions (Mishra et al., 2019).

$SAM = \frac{1}{N}\sum_{i=1}^{N} M_i$…….(eq.5)

Where M_i is the i^{th} model data and N is the number of models

2.3.6. Tools for processing the data

After completing the full data quality control process, several software packages and analytical tools were used for data processing and the spatiotemporal analysis of historical and future rainfall and temperature performance: such as,

1. Climate Data Operators (CDO): Used to re-grid the different model resolutions to a common 0.0375° x 0.0375° grid resolution and to convert rainfall units from kg/m²/s to mm/month and temperature unit from kelvin/ m²/s to °c/month.
2. Climate Data Tools (CDT): Used for temporal aggregation, including converting daily data to monthly, and monthly data to seasonal and annual timescales.
3. Climate Data Bias Correction (CDBC): Used for adjusting climate model outputs to remove systematic errors so they better match ENACTS data.
4. Python: Used for extracting model data at the ENACTS 165 station points, converting data from NetCDF to Excel formats, and performing temporal analyses of historical and future rainfall and temperature under medium and high-emission climate scenarios. This includes trend analysis of rainfall and temperature at monthly, seasonal and annual timescales.
5. ArcGIS: Used for spatial analysis and visualization of rainfall, Tmax and Tmin distribution across annual and seasonal periods.

3. Results and Discussions

3.1. Rainfall

3.1.1. Statistical model performance

This study examined the future trends and climate projection of rainfall changes over Ethiopia using a medium-emission scenarios (SSP2-4.5), and under the high-emission scenario (SSP5-8.5) for mid- term (2050), and long-term (2080) periods. Performances of the models were evaluated by employing the bias correction method in order to check the degree of agreement between the projected and observed data.

Therefore the study were used ENACTs data from 165 point stations 4 x4 km resolutions and 10 best CMIP6 model data out of 50 available CMIP6 models based on statistical metrics and Taylor diagram results such as HadGEM3-GC31-LL, AWI-CM-1-1-MR, UKESM1-0-LL, MPI-ESM1-2-LR, KACE-1-0-G, ACCESS-CM2, CAMS-CSM1-0, INM-CM5-0, NESM3 and EC-Earth3-Veg-LR. The details information about selected models is summarized in the following table and Taylor diagram figure (table 3 and Figure 3).

Table 5: statistical values for mean monthly rainfall and overall ranks of 15 best CMIP6 models based on statistical values from 50 CMIP6 models with respect to ENACTS for the period 1985–2014

No	Models Name	RMSE	MAE	IOA	CC	BIAS	Remarks
1	HadGEM3-GC31-LL	76.9	52.8	0.79	0.65	-0.7	Selected
2	AWI-CM-1-1-MR	78.0	52.9	0.77	0.64	-4.9	Selected
3	UKESM1-0-LL	78.7	52.0	0.76	0.63	-16.0	Selected
4	MPI-ESM1-2-LR	82.9	54.6	0.70	0.59	-22.6	Selected
5	KACE-1-0-G	82.9	61.5	0.75	0.60	-19.4	Selected
6	ACCESS-CM2	84.6	57.6	0.71	0.56	-9.8	Selected
7	CAMS-CSM1-0	85.4	57.9	0.65	0.53	-12.4	Selected
8	INM-CM5-0	87.9	67.5	0.74	0.61	40.7	Selected
9	NESM3	88.3	58.6	0.66	0.52	-23.5	Selected
10	EC-Earth3-Veg-LR	92.5	66.0	0.74	0.55	16.6	Selected

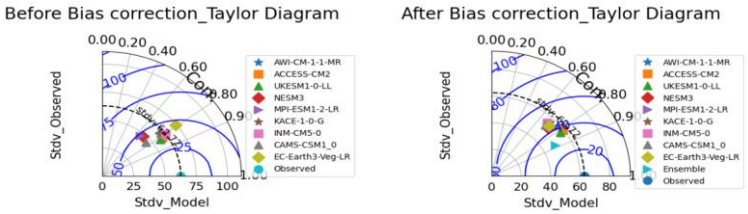

Figure 3: illustrates for the results of Taylor diagrams before and after model data bias corrections

3.1.2. Spatial analysis for comparisons on ENACTs and ensemble CMIP6 model data sources (1985-2014)

After improved data qualities of 10 selected CMIP6 model data; next process was ensemble model data by using Simple arithmetic mean (SAM) method. When comparing ENACTs data and ensemble model data based on seasonal and annual time scales: In Annual and Kiremt season both data source were almost similar value captured and ensemble model data highly fitted with ENACTs data source and most of western parts of the country dominated highest rainfall amount and decreasing rainfall amount from western to eastern direction. Whereas in Belg and Bega season: ensemble model data have little bit over estimated especially Bega season over north eastern, eastern and southern parts of the country captured over estimate compared with ENACTs data sources and in Belg season the model were little bit under estimate over southern parts of the country and over estimate at north western and western parts of the country. In generally, ensemble model data have a good similarity values from ENACTs data source over most of the country in annual and seasonal time scales (Figure 4).

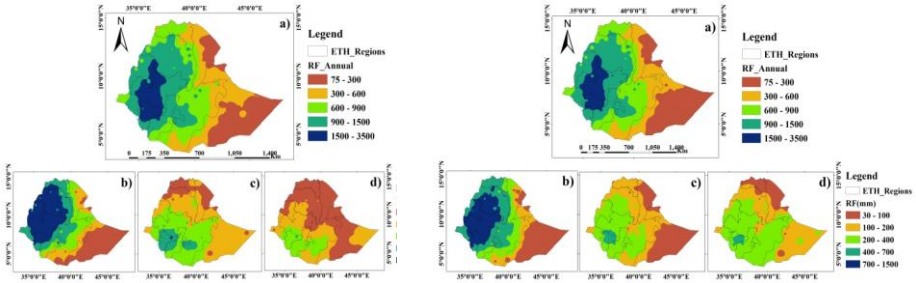

Figure 4: Comparisons between ENACTs and Ensemble model CMIP6 data

<u>Note:</u> The letter a) represents annual rainfall, b) Kiremt season, c) Belg season and d) Bega season rainfall spatial distribution; and left side map represented ENACTs data result and right side map represented ensemble model data results

3.1.3. Spatial analysis of mid-term (2041-2070) and long-term (2071-2100) periods rainfall future projection

Annual rainfall future projection

Historical rainfall spatial distribution shows; western areas have high rainfall amount than eastern parts of the country and this rainfall distribution will also expect on future projection in both climate scenarios and periods. Regarding to this ensemble model data shows future rainfall of spatial distribution annual rainfall will expects increasing over mid-term and long-term periods based on medium (SSP2_4.5) and worst (SSP5_8.5) climate scenarios. Figure 4 indicates slightly increasing annual rainfall over most of the country in mid and long term periods at medium (SSP2_4.5) scenario and highly increasing rainfall amount especially over western parts of the country at worst (SSP5_8.5) climate scenario compared with historical or reference time (1985-2014) periods.

From figure 5; the rainfall legend categories from 1500-3500mm highly expands over western parts of the country in worst climate scenario at mid and long-term periods. Whereas; eastern lowlands of the country will also expect changing or increasing from 80-300mm rainfall categories to 300-600mm rainfall categories. Generally future rainfall projection of CMIP6 ensemble model data shows slightly increasing in mid (2041-2070) and long (2071-2100) periods over both medium and worst climate scenarios.

In general the projected annual rainfall spatial analysis shows substantial variations and trends across emission scenarios. In medium-emission scenarios of SSP2-4.5 rainfall is expected no significant changes over the century that compared with climatology, which may lead to water shortages, affecting agriculture and other water-dependent sectors. In contrast, under the high-emission scenario (SSP5-8.5), seasonal rainfall is projected likely to increase by 2100. However, analyzed result of the highest emission scenario shows high variability, with frequent extreme events like heavy rainfall and occasional dry years impelling unpredictability could make water resource management and agricultural planning more challenging in the long term periods of end of 21st century (see Figure 5).

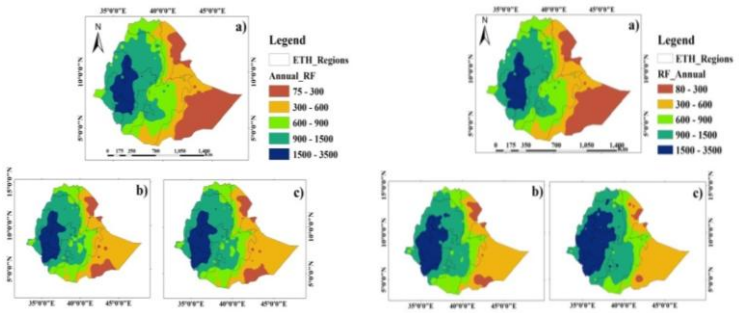

Figure 5: Spatial distributions of annual rainfall over Ethiopian
Note: The letter a) represents historical annual rainfall of ensemble models b) represents mid-term future projection and c) represents long-term future projection for both maps; and left side map represents medium (SSP2_4.5) and right side represents worst (SSP5_8.5) climate scenarios.

Belg (FMAM) season rainfall projection

Belg season historically known as mostly happen over southern parts of Ethiopia and ensemble model historical data over this season also confirms this statement. Most of south western Ethiopia and tip of southern parts of western oromia regions experienced high rainfall amount ranging from 400-600mm, pocket areas of south western Ethiopian region have 600-900mm rainfall and the rest of western parts like western Oromia, southern parts of western Amhara, Benshangul Gumuz, central and southern Ethiopia, Sidama and most of Southern Oromia regions have ranging from 200-400mm rainfall amounts. Whereas western, northern and eastern low lowland parts of the country like north western and eastern Amhara, Tigray, Afar and Somali regions experienced less amounts of rainfall compared with western parts of the country (20-200mm). According to historical rainfall performance; Belg season future projection of rainfall will expect increasing in most parts of the country in mid and long term periods under medium (SSP2_4.5) and worst (SSP5_8.5) climate scenarios. When comparing two climate scenarios; the model output shows both medium and worst climate scenarios will be expand rainfall distribution from western to eastern direction and also over northern parts of the country. Additionally, under worst (SSP5_8.5) rainfall projection will expect highly increased over most of the country particularly over western Ethiopia compared to under medium (SSP2_4.5) climate scenario (see Figure 6).

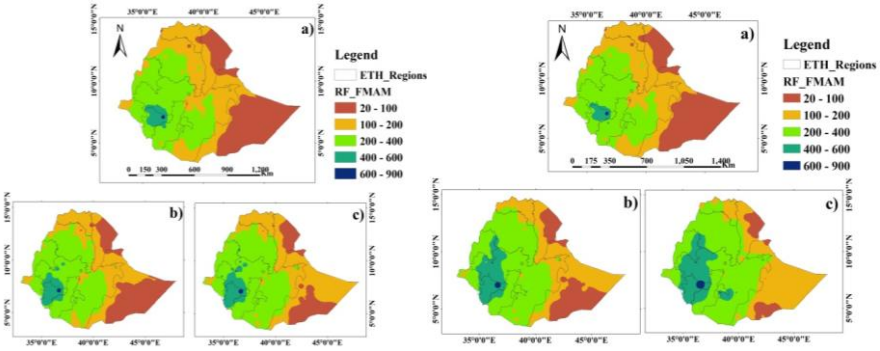

Figure 6: Spatial distributions of Belg rainfall over Ethiopian

Note: The letter a) represents historical Belg rainfall of ensemble models b) represents mid-term future projection and c) represents long-term future projection for both maps; and left side map represents medium (SSP2_4.5) and right side represents worst (SSP5_8.5) climate scenarios

Kiremt (JJAS) Season rainfall projection

Kiremt (JJAS) rainfall contributes from 50–80 % of the total annual rainfall over the Ethiopia with high agricultural productivity and major water reservoirs. About 85 to 95 % of the food crop of the country is produced during this season (Bekana, 2025). Therefor this season is the main rainy season for northern half of the country and most agricultural activities are depends on this season. Figure 7(a) shows historical kiremt (JJAS) season that explains western parts of the country received high amount of rainfall ranging from 700-1500mm and north western, northern and central mid-latitude areas are also received from 400-700mm whereas eastern parts of the country were experienced up to 400mm in kiremt season.

According to figure 7(b and c) that represents rainfall projection based on mid and long term periods under SSP2_4.5 and SSP5_8.5 climate scenarios in both maps. Although the figure indicates future rainfall projection will slightly increasing over most parts of Kiremt benefiting areas whereas eastern and south eastern areas will be similar situation from historical rainfall distribution. Comparing the two climate scenarios; long term period under SSP5_8.5 scenario shows rainfall increased in amount and distribution over western and north western parts of the country than both mid and long term periods under SSP2_4.5 and mid-term under SSP5_8.5 climate scenarios. On the other hands SSP2_4.5 in mid and long term periods will be expects similar (with slightly increments) rainfall amount and distribution from historical rainfall performance.

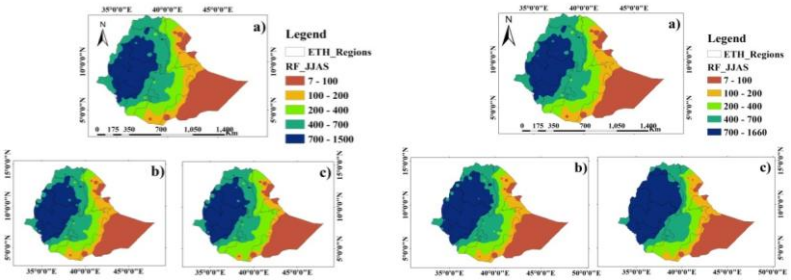

Figure 7: Spatial distributions of Kiremt rainfall over Ethiopian

Note: The letter a) represents historical Kiremt rainfall of ensemble models b) represents mid-term future projection and c) represents long-term future projection for both maps; and left side map represents medium (SSP2_4.5) and right side represents worst (SSP5_8.5) climate scenarios

Bega (ONDJ) Season rainfall projection

Bega season in Ethiopia covers from October to January and are the dry season with frost in morning especially in December over northern have of the country whereas over southern and south eastern parts of the country this season is known as second rainy season.

Figure 8(a) indicates ensemble models historical rainfall amount and distribution in Bega (ONDJ) seasons over Ethiopia. In this season most of northern half of the country received less amount of rainfall and southern half of the country experienced high amount of rainfall. Figure 8(b and c) also indicates future projection of rainfall amount and distribution in mid and long term periods under medium (SSP2_4.5) and worst (SSP5_8.5) climate scenarios.

The projection shows; in bega season most of the country will be increased rainfall specially over Bega rainfall benefiting areas and also increase over north western and western parts of non bega rainfall benefiting areas. In addition to this; under worst (SSP5_8.5) scenario and mid and long term periods will be expect expanded amounts and distributions of rainfall ranging from 450-850mm over southern and south western parts of the country particularly under SSP5_8.5 long term periods. This future projection also shows Bega (ONDJ) season spatial rainfall distribution will be highly increasing in both mid and long term periods under both climate scenarios compared to the other two seasons in Ethiopia.

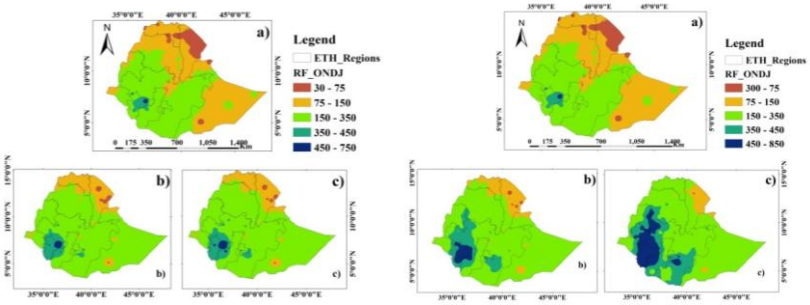

Figure 8: Spatial distributions of Bega rainfall over Ethiopian

Note: The letter a) represents historical Bega rainfall of ensemble models b) represents mid-term future projection and c) represents long-term future projection for both maps; and left side map represents medium (SSP2_4.5) and right side represents worst (SSP5_8.5) climate scenarios

3.1.4. Projection of rainfall trend analysis over Ethiopia at 21st century (1981-2100)

In this part of the study can observe how the rainfall decreasing or increasing trends and variability at historical (1981-2014) and future projection (2015-2100) over all the century in Ethiopia and over each twelve homogeneity zones.

Figure 9 also show historical and future projection of annual rainfall trends and variability over Ethiopia and its homogeneity zones under two climate scenarios. Over all in Ethiopia; historical rainfall from 1981-2014 was varying from 600 to 850mm and slightly increasing but this increasing trend was not significant and the model shows future projection will be expect slightly increasing compared with climatology up to 2060 under both climate scenarios. After the end of 2060 G.C. the two climate scenarios trend will be expect opposite direction; such as under SSP2_4.5 the projection show decreasing from the previous and more or less similar with historical rainfall trends whereas under SSP5_8.5 the projection indicates increasing from the previous up to the end of century. In general future rainfall projection will have high variability and varying from 700-1200mm from 2015 to 2100 under two scenarios.

The same is true over homogeneity zone one to homogeneity zone ten indicates increasing rainfall trends over time, with the projections showing more variability and higher rainfall amounts, especially under the SSP5_8.5 scenario, which experiences more frequent and intense fluctuations. Whereas homogeneity zone eleven and twelve will be experienced exceptionally different from the rest homogeneity zones: such as;

In homogeneity zone eleven indicates overall increasing trend in rainfall over time, with more pronounced fluctuations in the projections, especially under the SSP5_8.5 scenario, which shows higher and more variable rainfall amounts in the future and SSP2_4.5 shows almost similar trends with historical rainfall

performance. Whereas in homogeneity zone twelve displays the trend below historical baseline but overall increasing trend in rainfall over time, with higher and more variable rainfall patterns projected under the SSP5_8.5 scenario, especially after 2000. The projections suggest more frequent and intense rainfall fluctuations in the future, with significant variations around the 2050s to 2100s. In general future projection of rainfall will be increasing under SSP5_8.5 over all homogeneity zones with different varying intensity and under SSP2_4.5 almost similar trends with slightly increasing over the country and each homogeneity zones (see Figure 9).

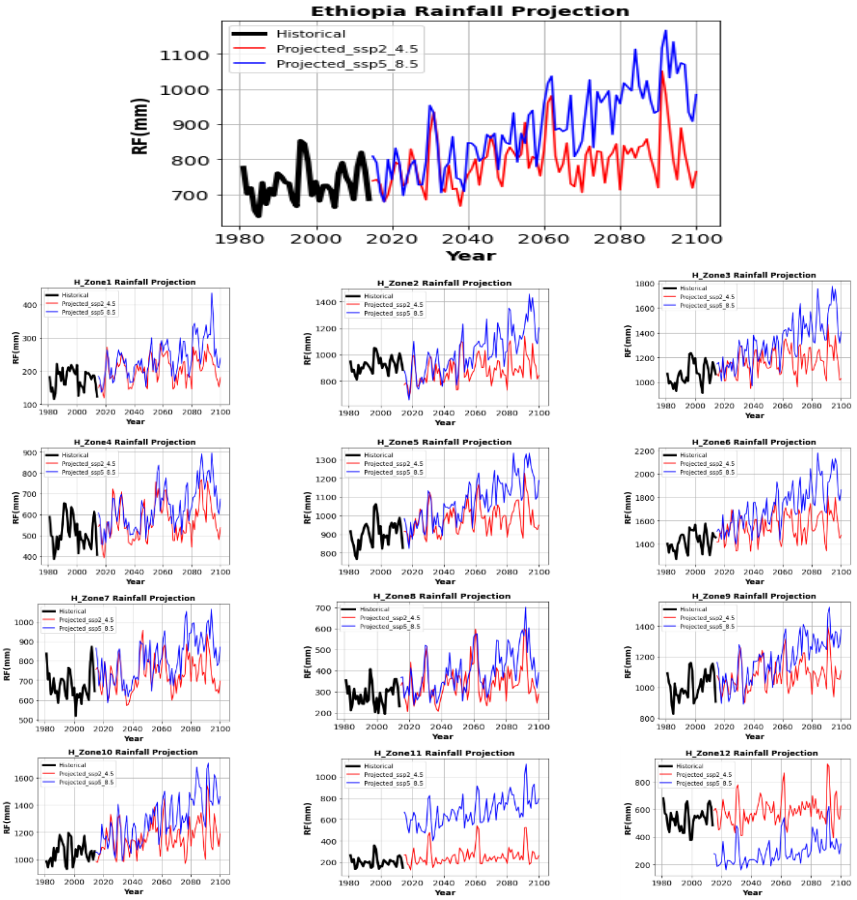

Figure 9: Ensemble model historical and future projection of rainfall over Ethiopia using twelve homogeneity zones from 1981-2100

3.1.5. Historical and future projection of Rainfall trend analysis in mid and long term periods

Figure 10 indicates historical baseline period and future projection in mid and long term rainfall temporal analysis under medium and worst climate scenarios over Ethiopia. Historical rainfall temporal analysis shows fluctuates significantly over the years with peaks around 1996 and 2012 and the trend displays slightly increasing from 1985 to 2014.

Projection of rainfall under medium (SSP2_4.5) scenario shows increasing variability of rainfall with peaks at 2062 and after this year the rainfall will expect decreasing trends whereas trend line shows normal rainfall performance in mid-term (2041-2070) period. In long term period of this climate scenario indicates less rainfall variability compared with mid-term period and rainfall peaks at 2091 with decreasing trends after this year up to the end of century. Trend line also shows almost normal rainfall performance from 2071-2100. The amount of rainfall ranging from 700-1000mm in mid-term and 700-1150mm in long term periods.

Projection of rainfall under worst (SSP5_8.5) scenario also shows increasing variability of rainfall with peaks at 2062 and after this year the rainfall will expect decreasing trends whereas trend line shows increased rainfall performance in mid-term (2041-2070) period. In long term period of this climate scenario indicates also significantly increasing rainfall variability compared with mid-term period and rainfall peaks at 2092 with decreasing trends after this year up to the end of century. Trend line also shows increasing rainfall performance from 2071-2100. Under this scenario the annual average amount of rainfall will be expect ranging from 700-1050mm in mid-term and 700-1200mm in long term periods.

In general temporal analysis of future rainfall projection displays significantly increasing rainfall performance will be expected under worst (SSP5_8.5) climate scenario in both mid and long term periods whereas under medium (SSP2_4.5) scenario indicates almost normal or similar trends will be expect compared to historical baseline period (see Figure 10). Rainfall projection over twelve homogeneity zones shows highly variable and has different intensity of variability in each homogeneity zones. Additionally trend lines shows also different over all zones like some homogeneity zones has increasing and other zones decreasing trends under both climate scenarios and both mid and long term periods. The details information about all homogeneity zones temporal analysis is summarized by figure in the Annex section from Figure 15 to Figure 26.

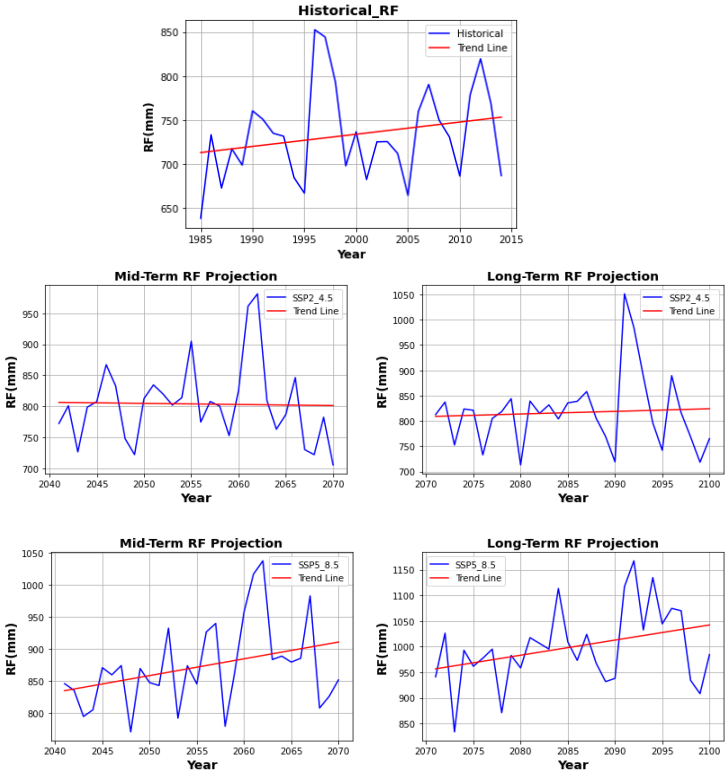

Figure 10: Historical and Future annual rainfall projection of mid and long-term periods under SSP245 and SSP585 climate scenarios over Ethiopia

3.1.6. Projection of rainfall anomalies under SSP2_4.5 and SSP5_8.5 in Mid-term (2041-2070) and long-term (2071-2100) periods

In this section discussing about future rainfall performance based on anomalies for each years compared to historical baseline periods (1985-2014) using two future periods such as mid-term (2041-2070) and long term (2071-2100) and also using two climate scenarios like medium (SSP2_4.5) and worst (SSP5_8.5) scenarios at each homogeneity zones and overall Ethiopia. Additionally discussing about future rainfall deficit or increasing trend over twelve homogeneity zones and over all Ethiopia. Therefore annual and seasonal rainfall anomalies of future rainfall detail discussion are the following:

Annual rainfall anomalies

Figure 11 indicates the difference between annual future rainfalls and historical baseline periods at mid and long term periods based on medium and worst climate scenarios. Under medium (SSP2_4.5) scenario; the rainfall will be have positive anomalies in most of years at medium and long term periods except negative anomalies on 2053,2053,2067 and 2068 in mid-term and 2076,2082,2098 and 2099 in long term periods. Besides 2061 and 2062 will be expect more wet years ranging from 200-300mm increasing in mid-term compare with historical baseline whereas 2091 and 2092 will be also expect more wet years ranging from 200-400mm increasing in long term periods compare with historical baseline periods. In general under this scenario future rainfall will be normal rainfall performance with slightly increments from historical baseline periods.

Whereas under worst (SSP5_8.5) positive anomalies will also dominated for the future projection of rainfall at mid and long term periods except 2053 and 2068 negative anomalies and significant increment rainfall will expect for the future under this climate scenario compare with historical baseline periods at both mid and long term periods. When comparing the two climate scenarios; worst (SSP5_8.5) will significantly increasing than medium (SSP2_4.5) scenarios especially at the time of long term period. Generally annual future rainfall from 2041-2100 over Ethiopia will be increasing compared with baseline (1985-2014) (see Figure 11).

Related to this annual rainfall future performance will also indicate similar trends all over homogeneity zones under both climate scenarios and periods. Detail information about those homogeneity zones annual rainfall anomalies also summarized at Annex section Figure 27 and 28 for Ethiopian level and Figure 35 and 36 for each homogeneity zones.

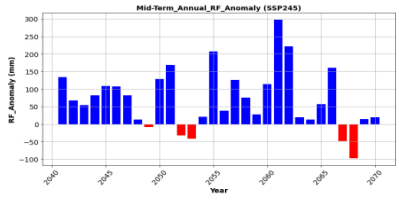

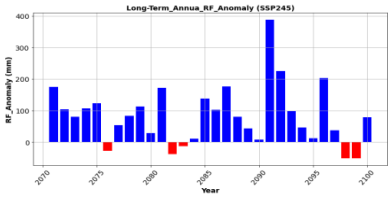

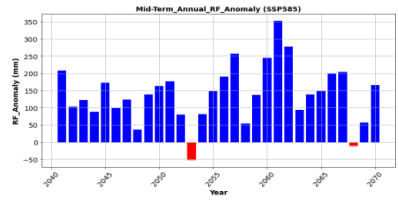

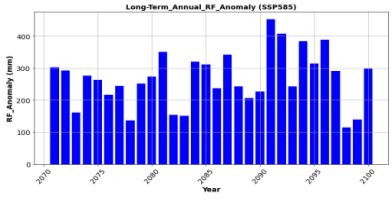

Figure 11: Annual rainfall anomalies under medium and worst climate scenarios with mid and long term periods

Table 4 shows average annual rainfall anomalies under medium and worst scenarios based on mid and long term periods over twelve homogeneity zones of Ethiopia. According to this table; most of homogeneity zones will have positive anomalies except homogeneity zone_2 (-29.8 and -18.1mm) under SSP2_4.5 at mid and long term periods respectively and homogeneity zone_12 (-242.0 and -181.0mm) under SSP5_8.5 at mid and long term periods respectively. Generally in Ethiopia future rainfall will increase by 71 and 83.6mm under SSP2_4.5 and 139.9 and 266.6mm under SSP5_8.5 scenarios at both mid and long term periods respectively (see Table 4).

Table 6: Annual rainfall average increasing and decreasing trends over Ethiopia and each homogeneity zones

Homogeneity Zone	SSP2_4.5		SSP5_8.5		Remark
	Mid-Term	Long-Term	Mid-Term	Long-Term	
Zone_1	30.9	33	49.1	98	
Zone_2	**-29.8**	**-18.1**	72.6	242.2	
Zone_3	101.5	119.2	225.6	420.8	
Zone_4	64.2	68.6	103.8	194	
Zone_5	81.3	93.7	153.9	277.4	
Zone_6	126.9	150.1	267.1	460.5	
Zone_7	79	83.5	124.4	234.5	
Zone_8	70.2	81.3	101.6	190.8	
Zone_9	84.5	100.5	160.4	306.5	
Zone_10	109.9	137	205.5	376.4	
Zone_11	62.2	66.9	457.1	578.8	
Zone_12	71.2	87.9	**-242.0**	**-181.0**	
Over all Ethiopia	71	83.6	139.9	266.6	

Belg (FMAM) season rainfall anomalies

This part also indicates about Belg (FMAM) season future rainfall anomalies that compare with historical baseline periods under both medium and worst scenarios depending on mid and long term periods. When SSP2_4.5 scenario; the rainfall anomalies will be negative at 2045, 2048, 2049, 2050, 2052, 2053, 2064, 2067 and 2068 by -2.3, -5, -38, -28.6, -19.9, -15.7, -33.3, -47.7 and -39.2mm respectively and the rest year will be positive anomalies ranging from 2.7-102.7mm in mid-term period. But these negative anomaly

Commented [C1]: Under

years will be decrease in long term period (2076, 2079, 2080, 2090, 2094 and 2098 will be decrease by -60.6, -8.8, -21.3, -12.6, -33.8 and -18.2mm respectively and the rest most years in this period will be have positive anomalies ranging from 7-108.7mm.

Whereas under SSP5_8.5 scenario; due to significantly increasing future rainfall under this scenario anomalies also positive values over most mid and long term periods. Comparing two periods; in mid-term except four years have negative anomalies like 2047, 2048, 2058 and 2068 with -22.2, -7, -34.8 and -50.0mm respectively most of the rest years will be positive anomalies ranging from 5-95mm. while in long term period will be expect positive anomalies over the whole years ranging from 8-140mm rainfall amount (see Figure 12).

On the other hand rainfall future performance in this season will also indicate that increasing the fluctuation of positive and negative anomalies all over twelve homogeneity zones under both climate scenarios and periods. Detail information about those homogeneity zones Belg rainfall anomalies also summarized at Annex section Figure 29 and 30 for Ethiopian level and Figure 37 and 38 for each homogeneity zones.

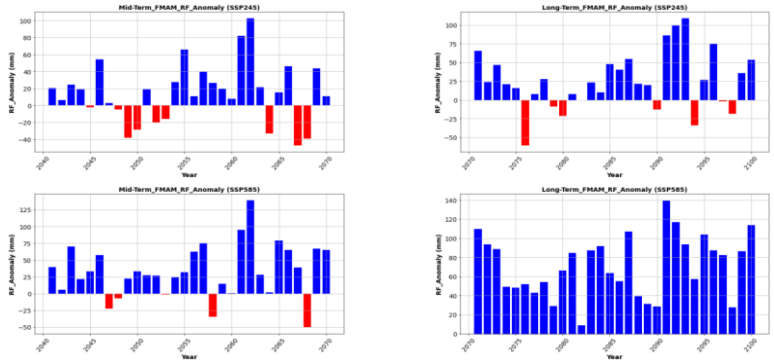

Figure 12: Belg rainfall anomalies under medium and worst climate scenarios with mid and long term periods

Table 5 also shows average Belg (FMAM) rainfall anomalies under medium and worst scenarios based on mid and long term periods over twelve homogeneity zones and Ethiopia. According to this table; most of homogeneity zones will have positive anomalies except homogeneity zone_2 (-36.3 and -8.7) under SSP2_4.5 and SSP5_8.5 scenarios at mid-term period respectively and homogeneity zone_12 (-109.8 and -84.5mm) under SSP5_8.5 at mid and long term periods respectively. Generally in Ethiopia future rainfall

will increase by 14.5 and 25.3mm under SSP2_4.5 and 33.6 and 71.3mm under SSP5_8.5 scenarios at both mid and long term periods respectively (see Table 5).

Table 7: Belg season rainfall average increasing and decreasing trends over Ethiopia and each homogeneity zones

Homogeneity Zone	SSP2_4.5		SSP5_8.5		Remark
	Mid-Term	Long-Term	Mid-Term	Long-Term	
Zone_1	6.9	27.2	11.9	26.8	
Zone_2	**-36.3**	9.9	**-8.7**	34.8	
Zone_3	23.8	-22.6	56.9	96.3	
Zone_4	13.9	30	24.5	58.3	
Zone_5	21.7	26.1	42.7	78.7	
Zone_6	28.6	31.9	68.0	111.1	
Zone_7	20.8	37.9	36.2	78	
Zone_8	13.2	35	19.7	49.1	
Zone_9	27.4	22.9	52.9	100.6	
Zone_10	33.8	42.7	57.5	105.4	
Zone_11	6.3	43.5	151.7	200.8	
Zone_12	14.2	16.3	**-109.8**	**-84.5**	
Over all Ethiopia	14.5	25.3	33.6	71.3	

Kiremt (JJAS) season rainfall anomalies

Kiremt season figure indicates rainfall anomaly data for two different climate scenarios (SSP245 and SSP585) over similar time periods, with both mid-term and long-term analyses. Under SSP2_4.5 projection indicates positive rainfall anomalies, peaking near 100 mm and negative rainfall anomalies, mostly around -20 to -40 mm. Fluctuations are irregular, with some periods showing significant positive anomalies and others with noticeable negative anomalies at mid-term period whereas in long term period dominated by negative anomalies reaching below -100 mm and Minor positive anomalies are present but less prominent with overall trend suggests increasing negative rainfall anomalies over time.

Under SSP5_8.5 projection show in mid-term period will be more frequent and larger positive anomalies, often exceeding 100 mm and negative anomalies are also present but less severe compared to positive anomalies with indicates greater variability and intensity in rainfall anomalies. Whereas in long term period the projection shows increasing positive anomalies initially, followed by fluctuations and a significant negative anomaly appears around the late 2090s or early 2100s, approaching -50 mm but dominate, especially in earlier years, indicating persistent positive anomalies.

In general the figure shows depict rainfall anomaly trends in different SSP scenarios over time like SSP2_4.5 shows a trend of increasing negative RF anomalies in the long term and SSP5_8.5 exhibits higher variability and more intense positive anomalies, with some late-century negative anomalies in mid-

term period. These trends can inform climate impact assessments related to radiative forcing and regional climate behavior (see Figure 13).

According to the results rainfall future performance in this season will be indicate that increasing the fluctuation of positive and negative anomalies all over twelve homogeneity zones under both climate scenarios and periods compared to Belg and Bega seasons. Detail information about those homogeneity zones Kiremt rainfall anomalies also summarized at Annex section Figure 31 and 32 for Ethiopian level and Figure 39 and 40 for each homogeneity zones.

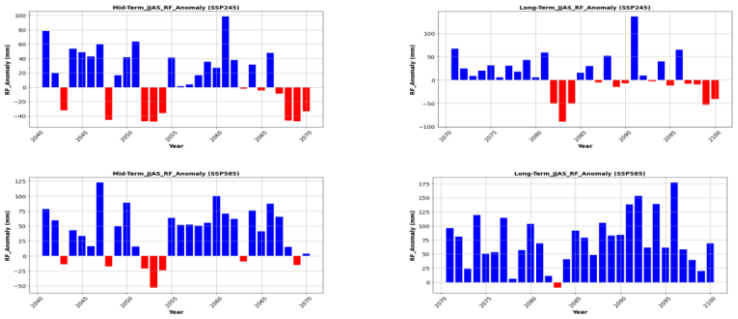

Figure 13: Kiremt rainfall anomalies under medium and worst climate scenarios with mid and long term periods

Under SSP5-8.5 consistently shows higher RF anomalies (both positive and negative) compared to SSP2-4.5, reflecting more extreme climate impacts under this scenario. The long-term values under SSP5-8.5 are significantly elevated, indicating worsening conditions over time.

Zone_6 has the highest positive anomalies in both scenarios (e.g., 50.2 under SSP2-4.5 and 174.6 under SSP5-8.5 in the long term) and Zone_12 stands out with negative anomalies under SSP5-8.5 (-118.3 mid-term, -116.7 long-term), it is suggesting unique localized effects. Zone_3 and Zone_6 show the most severe positive anomalies under SSP5-8.5 whereas Zone_7, Zone_8, Zone_9, and Zone_12 exhibit negative anomalies, with Zone_9 showing the steepest decline (-7.4 under SSP2-4.5, 57.8 under SSP5-8.5). Overall Ethiopia: The average rainfall anomaly for Ethiopia is 13.8 (mid-term) and 10.6 (long-term) under SSP2-4.5, but jumps to 38.3 (mid-term) and 74.1 (long-term) under SSP5-8.5 (Table 6).

Table 8: Kiremt season rainfall average increasing and decreasing trends over Ethiopia and each homogeneity zones

Homogeneity Zone	SSP2_4.5		SSP5_8.5		Remark
	Mid-Term	Long-Term	Mid-Term	Long-Term	
Zone_1	5.6	2.5	13.6	25.4	
Zone_2	23.4	15.5	74.1	140.4	

Zone_3	34.0	37.7	89.8	175.6	
Zone_4	10.0	0.6	26.1	43.1	
Zone_5	20.7	17	51.0	91.2	
Zone_6	43.5	50.2	96.3	174.6	
Zone_7	8.2	**-2.7**	22.8	44.5	
Zone_8	1.8	**-0.7**	8.5	18.5	
Zone_9	1.7	**-7.4**	22.4	57.8	
Zone_10	14.9	18	44.8	92.7	
Zone_11	0.3	**-1.8**	128.5	142.6	
Zone_12	1.7	**-1.2**	**-118.3**	**-116.7**	
Over all Ethiopia	13.8	10.6	38.3	74.1	

Bega (ONDJ) season rainfall anomalies

Bega season anomalies under SSP2_4.5 scenario positive anomalies dominate with peaking around 200 mm and negative anomalies are minimal, mostly below -20 mm with Variability: Fluctuations are moderate, with no extreme outliers in mid-term period. While in long term period positive anomalies remain prevalent but decline slightly, ranging 100–175 mm with negative anomalies are rare and mild. This Implication: Stable but slightly reduced rainfall anomalies compared to mid-term.

Whereas anomalies under SSP5_8.5 scenario; Higher variability than SSP245, with positive anomalies reaching 120 mm and negative anomalies are more frequent but still minor (e.g., -25 mm), More erratic swings, suggesting greater climate instability in mid-term period. Beside the trend shows sharp in positive anomalies (25–200mm) and there is no negative anomalies become. This is also significant increasing in rainfall anomalies; potentially indicating wet conditions in both mid and long term climate scenarios (see Figure 14).

Rainfall future performance in this season will also indicate that increasing the fluctuation of positive and decreasing in negative anomalies all over twelve homogeneity zones under both climate scenarios and periods. Detail information about those homogeneity zones Bega rainfall anomalies also summarized at Annex section Figure 33 and 34 for Ethiopian level and Figure 41 and 42 for each homogeneity zones.

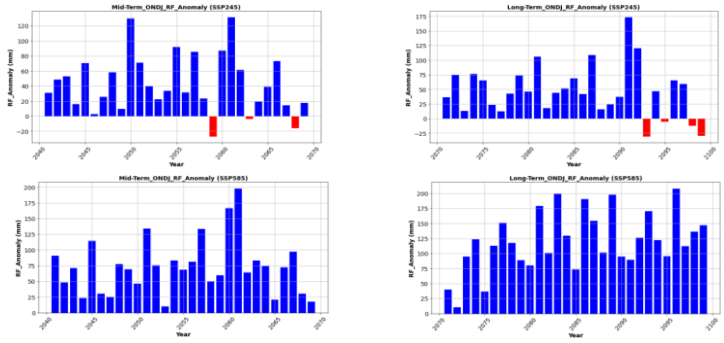

Figure 14: Bega rainfall anomalies under medium and worst climate scenarios with mid and long term periods

Table 7 shows average Bega season rainfall anomalies under medium and worst scenarios based on mid and long term periods over twelve homogeneity zones and Ethiopia. According to this table; most of homogeneity zones will have positive anomalies except homogeneity zone_2 (-16.4 and -11.6mm) under SSP2_4.5 at mid and long term periods respectively and homogeneity zone_12 (-13.9mm) under SSP5_8.5 at mid-term period. Generally in Ethiopia future rainfall will increase by 42.7 and 47.1mm under SSP2_4.5 and 72.9 and 121.4mm under SSP5_8.5 scenarios at both mid and long term periods respectively (see Table 7).

Table 9: Bega season rainfall average increasing and decreasing trends over Ethiopia and each homogeneity zones

Homogeneity Zone	SSP2_4.5		SSP5_8.5		Remark
	Mid-Term	Long-Term	Mid-Term	Long-Term	
Zone_1	18	20.3	22.9	46.2	
Zone_2	**-16.4**	**-11.6**	78.6	67.1	
Zone_3	45.1	52	70.1	150.8	
Zone_4	39.8	40.8	51.9	92.5	
Zone_5	38.4	43.2	58.3	106.7	
Zone_6	56.1	61.9	102.5	177.1	
Zone_7	50.3	50.7	64.5	112.8	
Zone_8	55.7	59.7	72.9	124.4	
Zone_9	54.1	62.8	82.2	146.5	
Zone_10	60.8	73.7	101.7	177.6	
Zone_11	55.7	51.5	174.7	234.5	
Zone_12	55.5	60.3	**-13.9**	20.6	
Over all Ethiopia	42.7	47.1	72.9	121.4	

As a discussion; this findings aligns with projected result of a reduction in annual rainfall under lower-emission scenarios (Mengistu et al., 2021) and while contrary to the projected an upward trend in seasonal precipitation during the major rainy months (June, July, August, and September) and minor rainy months

(March, April, and May) reported (T. A. Feyissa et al., 2023). The more pronounced rise is projected under the SSP5-8.5 scenario, with increases of 139.9mm in mid-term and 266.6mm in long term annually, 38.3mm in mid-term and 74.1mm in long term at Kiremt (JJAS) season and 33.6mm in mid-term and 71.3mm in long term period at belg (FMAM) season. Different studies disclosed that anticipated increasing trends of annual precipitation under different climate scenarios were reported (Alaminie et al., 2021; Gebisa et al., 2023; Getachew & Manjunatha, 2021; Moges & Bhat, 2021). Another study conducted in southwest Ethiopia using regional climate models project these calls for the need for tailored adaptation strategies and decreasing rainfall need water conservation measures, while regions of increasing rainfall require flood management infrastructure to ensure sustainable water use and agricultural productivity.

3.2. Maximum Temperature

3.2.1. Statistical model performance

In this section also examined the future trends and climate projection of maximum temperature changes over Ethiopia using a medium-emission scenarios (SSP2-4.5), and under the high-emission scenario (SSP5-8.5) for mid- term (2050), and long-term (2080) periods. Performances of the models were evaluated by employing the bias correction method in order to check the degree of agreement between the projected and observed data. Besides this study also used ENACTs data from 165 point stations, 4 x4 km resolutions, and 10 best CMIP6 model data out of 33 models based on statistical metrics result (ACCESS-CM2, AWI-CM-1-1-MR, Can ESM5-canOE, EC-Earth3-Veg-LR, EC-Earth3-CC, FGOALS-g3, HadGEM3-GC31-LL, INM-CM4-8, INM-CM5-0, and MIROC-ES2L. The Taylor diagram also evaluates the performance of multiple climate models in simulating a target climate variable (likely temperature) against observational data, before and after bias correction by comparing models based on key statistical metrics like Correlation Coefficient (Corr), Standard Deviation (Stdev) and Root Mean Square Error (RMSE).The details information about selected models is summarized in the following table 3 and Figure 15.

Table 10: The monthly performance evaluation statistical value of the CMIP6 climate model output and ranks

No	Models Name	RMSE	MAE	IOA	CC	BIAS	Remarks
1	ACCESS-CM2	4.6	3.6	0.5	0.28	-6.4	Selected
2	AWI-CM-1-1-MR,	4.2	3.4	0.6	0.40	-2.0	Selected
3	CanESM5-canOE	4.5	3.5	0.5	0.26	0.7	Selected
4	EC-Earth3-Veg-LR	5.2	4.1	0.5	0.37	-11.6	Selected
5	EC-Earth3-CC	5.0	3.9	0.6	0.38	-9.6	Selected
6	FGOALS-g3,	4.8	3.7	0.5	0.37	-9.5	Selected
7	HadGEM3-GC31-LL	4.6	3.6	0.5	0.26	-5.5	Selected
8	INM-CM4-8	5.2	4.0	0.5	0.24	-10.3	Selected
9	INM-CM5-0	5.1	3.9	0.5	0.23	-9.5	Selected
10	MIROC-ES2L	5.2	4	0.5	0.26	-10.3	Selected

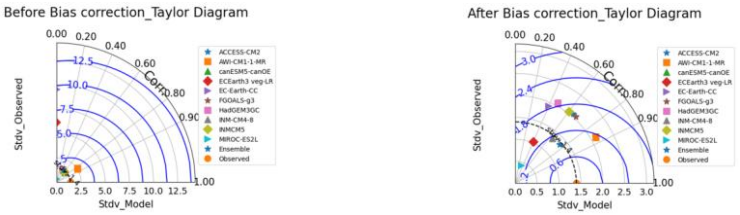

Figure 15: Taylor diagram (after bias correction) of mean monthly-simulated Tmax concerning ENACTS over Ethiopia from 1985_2014.

3.2.2. Spatial analysis for comparisons on ENACTs and ensemble CMIP6 model data sources (1985-2014)

The enhancement of data quality from 10 selected CMIP6 models, the next step involved generating an ensemble dataset using the Simple Arithmetic Mean (SAM) method. When comparing ENACT's data and ensemble model data based on seasonal and annual time scales, during the annual and Kiremt seasons, both data sources showed closely aligned values, with the ensemble model data closely matching the ENACTS dataset. High maximum temperatures were predominantly observed in the northeastern, southeastern, and some limited areas of the northwestern regions, while a decreasing trend in maximum temperature was noted from the western toward the central parts of the country. In contrast, during the Bega and Belg seasons, the ensemble model slightly overestimated temperatures, particularly in the northeastern, eastern, and certain pockets of the western regions during the Bega season, when compared to the ENACTS data. In the Belg season, the model slightly underestimated temperatures in parts of the western regions, while overestimating them in the northeastern areas. Spatial distribution of annual maximum temperature in Ethiopia (based on ENACTS observational data) highlights significant spatial variations in annual maximum temperatures across Ethiopia this distribution also similar to ensemble model results.

The hottest regions, particularly the Afar region in northeastern Ethiopia, experience the highest annual maximum temperatures due to their arid and semi-arid conditions. In contrast, cooler temperatures are observed in the central, southwestern, western, and southern highlands, where higher elevations result in a milder climate despite Ethiopia's equatorial location.

The highest maximum temperatures are predominantly found in Afar and the surrounding lowland areas, characterized by extreme daytime heat and dry conditions. Lowest maximum temperatures are concentrated in the central highlands (e.g., Addis Ababa), parts of Oromia, and the Southern part, all regions where elevation moderates temperatures. High temperatures in lowland areas can reduce crop yields due to heat stress, exacerbate water scarcity through increased evaporation, and heighten the risk of

heat-related illnesses in arid regions, necessitating improved water management and public health interventions. The ENACTS dataset provides a reliable observational baseline for climate studies, supporting evidence-based planning and adaptation strategies.

The spatial distribution of maximum temperature (Tmax) across Ethiopia simulated by the CMIP6 ensemble model for the annual scale and three major seasons, Kiremt, Belg (short rainy season), and Bega (dry season).

The hottest zones (43–54°C) are found in northeastern Ethiopia, particularly Afar, due to arid lowland conditions, while cooler zones (22–38°C) prevail in the central, southwestern, and southern highlands such as Oromia, Sidama, South West, Central Ethiopia, and Amhara—demonstrating elevation's moderating effect on temperature.. Seasonal variations of Kiremt Cooler temperatures prevail in the central highlands, where increased cloud cover and rainfall reduce Tmax. Persistent heat in the northeast (Afar) and the remaining areas are dry during this season. Belg season is generally warmer than Kiremt, especially in eastern and northeastern regions. High Tmax again dominates Afar and the surrounding lowlands. Bega (Dry Season) Warm conditions persist in eastern and northeastern Ethiopia due to clear skies and minimal rainfall. Highlands exhibit lower Tmax, while lowlands (Afar, Somali, and eastern Oromia) remain hot. Generally, the CMIP6 ensemble model outputs reveal a consistent spatial pattern, with lowland regions experiencing significantly higher Tmax than highland areas across all seasons. Seasonal variations are evident, with Belg and Bega exhibiting more extensive areas of elevated temperatures compared to Kiremt. These findings are critical for Climate adaptation planning, particularly in heat-sensitive sectors like agriculture and health.

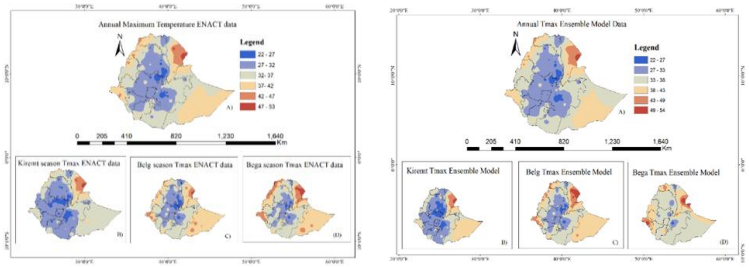

Figure 16: Spatial distribution of comparisons between observed and ensemble model CMIP6 data Tmax

3.2.3. Spatial analysis of mid-term (2041-2070) and long-term (2071-2100) periods maximum temperature future projection

Annual maximum temperature future projection

Figure 16 indicates spatial distribution of annual maximum temperature (Tmax) in Ethiopia CMIP6 Ensemble Projections under SSP2-4.5 and the figure illustrates the distributions of annual maximum temperature (Tmax) across Ethiopia, comparing historical (1985–2014) and future projections (SSP2-4.5 scenario) from CMIP6 ensemble models. The coolest regions (22–33°C) are concentrated in the central and southwestern highlands (Oromia, Sidama, and Amhara), while the hottest zones (43-54°C) appear in the northeast (Afar) and southeastern lowlands, this also reflecting Ethiopia's strong elevation-temperature gradient. The mid-term future (SSP2-4.5) moderate warming is evident, with previously cooler areas (33-38°C) shifting to warmer ranges (38–43°C). The highlands show slight warming (greener tones fading), while the Afar and eastern lowlands exhibit intensified heat stress (expanding red zones). The long-term future (SSP2-4.5) pronounced warming trend emerges, with extreme temperatures (49-54°C) expanding further into the northeast and southeast. Highland regions warm significantly (33-38°C and above), signaling a systematic rise in Tmax nationwide. The highlands remain relatively cooler but face measurable warming, while the lowlands (Afar, Somali regions) endure extreme heat increases. Progressive warming is clear-century shows moderate shifts, but end-century projections reveal severe heat stress, particularly in vulnerable regions. This analysis underscores Ethiopia's growing exposure to extreme temperatures under SSP2-4.5, emphasizing the urgency of region-specific adaptation strategies and Separated into logical sections.

Spatial projections of annual maximum temperature under the SSP5-8.5 Scenario indicates at the figure presents the evolution of maximum annual temperature (Tmax) from historical conditions to future projections (mid-term and long-term) under the high-emission SSP5-8.5 scenario, revealing distinct spatial patterns. Historical Baseline Clear thermal gradient Cooler central/southern regions (22-33°C) contrast with hot northern/northeastern zones (43-54°C). Mid-term projection northern/northeastern hotspots intensify, warming expansion 33-43°C zones grow significantly, and thermal shift. Cool areas (22-27°C) begin shrinking. Long-term projections of extreme heat dominance 43-54°C zones expand dramatically, and northern/northeastern regions face unprecedented Tmax levels. Geographical disparity, northern/eastern regions face the most severe warming. Scenario Severity SSP5-8.5 drives extreme temperature threshold, adaptation is urgent. The SSP5-8.5 scenario projects alarming Tmax increases across the region, particularly in northern/northeastern zones. Current hot areas will face dangerous

extremes, while previously temperate regions will experience unprecedented warming. These spatial patterns demand immediate, location-specific adaptation measures to address the growing heat threats to ecosystems and human systems.

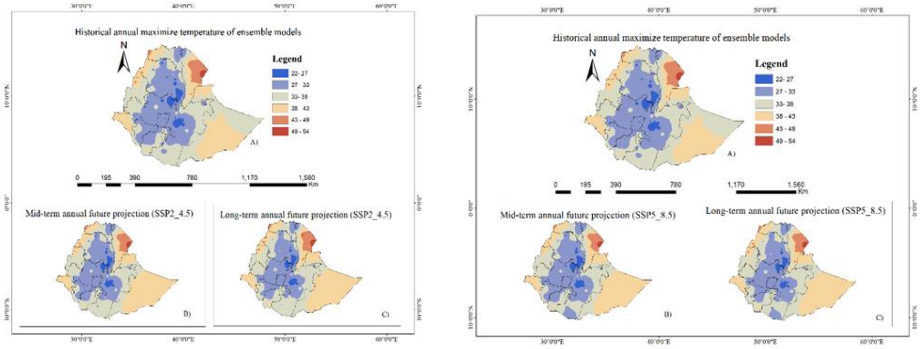

Figure 17: Spatial distributions of annual maximum temperature over Ethiopia

Note: The letter a) represents historical annual Tmax of ensemble models, b) represents mid-term future projection, and c) represents long-term future projection for both maps; and the left side map represents medium (SSP2_4.5) and the right side represents worst (SSP5_8.5) climate scenarios.

Belg (FMAM) season maximum temperature projection

The spatial distribution of maximum temperature (Tmax) during the Belg season under the SSP2-4.5 moderate emissions scenario reveals important trends when comparing historical conditions with mid-term (2041–2070) and long-term (2071–2100) projections. In the historical baseline, cooler conditions (22–30°C) dominate most regions, with localized heat extremes (37–45°C) occurring primarily in the northern and northeastern lowlands, particularly the Afar region. This reflects the present climate variability during Ethiopia's short rainy season. In the mid-term projections, a gradual warming trend emerges nationwide like northern and eastern regions begin shifting into higher temperature categories (30–37°C), accompanied by a moderate expansion of warmer zones and a partial reduction of the coolest areas.

Long-term projections indicate accelerated warming, with historically hot regions like northeast Ethiopia experiencing even higher dominant temperatures (37–45°C); while newly vulnerable areas emerge as the 30–37°C zones expand westward. The extent of areas with sub-30°C Tmax shrinks significantly, persisting only in the highest elevations of the highlands. Spatially, strong north-south thermal gradient remains, but it intensifies over time, with lowland regions warming at a faster rate than the highlands. Temporally, the

analysis indicates progressive warming across all future periods, with the most dramatic changes projected in the long term. Although SSP2-4.5 represents a moderate warming path less severe than SSP5-8.5, the projected changes are still substantial.

The SSP2-4.5 scenario suggests consistent warming during the Belg season, with the northern and northeastern lowlands expected to experience the most significant increases in Tmax. While highland areas are projected to remain relatively cooler, all regions exhibit upward shifts in temperature categories. These changes imply longer periods of heat stress, particularly in already vulnerable areas, and pose potential risks to Belg-season agricultural activities. As such, climate-resilient planning and adaptive strategies are essential, even under moderate emissions scenarios. The evolving spatial patterns emphasize the urgency of proactive measures tailored to regional vulnerabilities, ensuring sustainable development amid changing climate conditions. The historical spatial distribution and projected changes in annual maximum temperature (Tmax) over Belg under the SSP5-8.5 high-emission climate scenario are illustrated through comparisons between historical data and mid-term (2041–2070) and long-term (2071–2100) future projections. During the historical period, cooler regions (22–26°C and 26–30°C) dominate much of Belg, while warmer zones (37–41°C and 41–45°C) are primarily confined to the northern and northeastern areas. This historical distribution establishes the baseline, reflecting the current spatial variability of Tmax across the region.

In the mid-term projection, a noticeable warming trend emerges, with a significant decline in cooler zones (22–26°C) and an expansion of warmer temperature classes (30–33°C and 33–37°C), indicating a clear shift toward higher Tmax values across broader areas. The long-term projection intensifies this trend, with a widespread increase in the hottest temperature categories (37–41°C and 41–45°C), suggesting that much of Belg could transition from relatively moderate conditions to consistently hot climates.

Overall, the projections under SSP5-8.5 demonstrate a continuous rise in Tmax from the historical baseline to the end of the century. Regional variability is pronounced, with the northern and northeastern parts of Belg projected to experience the most substantial increases. These findings emphasize the heightened risk of frequent and extreme heat events in the future, underscoring the urgent need for effective climate adaptation and mitigation strategies to safeguard vulnerable regions.

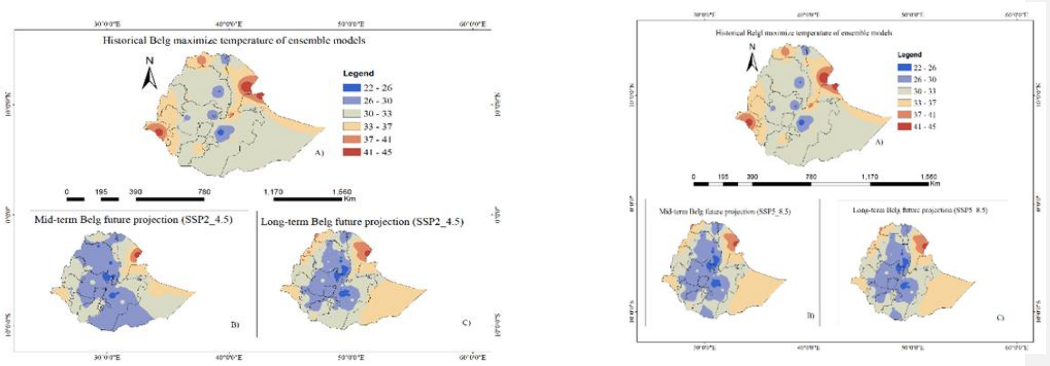

Figure 18 Spatial distributions of Belg maximum temperature over Ethiopian

Kiremt (JJAS) Season maximum temperature projection

The figure 18 at below displays a series of maps showing the spatial distribution of maximum temperatures during the Kiremt season, Ethiopia's main rainy season, based on various climate model projections. The historical kiremt Tmax map illustrates past observed maximum temperatures, using color gradients to represent temperature ranges from 20–25°C, 25–30°C, 30–35°C, 35–39°C, 39–44°C, to 44–49°C. The mid-term future projection map depicts projected temperatures for 2041–2070 under the SSP2-4.5 scenario, while the Long-term future projection map shows projections for 2071–2100 under the same scenario.

This analysis examines the spatial distribution of maximum temperatures during Ethiopia's Kiremt season (the main rainy season) under the high-emission SSP5-8.5 scenario, comparing historical data with mid-term (2041–2070) and long-term (2071–2100) projections. Historical baseline Maximum temperatures ranged from 22°C to 38°C across much of the central and western highlands, while extreme heat (43–54°C) was confined to localized areas in the northeastern lowlands (Afar region).

Mid-term projection (2041–2070) significant warming is projected, particularly in lowland regions, with temperature increases of 3–5°C. Areas with 38–43°C expand into central transitional zones, and cooler highland zones below 30°C begin to shrink noticeably. Long-term projection (2071–2100), a dramatic expansion of extreme heat is expected. Temperatures of 49–54°C are projected to cover up to 40% of lowland areas. The highlands could warm by 4–7°C compared to the historical baseline, with sub-27°C zones nearly disappearing.

The most severe warming occurs in lowland regions like Afar and the east, while highlands lose their cooling effect, with cooler zones shrinking to only the highest elevations. Overall, the SSP5-8.5 scenario projection will be expected catastrophic warming during Ethiopia's main growing season. Extreme heat in

the lowlands could render some areas uninhabitable, while highlands lose their historical climate resilience. These trends call for urgent, location-specific adaptation strategies to protect food security, water access, and human health.

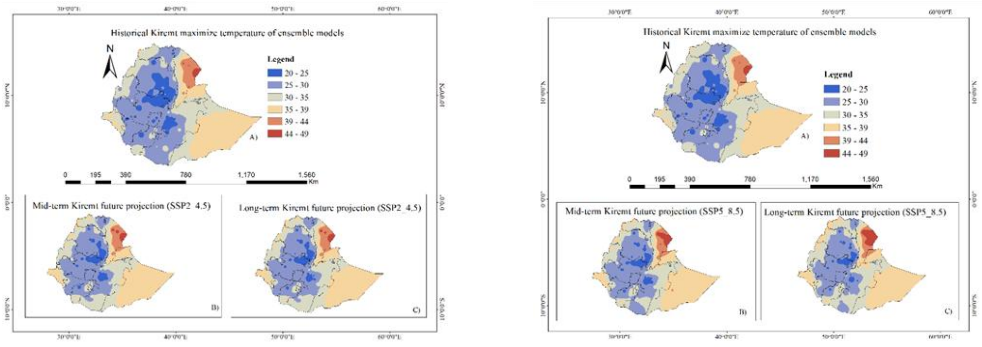

Figure 19 Spatial distributions of the Kiremt maximum temperature over Ethiopia

Note: The letter a) represents the historical Kiremt maximum temperature of the ensemble model, b) represents the mid-term future projection, and c) represents the long-term future projection for both maps; and the left side map represents medium (SSP2_4.5) and the right side represents worst (SSP5_8.5) climate scenarios.

Bega (ONDJ) Season maximum temperature projection

The maximum temperatures during Ethiopia's Bega season are projected to change under the SSP2-4.5 scenario, comparing historical conditions with mid-term (2041–2070) and long-term (2071–2100) futures. During the historical period, Bega season maximum temperatures ranged from 25–34°C across much of the country. Cooler temperatures (21–25°C) were concentrated in the central and western highlands, while warmer zones (38–46°C) were found in the northeastern lowlands (Afar) and parts of the eastern and southeastern lowlands, driven by low elevation and arid conditions.

Mid-term projection shows significant warming is expected in as once within the 25–29°C range shifting 29–34°C. The northeastern lowlands see an expansion into 42–46°C, while highland regions experience moderate warming and a reduction of cooler zones (<25°C). Transitional areas, especially in central and eastern Ethiopia, warm into the 34–38°C range. Long-term projection warming intensifies further regions exceeding 38°C, spreading deeper into lowland and transitional areas. Cool highland zones (21–25°C) become increasingly rare, limited to the highest elevations. Afar and eastern Ethiopia are projected to face extreme heat (42–46°C), reflecting severe climate vulnerability.

Trends are a clear northward and eastward shift of heat extremes over time such as Cool zones shrink, while hotter temperature ranges (above 34°C) expand into previously moderate areas. Generally, under the SSP2-4.5 scenario, Ethiopia's Bega season is projected to warm significantly, especially in lowland and transitional areas and cooler highland zones will shrink, while extreme heat (above 38°C) expands, particularly in the Afar and eastern regions. The figure also presents projected changes in Ethiopia's Bega season maximum temperatures (Tmax) based on ensemble climate model outputs under the high-emission SSP5-8.5 scenario. In the historical period, Tmax ranged from 21–46°C. Cool zones (21–25°C) were concentrated in the central and western highlands, while moderate temperatures (25–34°C) covered much of the country. Hot zones (38–46°C) were mainly limited to the northeastern lowlands (Afar) and parts of the eastern and southeastern lowlands.

Mid-term projections show a clear warming trend are Cool areas below 25°C contract significantly, while 29–34°C zones expand into transitional and lower highland regions. Extreme heat (42–46°C) extends further across the northeastern and eastern lowlands. In the long-term projections, warming becomes more severe. 21–25°C zones nearly disappear, remaining only in isolated high-elevation pockets. 34–42°C temperatures become widespread, and 42–46°C zones dominate large areas of the Afar, Somali, and Oromia lowlands, indicating intense heat amplification. The trends Pronounced northward and eastward

spread of extreme heat, Gradual loss of cooler highland zones, Expansion of hot zones (>38°C) into previously moderate regions, and the Afar and Somali regions emerge as severe heat hotspots.

The increased heat stress could reduce crop productivity in highland and transitional farming zones. Water resources are higher temperatures may intensify evaporation, lowering water availability during the dry Bega season. Health & Livelihoods populations in lowland regions, particularly afar and Somali will face greater exposure to heat-related health risks and diminished habitability. Overall, under the SSP5-8.5 scenario, Ethiopia's Bega season is projected to experience sharp temperature increases, with expanding extreme heat zones and the disappearance of cooler climates, posing critical challenges for agriculture, water resources, and public health.

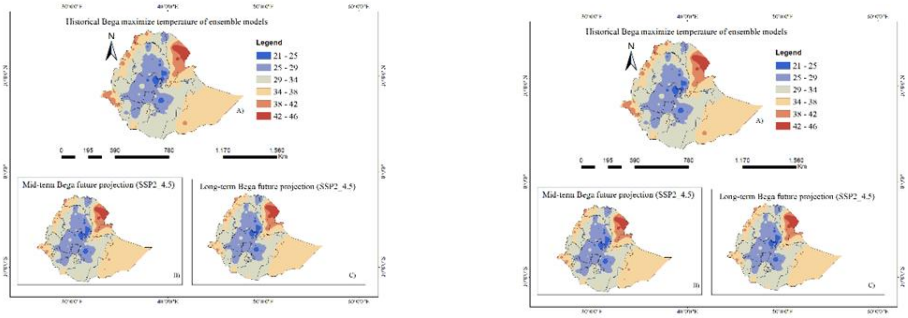

Figure 20: Spatial distributions of the Bega maximum temperature over Ethiopia

Note: The letter a) represents the historical Bega maximum temperature of ensemble models, b) represents the mid-term future projection, and c) represents the long-term future projection for both maps; and the left side map represents the medium (SSP2_4.5) and the right side represents the worst (SSP5_8.5) climate scenarios

3.2.4. Projection of maximum temperature trend analysis over Ethiopia at 21st century (1981-2100)

Figure 20 below illustrates a time series of maximum temperature (Tmax) over Ethiopia from 1981 to 2100. Historical Data (1980–present) Observed records show a gradual warming trend with natural year-to-year fluctuations. Since 1980, temperatures have risen by about 2–3°C. Future Projections (SSP2-4.5) under a moderate emissions pathway with some mitigation efforts, temperatures continue to rise steadily, reaching about 38°C by 2100. Future Projections (SSP5-8.5) under a high-emissions scenario dominated by fossil fuel use and limited climate action, temperatures increase much more sharply, surpassing 39°C by 2100. Comparison SSP2-4.5 suggests that moderate mitigation can limit extreme warming, while SSP5-8.5 highlights the severe consequences of unchecked emissions, with major risks for Ethiopia's ecosystems and human systems. Overall, the figure underscores how emissions choices today shape vastly different temperature outcomes for Ethiopia by the end of the century.

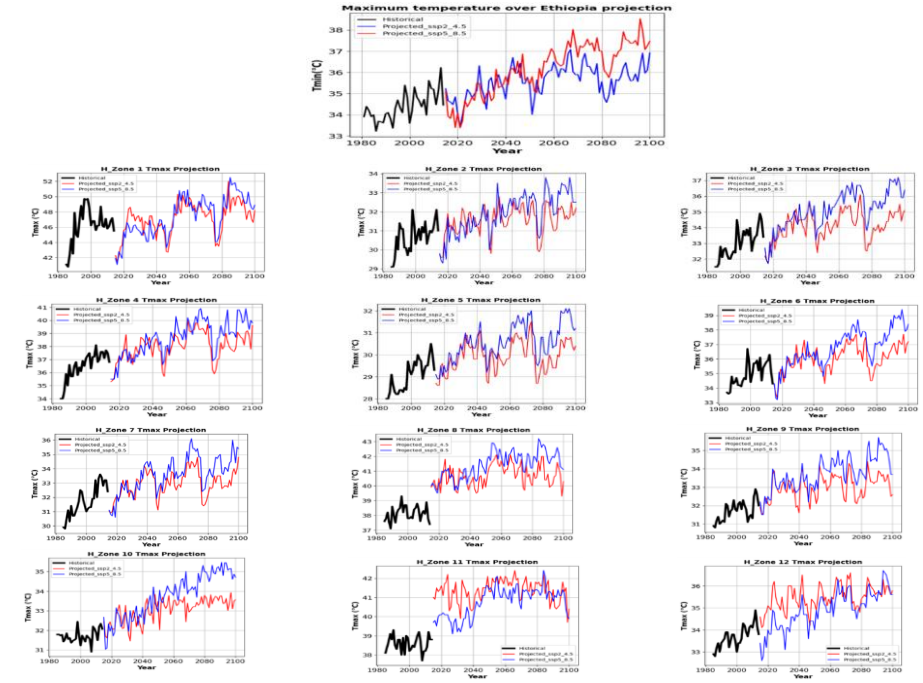

Figure 21: Maximum temperature Annual trend analysis over Ethiopia (1981-2100)

3.2.5. Historical and future projection of the maximum temperature trend analysis

The trend analysis of maximum temperatures (1985–2014) plots temperature values (33.0°C–35.5°C) with a blue line depicting historical data that fluctuates annually between peaks and dips. The red trend line, cuts through these variations filtering out short-term noise to reveal a clear long-term warming pattern. The analysis reveals a clear upward trajectory in maximum temperatures over these 30 years. Despite year-to-year variability, the consistent slope of the trend line indicates a sustained warming pattern. This finding aligns with broader climate change expectations, demonstrating a gradual but definite increase in maximum temperatures in the region. The visualization effectively separates natural annual variability from the underlying warming trend, providing clear evidence of climate change impacts over recent decades.

The four subplots display maximum temperature (Tmax) projections across different timeframes and scenarios, with the top-left plot showing mid-term projections (2041-2070) where annual Tmax data points follow an upward trend. The top-right plot presents long-term projections (2071-2100), exhibiting a similar but more intensified warming pattern compared to the mid-term outlook. The bottom panels analyze a high-emission scenario (SSP5-8.5), with the left plot showing mid-term projections (2041-2070) exhibiting heightened variability and accelerated warming. The right plot reveals the most extreme temperature increases in century-scale projections (2071-2100) under the same scenario, where blue lines track annual Tmax variations and red trend lines emphasize persistent warming patterns.

Over the entire 21st century (2015–2100), the average maximum temperature over the country is projected to rise by 1.7°C in mid-term and 1.6°C in long term under SSP2-4.5, and 2.1°C in mid-term and 2.7°C in long term under SSP5-8.5 indicating the highest temperatures in highest emission scenario. The Computed result of analysis indicates that both SSPs project an increase in mean maximum temperatures in the mid-term and long-term period of the 21st century, reflecting global warming due to rising GHG emissions. SSP5-8.5, while the high-emission scenario, shows the largest increases. These projections highlight the variability in warming across different emission pathways, emphasizing the critical role of emissions control in shaping future climate outcomes. Warming is expected to be more significant in the distant future (2070–2100), with the highest increases under SSP5-8.5, strengthening the connection between emissions levels and temperature rise.

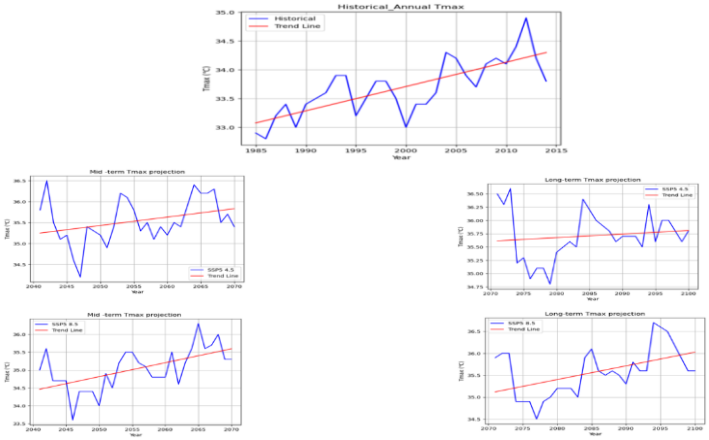

Figure 22: Future annual Tmax projection of mid and long-term periods under SSP245 and SSP585 climate scenarios over Ethiopia

3.2.6. Annual maximum temperature anomalies over twelve homogeneity zones

Figure 23 illustrates projected annual maximum temperature (Tmax) anomalies for Ethiopia's homogeneity zones during the mid-term period (2041–2070) under the moderate-emission scenario (SSP2-4.5). Each subplot corresponds to a specific zone (Zone 1-12), depicting yearly deviations from a historical baseline. Positive anomalies (red bars), indicating warmer-than-baseline years, predominate across most zones (Zone 3, Zone 5, Zone 10), confirming a persistent warming trend. Negative anomalies (blue bars), although present in some zones (Zone 2, Zone 9), decrease in frequency and magnitude over time, particularly by 2070.

Temporal variability zones exhibit distinct patterns like Zone6 show steady warming, while others display higher inter-annual variability. The intensity of anomalies varies regionally, underscoring Ethiopia's heterogeneous climate response. Scenario Implications Even under SSP2-4.5, all zones trend toward higher Tmax values, with cooler years becoming increasingly rare. The findings align with global projections but emphasize localized risks, necessitating zone-specific adaptation measures. The mid-term projections strengthen the urgency of climate resilience planning, as warming persists across all zones despite the moderate-emission pathway. The spatial heterogeneity highlights the need for tailored strategies to address regional vulnerabilities.

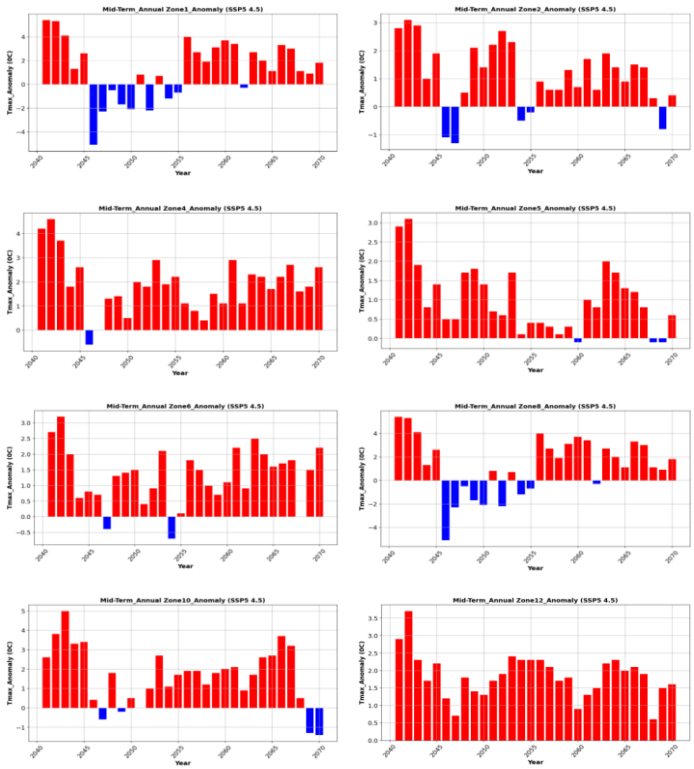

Figure 23: Future projection Annual Tmax anomalies under SSP2_4.5 climate scenarios for the mid-term period

Figure 23 also shows six bar charts illustrating projected annual maximum temperature (Tmax) anomalies under the SSP2-4.5 climate scenario with long term period, which represents a moderate emissions pathway. Each chart shows temperature deviations from a historical baseline, where red bars indicate warmer-than-normal years and blue bars indicate cooler-than-normal years. The predominance of red bars suggests a general trend toward higher temperatures in the future. A clear long-term warming trend is evident, with both the frequency and intensity of positive anomalies increasing over time. Meanwhile, negative anomalies (blue bars) become less frequent and less pronounced, indicating a reduced likelihood of cooler-than-normal years as climate change advances. The alternating red and blue bars reflect short-term variability and uncertainty, yet the overall direction points to sustained warming. In the earlier part of the projection period (near the 2020s), charts show more frequent neutral or negative anomalies. In

contrast, the later periods (2050s to 2100) are dominated by stronger and more frequent positive anomalies. This pattern highlights the anticipated progression of warming under the SSP2-4.5 scenario: while variability remains, the long-term signal is a clear and intensifying rise in temperature anomalies.

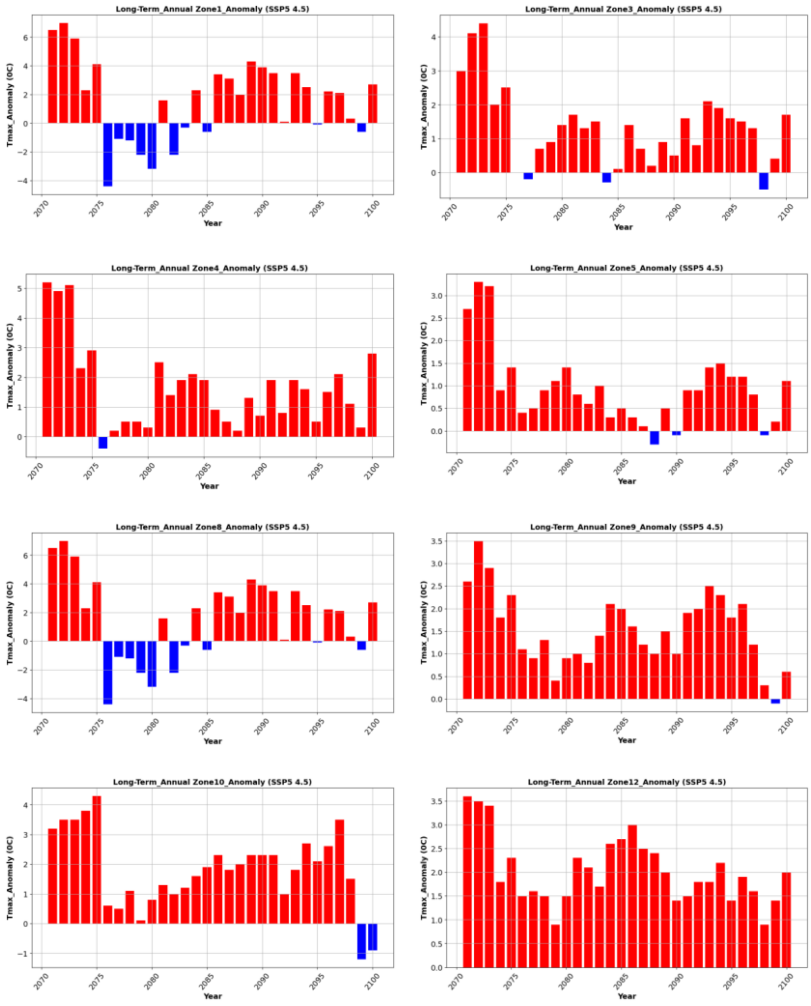

Figure 24: Future projection Annual Tmax anomalies under SSP2_4.5 climate scenarios for long-term period

The figure 25 at below presents six bar charts illustrating the future projections of annual Tmax (maximum temperature) anomalies under the SSP5-8.5 climate scenario, which represents a high-emission pathway with minimal mitigation efforts. Most bars are red which indicating positive temperature anomalies and this suggests a trend toward rising temperatures. The anomalies tend to be larger and more frequent during the mid-term, reflecting significant warming under this high-emission scenario. Frequency and magnitude of anomalies charts demonstrate a consistent presence of positive (warm) anomalies across the mid-term period. The size of the red bars increases and that indicating more intense hot years progresses and there are relatively fewer blue bars compared to the SSP2-4.5 scenario, reflecting fewer cooler-than-normal periods. Variability Despite the dominant warming trend, there is noticeable variability, with some blue bars indicating occasional cooler periods.

The overall pattern suggests that, under SSP5-8.5, the climate system is expected to experience more frequent and intense heat anomalies in the mid-term, but with some fluctuations. The charts underscore the severe warming implications of the SSP5-8.5 scenario during the mid-term, characterized by frequent hot years and fewer cold periods. This highlights the urgency for climate mitigation to prevent such high-end projection scenarios. Under the SSP5-8.5 high-emission scenario, the mid-term future shows a clear trend toward increased maximum temperature anomalies. The projections indicate more frequent and intense hot years, with fewer occurrences of cooler days, emphasizing the substantial warming impact expected if emissions continue unabated.

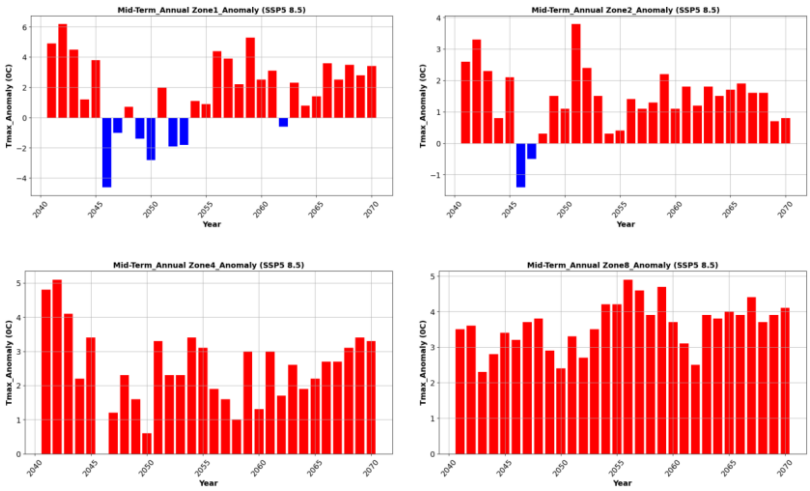

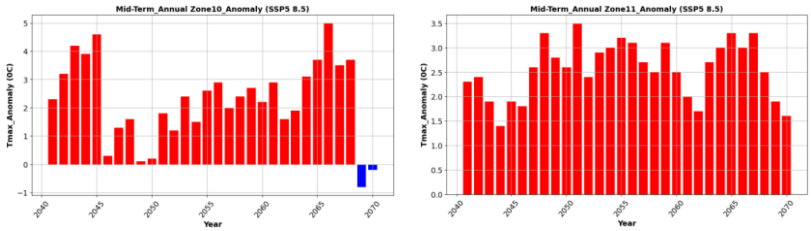

Figure 25: Future projection Annual Tmax anomalies under SSP5_8.5 climate scenarios for the mid-term period

The figure 26 shows six bar charts illustrating the long-term projections of annual Tmax (maximum temperature) anomalies under the SSP5-8.5 climate scenario, which represents a high-emission pathway with minimal mitigation efforts. The majority of the bars are red, indicating positive temperature anomalies, which signifies a consistent trend of increasing maximum temperatures over the long term under this high-emission scenario. The magnitude of anomalies tends to be larger, suggesting significant warming compared to the baseline period. The early years (left side of the charts) show higher variability with some negative anomalies (blue bars), but these become less frequent over time. In later periods, positive anomalies dominate, with many bars reaching higher values, indicating more frequent and severe warm years. Variability and Uncertainty Despite the overall warming trend, there are fluctuations, reflecting the natural variability within the climate system. The periods towards the end of the timeline show an increase in the intensity and frequency of warm anomalies, emphasizing the long-term impacts of continued high emissions. Long-term, these projections suggest a sustained increase in maximum temperatures over the long term, with a marked decline in cooler periods. The results highlight the potential for ongoing and intensifying heat-waves and temperature extremes if high emission levels persist. Under the SSP5-8.5 scenario, the long-term future indicates a persistent and significant rise in Tmax anomalies, with more frequent and intense high-temperature years. This underscores the severe warming trajectory associated with continued high greenhouse gas emissions.

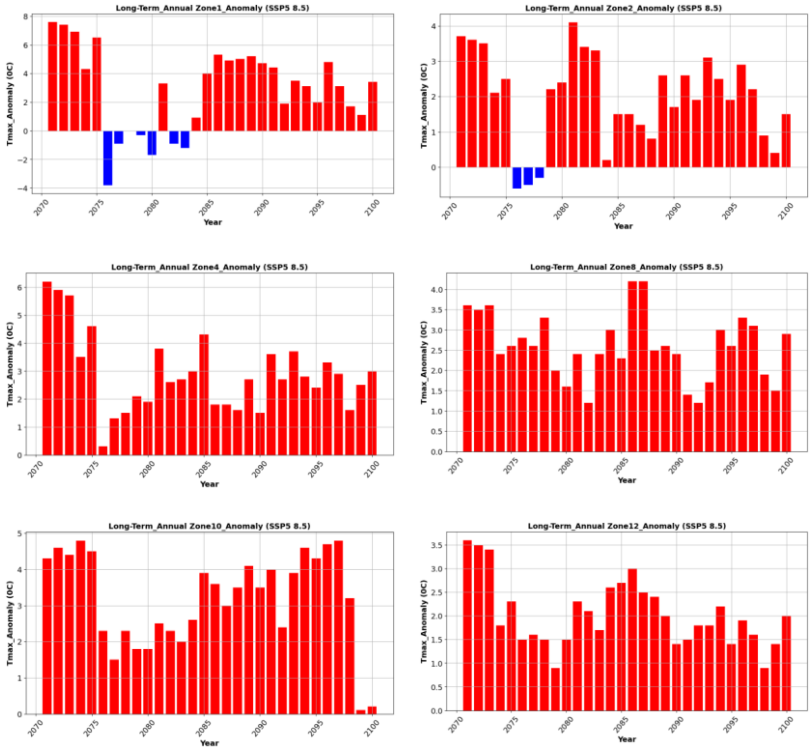

Figure 26: Future projection Annual Tmax anomalies under SSP5_8.5 climate scenarios for the long-term period

3.2.7. Analysis of Maximum Temperature variation for Projections across Ethiopia's 12 Homogeneity Zones

The table below analysis highlights projected Tmax anomalies across Ethiopia under moderate (SSP2-4.5) and high (SSP5-8.5) emission scenarios for 2041–2070 and 2071–2100. Under SSP2-4.5, warming is moderate and stabilizes over time (national average: 1.7°C to 1.6°C). In contrast, SSP5-8.5 shows stronger, accelerating warming (2.1°C to 2.7°C), with Zones 8 and 11 most affected. Zone 12 warms least, while Zones 2 and 5 show minimal but notable increases. SSP5-8.5 leads to ~1.0°C more warming by 2100, posing serious risks. Urgent adaptation is needed for vulnerable zones, and mitigation efforts are essential to avoid extreme outcomes.

Table 11: Maximum temperature variation for projections across Ethiopia's 12 homogeneity zones

Homogeneity Zone	SSP2_4.5		SSP5_8.5	
	Mid-Term	Long-Term	Mid-Term	Long-Term
Zone_1	1.3	1.6	1.8	2.9
Zone_2	1.1	1.0	1.4	2.0
Zone_3	1.3	1.3	2.3	2.9
Zone_4	1.9	1.6	2.5	2.9
Zone_5	1.0	1.0	1.6	2.0
Zone_6	1.3	1.3	2.0	2.7
Zone_7	1.5	1.4	2.1	2.6
Zone_8	2.8	2.6	3.6	3.8
Zone_9	1.4	1.5	2.1	2.7
Zone_10	1.7	1.8	2.3	3.2
Zone_11	3.0	2.7	2.6	2.6
Zone_12	1.9	2.0	1.3	1.9
Over all Ethiopia	1.7	1.6	2.1	2.7

As a discussion; the results of this study is highly related from different previous studies such as; Sixth Assessment Report (AR6) of the IPCC ((Lee et al., 2023) confirms that global warming is intensifying with projected temperature increases of + 2 °C to + 3 °C under SSP2-4.5 and + 4 °C or more under SSP5-8.5 by 2100 (IPCC,2023). Ethiopia, including its highland watersheds, is already experiencing these shifts. Under SSP2-4.5, maximum temperatures (Tmax) are projected to rise by + 2.0 °C to + 2.5 °C under SSP2-4.5, and by + 3.3 °C to + 4.5 °C under SSP5-8.5 and another study project that in the Blue Nile Basin, Tmax could increase by 2.1 °C and 2.8 °C under SSP2-4.5 and SSP5-8.5, respectively (Enyew et al., 2024).

Additionally; The finding of the study implies the rising mean maximum temperatures are consistent with several studies such as; According to Getachew & Manjunatha (2021) predicted a temperature increase of 1.38–3.59 °C by the 2080s in the Lake Tana sub-basin under the RCP4.5 scenario, also, an estimated a rise of 2.1, and 2.8 °C in the mean annual maximum temperature under the SSP2-4.5, and SSP5-8.5 scenarios from 2015 to 2100 (Enyew et al., 2024), Similarly according to Alaminie et al. (2021) reported comparable increases by predicting temperature rises of 1.3, 1.7, 2.0, and 2.6 °C under the SSP1-2.6, SSP2-4.5, SSP3-3.7, and SSP5-8.5 scenarios, respectively and according to Gebisa et al. (2023) projected an increase of 1.4 and 1.8 °C in the Baro River Basin under the SSP2-4.5 and SSP5-8.5 scenarios.

3.3. Minimum temperature

3.3.1. Statistical and spatial models performance

Baseline observation data are the standard for finding changes in climate projections and also for evaluating the performance of the models. To evaluate models to use in temperature projection analysis, the study therefore used ENACTS data from 165 baseline stations covering all parts of Ethiopia. Using this data, the study selected models for the projection analysis of minimum temperature (Tmin) and the models were also ranked according to their performance against statistical metrics such as Root Mean Square Error (RMSE), Mean Absolute Error (MAE), Index of Agreement (IOA), Correlation Coefficient (CORR), and Percent Bias (PBIAS). These metrics facilitated the selection of the best performing models. Thus, out of the 24 models in the Historical, SSP2-4.5, and SSP5-8.5 scenarios, the highest 10 models (highlighted in blue in Table 10) were utilized in this study.

Table 12: Statistical performance of selected models for Tmin

Model	RMSE	MAE	IOA	CORR	PBIAS
FGOALS-g3	**0.522**	**0.38**	**0.78**	**0.44**	**1%**
NRM-ESM2-1	**0.609**	**0.5**	**0.75**	**0.52**	**2%**
IPSL-CM6A-LR	**0.658**	**0.74**	**0.72**	**0.56**	**4%**
CanESM5-CanOE	**0.652**	**0.7**	**0.68**	**0.56**	**3%**
MRI-ESM2-0	**0.66**	**0.61**	**0.67**	**0.56**	**5%**
EC-Earth3-CC	**0.671**	**0.61**	**0.73**	**0.57**	**7%**
GFDL-ESM4	**0.652**	**0.56**	**0.61**	**0.56**	**6%**
CNRM-CM6-1	**0.698**	**0.85**	**0.63**	**0.59**	**10%**
EC-Earth3-Veg-LR	**0.754**	**0.8**	**0.68**	**0.64**	**14%**
HadGEM3-GC31-LL	0.664	0.41	0.61	0.57	8%

Figures 27 show the ENACT observational data and historical ensemble model for annual and seasonal minimum temperature (Tmin) distributions over Ethiopia for respective figures. In both figures, the upper side represents annual Tmin from observational data from ENACT and ensemble of historical climate model outputs and down side represents seasonal Tmin from observational data from ENACT and ensemble of historical climate model outputs. Both the annual and seasonal maps an identical uniform color gradient showing Tmin values from cold (3.63-6.84°C in blue) to hot (19.8-22.9°C in red). Spatially, both datasets exhibit similar patterns: colder Tmin dominates in the highland regions of central and northern parts, particularly, warmer Tmin values over the eastern, southeastern, and southwestern lowland

regions. Such spatial agreement indicates satisfactory coincidence between ENACT and the historical ensemble model, which implies the ability of the model to reproduce past climatic conditions. However, the ensemble model slightly underestimates Tmin values in the northern and central regions of Ethiopia. Although this, the model describes rather well the main climatic characteristics present in the ENACT data, and it is hence justified as being applicable to future climate projections and impact assessments.

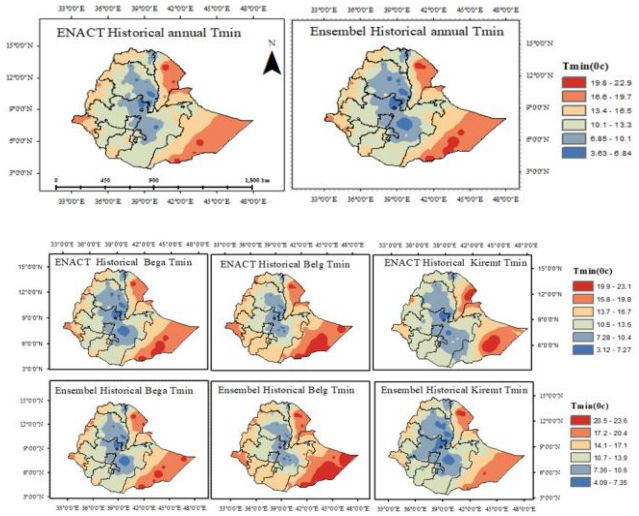

Figure 27: Annual and seasonal ENACT and Ensemble historical performance

3.3.2. Spatial annual projection of minimum temperature in mid and long term period

Figure 28 present the spatial pattern of annual minimum temperature (°C) across Ethiopia throughout the historical period (1985-2014) and under two scenarios of future climate (SSP2-4.5 and SSP5-8.5) for mid-term (2041-2070) and far-term (2071-2100) periods. Historically, Tmin ranged from approximately 3.6°C in highlands to approximately 23°C in eastern and southern lowlands. Under SSP2-4.5 and SSP5-8.5 scenarios, there is clear warming trend of Tmin over the nation. The lowest temperatures increase in the highlands, yet even more significantly in the lowlands. Compared to the previous baseline, Tmin increases by about 1.7°C in the mid-term and 2.3°C in the far-term under SSP2-4.5. Under high-emission SSP5-8.5 scenario, the increase is even higher 1.8°C in the mid-term and 2.8°C in the far-term.

By the end of the century (2071–2100), SSP5-8.5 scenario projects widespread warming, with minimum temperatures of more than 25°C in the majority of the northeastern and southeastern lowlands. Even the cooler highlands will presumably warm significantly. In general, the projections are that Ethiopia will

experience substantial increases in minimum temperatures, especially under the high-emission scenario, necessitating the imperative of effective climate mitigation actions.

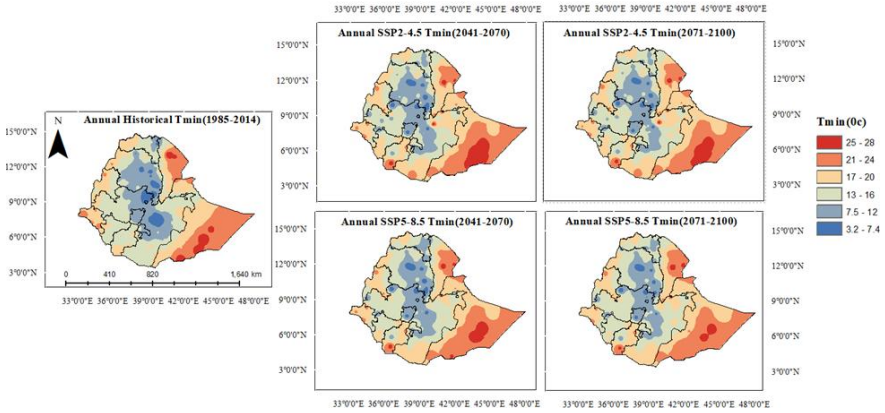

Figure 28: Annual Tmin projections under SSPS2-4.5 and SSP5-8.5 scenarios

3.3.3. Seasonal spatial trend of minimum temperature

Ethiopian regions are expected to have a uniform rising trend of minimum temperature (Tmin) over all seasons and geographical regions by the end of the 21st century. With reference to the historical baseline period (1985-2014) present under SSP2-4.5 scenarios, increase in Tmin for the Bega, Belg, and Kiremt seasons in both the mid-century period (2041-2070) and long century period (2071-2100). Lowlands such as Afar and Somali show more accelerated warming, with Tmin expected to exceed 23°C towards the end of the century. Highland regions, particularly central and northern Ethiopia, will experience warming but will be somewhat cooler, with Tmin ranging from 12°C to 18°C.

On the other hands; presents Tmin projections for the Bega, Belg, and Kiremt seasons under the high-emission SSP5-8.5 scenario. There are much greater increases in Tmin from the projections. By the end of the 21st century, Tmin in most of the lowland areas would be over 25°C, while some parts would be over 27°C, indicating great warming in Tmin. Though highland regions will remain cooler, they too will experience significant Tmin increases to up to 18°C and above, particularly during the Kiremt season. The extent and severity of Tmin rising in the SSP5-8.5 scenario signify the probability of intensified heat stress, disruption of past agricultural schedules, and increased vulnerability of ecosystems and human health. These findings further underscore the need for effective mitigation measures to avoid future warming and reduce associated risks (see figure 29).

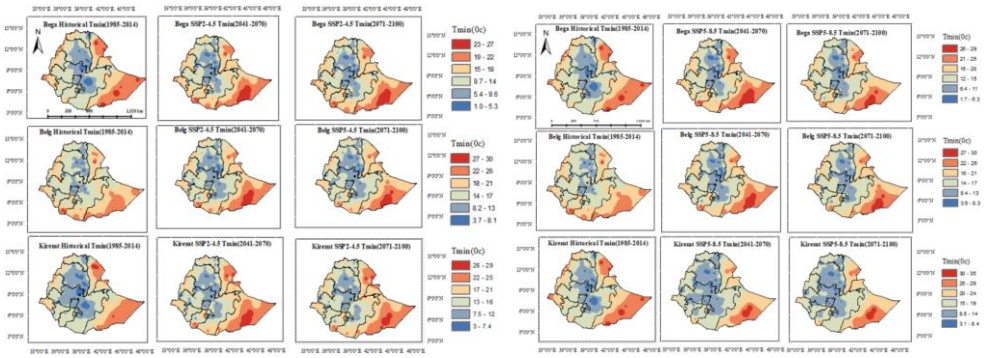

Figure 29: Bega, Belg and Kiremt Tmin projections under SSPS2-4.5 and SSP5_5.8 scenario

3.3.4. Projection of monthly Tmin trend in mid and long term period

Figures 30 show the simulated monthly minimum temperature (Tmin) changes of the Ethiopia in three time periods: the historical reference period (1985–2014), the mid-term (2041–2070), and the long term (2071–2100) under the SSP2-4.5 and SSP5-8.5 climate scenario. The result demonstrates an apparent increasing trend in Tmin in each month, representing a uniform warming trend. In comparison to the Historical periods, minimum temperatures are projected to increase at mid-term and end-term. April to August would be the warmest months, with July recording the highest Tmin values, in the end-century scenario. Relatively, December and January remain the coldest months but also continue to undergo considerable warming with increasing time under both scenarios. This projected warming of Tmin has broad implications for the Ethiopia, including potential impacts on agriculture, human health, ecosystems, and water resources. Warming of temperatures at night might change crop calendars, increase heat related health impacts, and affect biodiversity and hydrological processes. The projections serve to highlight the need for adaptation and mitigation efforts to address the anticipated patterns of warming in all parts of Ethiopia.

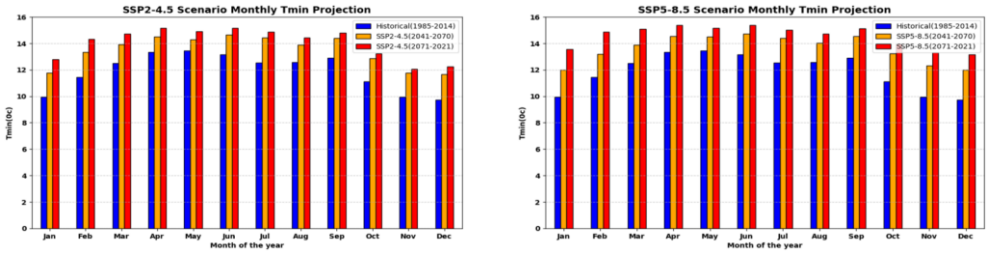

Figure 30: Monthly Tmin projection under SSP2-4.5 and SSP5_8.5 scenario

3.3.5. Projection of monthly trends of minimum temperature over twelve homogeneity zones

Figure 31 and 32 demonstrate the monthly projected Tmin under the SSP2-4.5 and SSP5-8.5 scenarios across all 12 rainfall homogeneity zone in Ethiopia show a consistent warming trend compared to the historical period (1985-2014). All climate zones experience a clear upward shift in monthly Tmin for both midterm (2041-2070) and long term (2071-2100) periods. In highland zones such as Zone 3 and Zone 5, Tmin rises steadily across all months, with more pronounced increases during the cooler months (October to January), suggesting reduced cold-season extremes. Zones 3 and 5, which also display a similar trend but with slightly higher Tmin values, indicating a progressive warming pattern throughout the year. This warming could have direct implications for agriculture, particularly for crops sensitive to cooling.

The lowland and warmer regions like, zones 1 and 11 are projected to experience the highest Tmin values, especially in the long period and in several months with a substantial increase from historical levels. In general in all months and zones, which likely exhibits relatively smaller absolute changes but still shows significant warming, especially in the dry months(October to January). These trends suggest increased thermal stress and possible challenges for heat-sensitive crops, livestock, and water resource management. The monthly breakdown highlights the importance of seasonal planning and targeted adaptation strategies, particularly in zones with the most extreme warming projections.

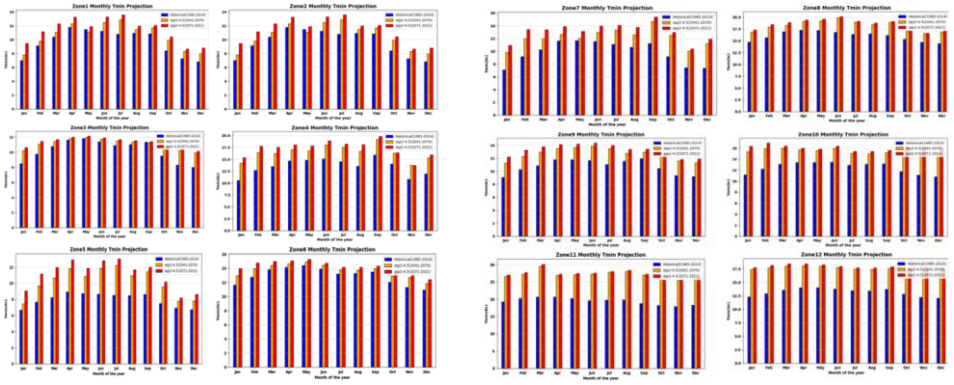

Figure 31: Zone1 to 12 Tmin monthly projection under SSP2-4.5 scenario

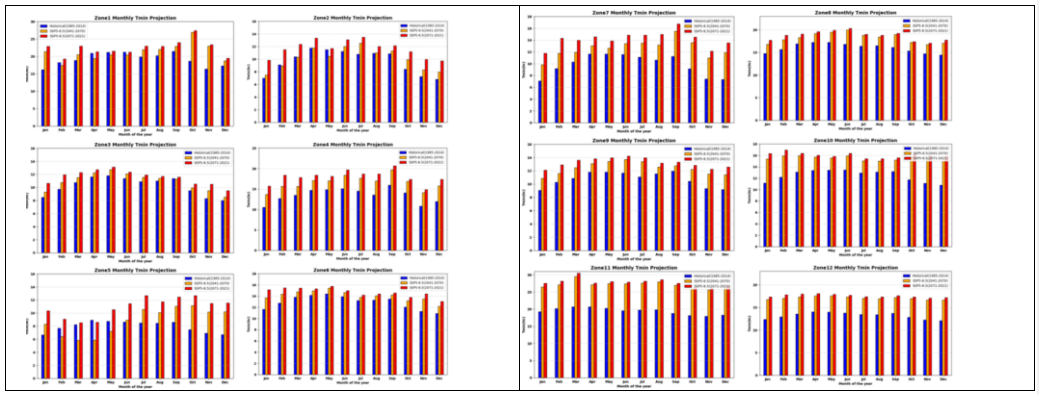

Figure 32: .Zone1 to 12 Tmin monthly projections under SSP5-8.5 scenario

3.3.6. Projection of minimum temperature trend analysis over Ethiopia at 21st century (1981-2100)

Figure 33 presents projected trends in annual mean temperature under two emissions scenarios SSP2-4.5 (moderate) and SSP5-8.5 (high) based on climate model simulations. The left panel shows mid-term projections, and the right panel shows long-term projections. Solid lines represent mean temperature; shaded areas indicate model uncertainty. Temperatures start around 13°C and rise gradually. By 2070, SSP2-4.5 projects approximately 18°C, while SSP5-8.5 reaches 20°C. By 2100, temperatures could hit approximately 25°C under SSP2-4.5 and 27°C under SSP5-8.5. The uncertainty grows over time, especially in the high-emissions scenario. The analysis emphasizes that without strong mitigation, Tmin

may rise by up to 10°C above historical averages, posing serious risks to ecosystems, health, agriculture, and water resources.

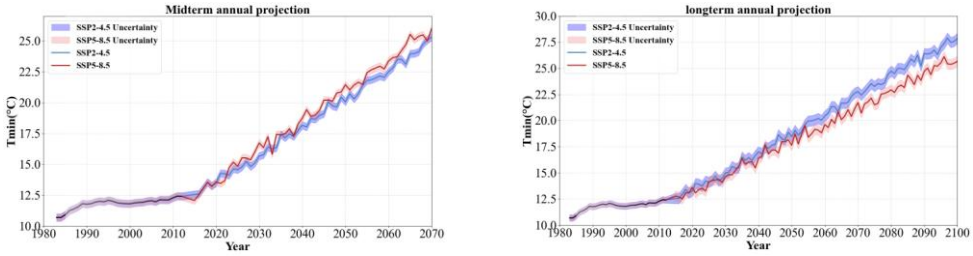

Figure 33: Annual Tmin projections with right (Mid-Term) and left (long-term)

3.3.7. Projection of maximum temperature trend analysis over Ethiopia at 21st century (1981-2100) over twelve homogeneous zones

Figure 34 and 35 Shows rainfall homogeneity Zone 1, 2, and 3 annual Tmin projections with long- and mid-term increments under two emissions scenarios using SSP2-4.5 (moderate) and SSP5-8.5 (high). Each zone includes a mid-term projection and a long-term projection, with shaded areas indicating model uncertainty. Across all zones, the Tmin warming trend is stronger and the uncertainty wider under the high emissions pathway, emphasizing the significant influence of emission choices.

The projected annual mean temperature trends for rainfall homogeneity Zone 4, 5 and 6 under SSP2-4.5 and SSP5-8.5, the projected from 2041-2070 mid-term and 2071-2100 compared to 1985 - 2014 for historical. All zones show a clear increasing Tmin trend, with the rate of warming varying by scenario. The SSP5-8.5 scenario indicates the highest rise in Tmin, highlighting the need of future adaptation and mitigation measures.

Additionally; the projected annual mean temperature trends for rainfall homogeneity Zone 7, 8 and 9 under SSP2-4.5 and SSP5-8.5, covering the period from 1985 to 2014 for historical, 2041-2070 mid-term and 2071-2100. All zones show a clear increasing Tmin trend, with the rate of warming varying by scenario. The SSP5-8.5 scenario indicates the highest rise in Tmin, highlighting the need of future adaptation and mitigation measures whereas projected annual Tmin trends for rainfall homogeneity Zone 10, 11 and 12 under SSP2-4.5 and SSP5-8.5, the projection from 2041-2070 mid-term and 2071-2100 compared to historical period 1985 to 2014 for historical. All zones show a clear increasing Tmin trend, with the rate of

warming varying by scenario. Among the zones, zone 11 highly increased. The SSP5-8.5 scenario indicates the highest rise in Tmin, highlighting the need of future adaptation and mitigation measures.

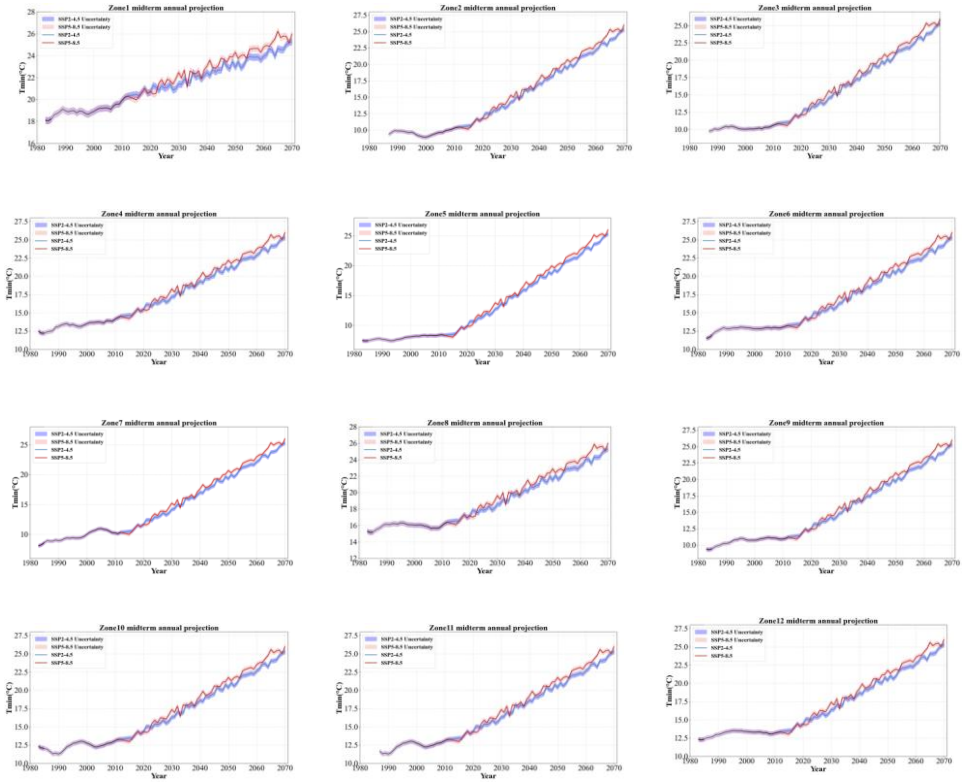

Figure 34: 12 homogeneity zones annual Tmin projections with midterm periods (2041-2070)

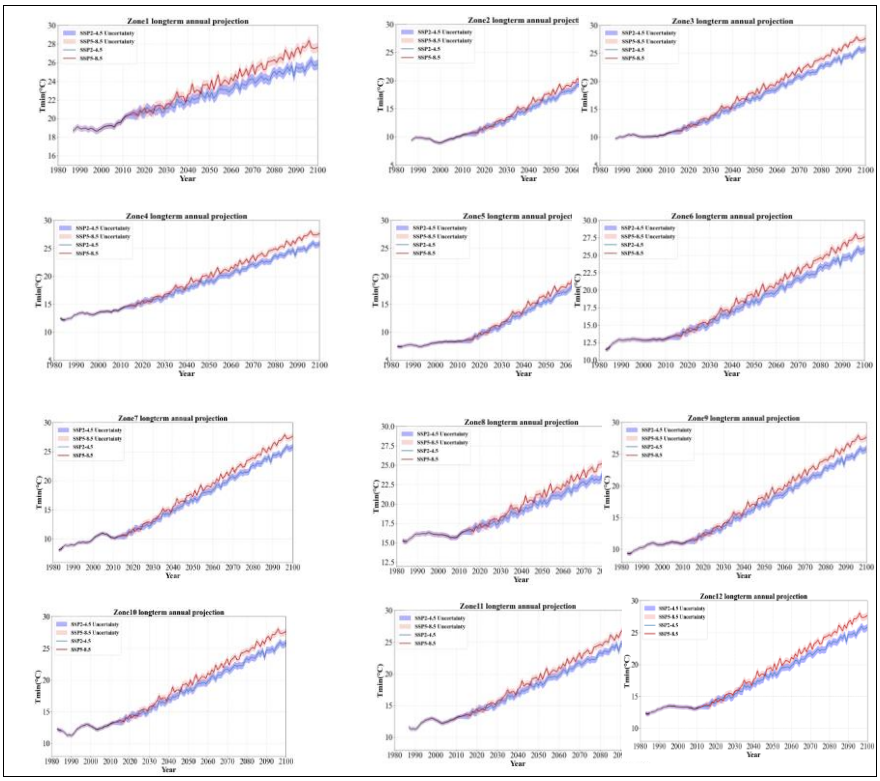

Figure 35: 12 homogeneity zones annual Tmin projections with long term periods (2071-2100)

Table 11 presents projected changes in change in Tmin for 12 rainfall homogeneity zones under two emission scenarios, SSP2-4.5 and SSP5-8.5, across mid-term (2041–2070) and long-term (2071–2100) periods, relative to the historical baseline (1985–2014). The data reveal a clear Tmin warming trend in all zones, with higher temperature increments under the (SSP5-8.5) high scenario compared to the (SSP2-4.5) intermediate scenario. Furthermore, Tmin increased are generally greater in the long term than in the mid-term, indicating progressive warming over time. Spatially, Zone 11 stands out with the most significant rise in minimum temperature, averaging 8.0°C across all projections, followed by Zone 12 (4.3°C), Zone 10 (3.2°C), and Zone 4 (3.6°C). Conversely, Zones 2 and 3 exhibit the smallest increases, averaging 1.3°C and 1.0°C, respectively. These projections underscore the urgent need for robust mitigation and adaptation

measures, particularly in zones experiencing the highest temperature increments, to minimize the adverse impacts of climate change on vulnerable sectors such as agriculture, health, and water resources.

Table 13: Tmin increments under SSP2-4.5 and SSP5-8.5 scenarios from baseline

RHZone	Mid-Term ΔTmin (°C) SSP2-4.5	Mid-Term ΔTmin (°C) SSP5-8.5	Long-Term ΔTmin (°C) SSP2-4.5	Long-Term ΔTmin (°C) SSP5-8.5	Average Increment
Zone 1	1.1	1.9	2.0	3.2	2.1
Zone 2	0.9	1.7	0.5	2.0	1.3
Zone 3	0.8	1.1	0.7	1.3	1.0
Zone 4	2.9	3.8	3.0	4.5	3.6
Zone 5	2.2	3.2	0.9	3.0	2.3
Zone 6	0.8	1.3	1.2	1.8	1.2
Zone 7	2.3	3.2	2.7	4.3	3.1
Zone 8	2.2	2.5	2.2	2.7	2.4
Zone 9	1.9	2.5	1.7	2.5	2.1
Zone 10	2.9	3.3	3.0	3.6	3.2
Zone 11	7.8	8.1	7.7	8.3	8.0
Zone 12	4.4	4.7	3.9	4.4	4.3

In general, the projected trends of minimum temperature (Tmin) in Ethiopia indicate a clear and consistent warming across the country; with both observational (ENACT) data and historical climate models showing similar spatial patterns for both annual and seasonal. Colder Tmin values are dominant in the central and northern highlands areas, while warmer Tmin prevails in lowland areas such as the east, southeast, and southwest. Although models slightly underestimate Tmin in the highlands, they reliably capture past climate conditions. Historical Tmin ranged from approximately 3.6°C to 23°C between 1985 and 2014. Future projections show significant increases under both moderate (SSP2-4.5) and high-emission (SSP5-8.5) scenarios reaching up to +2.3°C and +2.8°C, respectively, by the end of the century. Seasonal analyses reveal rising Tmin in all three main seasons (Bega, Belg, Kiremt), with lowland regions like Afar and Somali projected to exceed 25-27°C under SSP5-8.5 by 2100, and highland areas warming to around 18°C or more. Monthly trends indicate year-round warming, with implications for agriculture, human and animal health, biodiversity, and water resources. Across all 12 rainfall homogeneity zones, Tmin increases are evident, with Zones 1 and 11 showing the highest projected rise and highland zones like 3 and 5 experiencing notable warming during cooler months. Annual mean Tmin is projected to reach approximately 25°C under SSP2-4.5 and approximately 27°C under SSP5-8.5 by 2100, particularly impacting Zones 11 and 12. Quantitative estimates show Tmin increases as high as +8.0°C in Zone 11, while Zones 2 and 3 show more modest changes (1.0-1.3°C), emphasizing the greater vulnerability of lowland areas under long-term, high-emission scenarios.

Over all the finding of this study implies the rising mean minimum temperatures are consistent with several studies like all models consistently project increasing trends in maximum and minimum temperatures, while the majority of the models projected declining future precipitation from 2021-2100 compared to the base period of 1971–2005 using CORDEX Africa regional models (Geleta et al., 2022).

4. Conclusion

Robust warming signal: Tmax and Tmin are projected to rise across all Ethiopian regions and seasons, with the strongest warming under SSP5-8.5. This point to a sustained warming trajectory through 2041–2100 and complex, regionally variant rainfall: Rainfall changes are not uniform. Kiremt (JJAS) tends to increase overall, especially under higher emissions, while Belg (FMAM) and Bega (ONDJ) show spatially heterogeneous responses. The result is greater rainfall variability and pronounced inter-annual fluctuations at the zone level. Improved but bounded certainty: Bias-corrected CMIP6 multi-model ensembles aligned with ENACTS observations improve confidence, yet substantial zone-scale uncertainty remains due to internal climate variability and model spread. The 12-zone framework effectively captures spatial diversity, underscoring the need for localized planning. The implications of this result across different systems such as climate-induced changes will influence agriculture, water resources, infrastructure, health, and urban resilience. Zone-specific impacts, timing of rainfall and heat stress will drive adaptation needs.

In general based on this results the following recommendations can apply on different sectors and different areas of the country:

- Localized adaptation planning
  - ✓ Develop and implement zone-specific adaptation plans using the 12-homogeneity-zone framework.
  - ✓ Compare SSP scenarios (SSP2-4.5 vs SSP5-8.5) and time horizons (2041–2070 vs 2071–2100) to identify robust actions and understand trade-offs.
- Agriculture and food security
  - ✓ Promote climate-smart agriculture: drought-tolerant varieties, crop diversification, and season-specific planting calendars aligned to shifting Belg and Bega timings.
  - ✓ Invest in irrigation expansion and water-use efficiency where feasible; integrate crop-livestock systems to buffer variability.
- Water resources and infrastructure

- ✓ Enhance water storage, watershed management, and flood/drought risk governance to accommodate increased rainfall variability and higher Tmax/Tmin.
- ✓ Develop zone-tailored water allocation and storage strategies that reflect the projected shifts in Kiremt timing and magnitude.

- Health and urban resilience
  - ✓ Strengthen heat-health surveillance and community awareness, focusing on lowland and developing urban areas with pronounced Tmin/Tmax increases.
  - ✓ Integrate urban heat mitigation (green infrastructure, reflective surfaces) into city planning in high-risk zones.
- Risk management and early warning
  - ✓ Expand and synchronize early warning systems for heat stress and extreme rainfall events; ensure regional triggers are aligned with projected warming hotspots.
  - ✓ Incorporate climate-extremes indices (e.g., heavy rainfall days, drought frequency) alongside mean changes for risk assessments.
- Policy and data governance
  - ✓ Institutionalize routine updates of bias-corrected CMIP6 ENACTS-based projections as new data become available.
  - ✓ Support capacity-building for decision-makers to interpret scenario-based projections and apply them to sectoral planning.
- Further research and data needs
  - ✓ Extend analyses to extremes indices and compound events (heat + drought, flood frequency) for comprehensive risk profiling.
  - ✓ Validate and possibly expand downscaling approaches to reduce residual zone-level uncertainties.

References

Abbasnia, M. (2016). *Future changes in maximum temperature using the statistical downscaling model (SDSM) at selected stations of Iran*. https://doi.org/10.1007/s40808-016-0112-z

Akinsanola, A. A., Ongoma, V., & Kooperman, G. J. (2021). Evaluation of CMIP6 models in simulating the statistics of extreme precipitation over Eastern Africa. *Atmospheric Research*, *254*, 105509.

Alaminie, A. A., Tilahun, S. A., Legesse, S. A., Zimale, F. A., Tarkegn, G. B., & Jury, M. R. (2021). *Evaluation of Past and Future Climate Trends under CMIP6 Scenarios for the UBNB (Abay), Ethiopia. Water 2021, 13, 2110*. s Note: MDPI stays neutral with regard to jurisdictional claims in published ….

Ayugi, B., Jiang, Z., Iyakaremye, V., Ngoma, H., Babaousmail, H., Onyutha, C., Dike, V. N., Mumo, R., & Ongoma, V. (2022). East African population exposure to precipitation extremes under 1.5 C and 2.0 C warming levels based on CMIP6 models. *Environmental Research Letters*, *17*(4), 44051.

Babaousmail, H., Hou, R., Ayugi, B., Sian, K. T. C. L. K., Ojara, M., Mumo, R., Chehbouni, A., & Ongoma, V. (2022). Future changes in mean and extreme precipitation over the Mediterranean and Sahara regions using bias-corrected CMIP6 models. *International Journal of Climatology*, *42*(14), 7280–7297.

Bekana, T. H. (2025). *Drought Risk Management in Ethiopia : A Systematic Review*. *10*(1), 1–11.

Cheng, L., & Zhu, J. (2018). *2017 was the warmest year on record for the global ocean*. Springer.

Das, P., Zhang, Z., Ghosh, S., Lu, J., Ayugi, B., Ojara, M. A., & Guo, X. (2023). Historical and projected changes in Extreme High Temperature events over East Africa and associated with meteorological conditions using CMIP6 models. *Global and Planetary Change*, *222*, 104068.

Debela, N., Mohammed, C., Bridle, K., Corkrey, R., & McNeil, D. (2015). Perception of climate change and its impact by smallholders in pastoral/agropastoral systems of Borana, South Ethiopia. *SpringerPlus*, *4*(1), 236.

Dokken, D. (n.d.). *INTERGOVERNMENTAL PANEL ON CLIMATE CHANGE Drafting Authors :*

Dosio, A., Lennard, C., & Spinoni, J. (2022). Projections of indices of daily temperature and precipitation based on bias-adjusted CORDEX-Africa regional climate model simulations. *Climatic Change*, *170*(1), 13.

Dyer, E., Washington, R., & Taye, M. T. (2020). Evaluating the CMIP5 [Coupled Model Intercomparison Project Phase 5] ensemble in Ethiopia: creating a reduced ensemble for rainfall and temperature in Northwest Ethiopia and the Awash Basin. *Papers Published in Journals (Open Access)*, 40–46.

Easterling, D. R., Meehl, G. A., Parmesan, C., Changnon, S. A., Karl, T. R., & Mearns, L. O. (2000). Climate extremes: observations, modeling, and impacts. *Science*, *289*(5487), 2068–2074.

El Kenawy, A. M., Hereher, M., Robaa, S. M., McCabe, M. F., Lopez-Moreno, J. I., Domínguez-Castro, F., Gaber, I. M., Al-Awadhi, T., Al-Buloshi, A., & Al Nasiri, N. (2020). Nocturnal surface urban heat island over Greater Cairo: Spatial morphology, temporal trends and links to land-atmosphere influences. *Remote Sensing*, *12*(23), 3889.

Enyew, F. B., Sahlu, D., Tarekegn, G. B., Hama, S., & Debele, S. E. (2024). Performance evaluation of CMIP6 climate model projections for precipitation and temperature in the Upper Blue Nile Basin, Ethiopia. *Climate*, *12*(11), 169.

Eyring, V., Bony, S., Meehl, G. A., Senior, C. A., Stevens, B., Stouffer, R. J., & Taylor, K. E. (2016). Overview of the Coupled Model Intercomparison Project Phase 6 (CMIP6) experimental design and organization. *Geoscientific Model Development*, *9*(5), 1937–1958.

Feyissa, G., Zeleke, G., Gebremariam, E., & Bewket, W. (2018). GIS based quantification and mapping of climate change vulnerability hotspots in Addis Ababa. *Geoenvironmental Disasters*, *5*, 1–17.

Feyissa, T. A., Demissie, T. A., Saathoff, F., & Gebissa, A. (2023). Evaluation of general circulation models CMIP6 performance and future climate change over the Omo River Basin, Ethiopia. *Sustainability*, *15*(8), 6507.

Forster, P. M., Smith, C. J., Walsh, T., Lamb, W. F., Lamboll, R., Hauser, M., Ribes, A., Rosen, D., Gillett, N., & Palmer, M. D. (2023). Indicators of Global Climate Change 2022: annual update of large-scale indicators of the state of the climate system and human influence. *Earth System Science Data*, *15*(6), 2295–2327.

Gebisa, B. T., & Dibaba, W. T. (2024). Ensemble modeling of the hydrological impacts of climate change: A case study of the Baro River sub-basin, Ethiopia. *Hydrology Research*, *55*(11), 1143–1160.

Gebisa, B. T., Dibaba, W. T., & Kabeta, A. (2023). Evaluation of historical CMIP6 model simulations and future climate change projections in the Baro River Basin. *Journal of Water and Climate Change*, *14*(8), 2680–2705.

Gebrechorkos, S. H., Hülsmann, S., & Bernhofer, C. (2019). Changes in temperature and precipitation extremes in Ethiopia, Kenya, and Tanzania. *International Journal of Climatology*, *39*(1), 18–30.

Geleta, T. D., Dadi, D. K., Funk, C., Garedew, W., Eyelade, D., & Worku, A. (2022). Downscaled climate change projections in urban centers of Southwest Ethiopia using CORDEX Africa simulations. *Climate*, *10*(10), 158.

Getachew, B., & Manjunatha, B. R. (2021). Climate change projections and trends simulated from the CMIP5 models for the Lake Tana sub-basin, the Upper Blue Nile (Abay) River Basin, Ethiopia. *Environmental Challenges*, *5*, 100385.

Hamed, M. M., Salem, M., Shamsuddin, N., & Tarmizi, S. (2022). Thermal bioclimatic indicators over Southeast Asia : present status and future projection using CMIP6. *Environmental Science and Pollution Research*, 91212–91231. https://doi.org/10.1007/s11356-022-22036-6

Hassaan, M. A., Abdrabo, M. A., & Masabarakiza, P. (2017). GIS-based model for mapping malaria risk under climate change case study: Burundi. *Journal of Geoscience and Environment Protection*, *5*(11), 102–117.

Huang, W. T. K., Charlton-Perez, A., Lee, R. W., Neal, R., Sarran, C., & Sun, T. (2020). Weather regimes and patterns associated with temperature-related excess mortality in the UK: a pathway to sub-seasonal risk forecasting. *Environmental Research Letters*, *15*(12), 124052.

Iyakaremye, V., Zeng, G., Yang, X., Zhang, G., Ullah, I., Gahigi, A., Vuguziga, F., Asfaw, T. G., & Ayugi, B. (2021). Increased high-temperature extremes and associated population exposure in Africa by the mid-21st century. *Science of the Total Environment*, *790*, 148162.

Jaweso, D., Abate, B., Bauwe, A., & Lennartz, B. (2019). Hydro-meteorological trends in the upper Omo-Ghibe

river basin, Ethiopia. *Water*, *11*(9), 1951.

Kandji, S. T., Verchot, L., & Mackensen, J. (2006). *Climate Change and Variability in Southern Africa: Impacts and Adaptation Strategies in the Agricultural Sector*. UNEP.

Kisakye, V., Akurut, M., & Van der Bruggen, B. (2018). Effect of climate change on reliability of rainwater harvesting systems for Kabarole District, Uganda. *Water*, *10*(1), 71.

Koetse, M. J., & Rietveld, P. (2009). The impact of climate change and weather on transport: An overview of empirical findings. *Transportation Research Part D: Transport and Environment*, *14*(3), 205–221.

Lee, H., Calvin, K., Dasgupta, D., Krinner, G., Mukherji, A., Thorne, P., Trisos, C., Romero, J., Aldunce, P., & Barret, K. (2023). *IPCC, 2023: Climate change 2023: Synthesis report, summary for policymakers. Contribution of working groups i, II and III to the sixth assessment report of the intergovernmental panel on climate change [core writing team, h. Lee and j. Romero (eds.)]. IPCC, geneva, Switzerland.*

Macintyre, H. L., & Heaviside, C. (2019). Potential benefits of cool roofs in reducing heat-related mortality during heatwaves in a European city. *Environment International*, *127*, 430–441.

Madakumbura, G. D., Thackeray, C. W., Norris, J., Goldenson, N., & Hall, A. (2021). Anthropogenic influence on extreme precipitation over global land areas seen in multiple observational datasets. *Nature Communications*, *12*(1), 3944.

Makula, E. K., & Zhou, B. (2022). Coupled Model Intercomparison Project phase 6 evaluation and projection of East African precipitation. *International Journal of Climatology*, *42*(4), 2398–2412.

McSweeney, C., New, M., & Lizcano, G. (2008). UNDP climate change country profiles: Ethiopia. *Profiles for 52 Countries*.

Mengistu, A. G., Woldesenbet, T. A., & Dile, Y. T. (2021). Evaluation of the performance of bias-corrected CORDEX regional climate models in reproducing Baro–Akobo basin climate: AG Mengistu et al. *Theoretical and Applied Climatology*, *144*(1), 751–767.

Moges, D. M., & Bhat, H. G. (2021). Climate change and its implications for rainfed agriculture in Ethiopia. *Journal of Water and Climate Change*, *12*(4), 1229–1244.

Mwangi, K. K., & Mutua, F. (2015). Modeling Kenya's vulnerability to climate change–A multifactor approach. *International Journal of Science and Research*, *6*, 12–19.

Myhre, G., Alterskjær, K., Stjern, C. W., Hodnebrog, Ø., Marelle, L., Samset, B. H., Sillmann, J., Schaller, N., Fischer, E., & Schulz, M. (2019). Frequency of extreme precipitation increases extensively with event rareness under global warming. *Scientific Reports*, *9*(1), 16063.

Ngoma, H., Wen, W., Ayugi, B., Babaousmail, H., Karim, R., & Ongoma, V. (2021). Evaluation of precipitation simulations in CMIP6 models over Uganda. *International Journal of Climatology*, *41*(9), 4743–4768.

Obsi Gemeda, D., & Dafisa Sima, A. (2015). Journal of Ecology and the Natural Environment The impacts of climate change on African continent and the way forward. *Journal of Ecology and the Natural Environment*, *7*(10), 256–262. https://doi.org/10.5897/JENE2015.

Omondi, P., Awange, J., Forootan, E., Ogallo, L. A., Barakiza, R., Girmaw, G. B., Fesseha, I., Kululetera, V., Kilembe, C., & Mbati, M. M. (2014). Changes in temperature and precipitation extremes over the Greater Horn of Africa region from 1961 to 2010. *International Journal of Climatology*, *34*(4), 1262–1277.

Oreskes, N. (2004). The scientific consensus on climate change. *Science*, *306*(5702), 1686.

Rettie, F. M., Gayler, S., Weber, T. K. D., Tesfaye, K., & Streck, T. (2023). Comprehensive assessment of climate extremes in high-resolution CMIP6 projections for Ethiopia. *Frontiers in Environmental Science*, *11*, 1127265.

Sinore, T., & Wang, F. (2024). Impact of climate change on agriculture and adaptation strategies in Ethiopia: A meta-analysis. *Heliyon*, *10*(4).

Solomon, S., Qin, D., Manning, M., Chen, Z., Marquis, M., Averyt, K., Tignor, M., & Miller, H. (2007). IPCC fourth assessment report (AR4). *Climate Change*, *374*.

Tegegne, G., Melesse, A. M., & Alamirew, T. (2021). Projected changes in extreme precipitation indices from CORDEX simulations over Ethiopia, East Africa. *Atmospheric Research*, *247*, 105156.

Wilby, R. L., & Dawson, C. W. (2013). The Statistical Downscaling Model: insights from one decade of application. *International Journal of Climatology*, *33*(7).

Yigezu Wendimu, G. (2021). The challenges and prospects of Ethiopian agriculture. *Cogent Food & Agriculture*, *7*(1), 1923619.

Annex

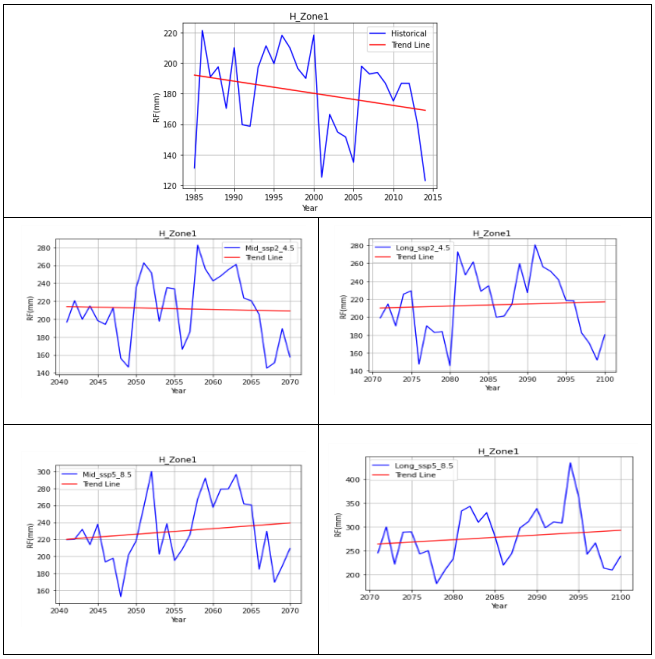

Figure 36: Ensemble model comparisons by SSP2_4.5 and SSP5_8.5 climate scenarios with historical (1985-2014) based on mid and long-term periods over homogeneity zone one

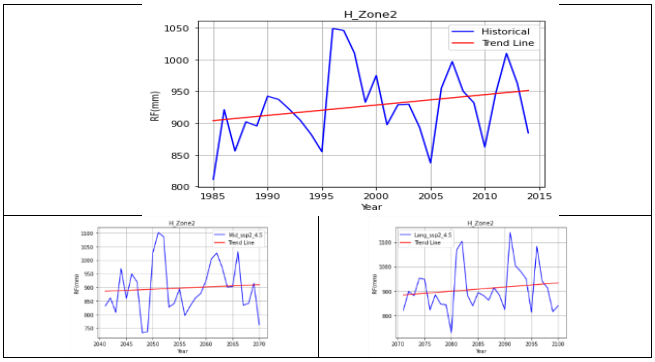

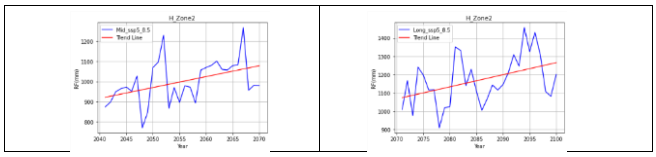

Figure 37: Ensemble model comparisons by SSP2_4.5 and SSP5_8.5 climate scenarios with historical (1985-2014) based on mid and long-term periods over homogeneity zone two

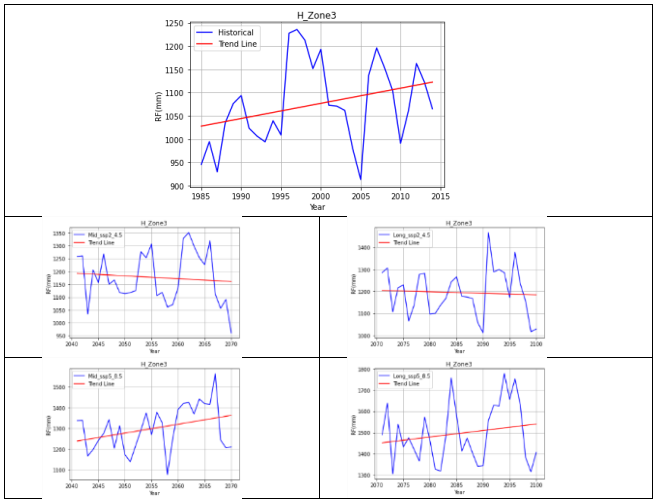

Figure 38: Ensemble model comparisons by SSP2_4.5 and SSP5_8.5 climate scenarios with historical (1985-2014) based on mid and long-term periods over homogeneity zone three

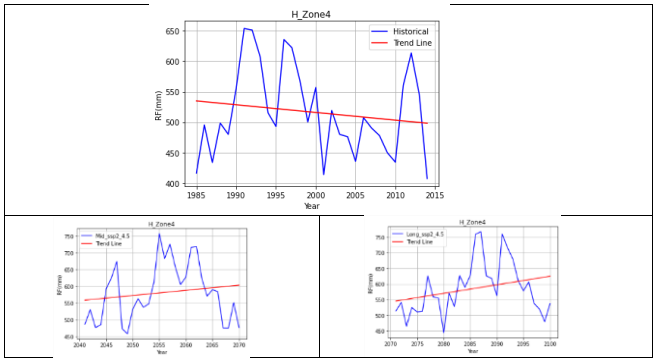

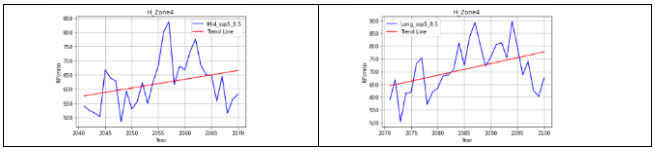

Figure 39: Ensemble model comparisons by SSP2_4.5 and SSP5_8.5 climate scenarios with historical (1985-2014) based on mid and long-term periods over homogeneity zone four

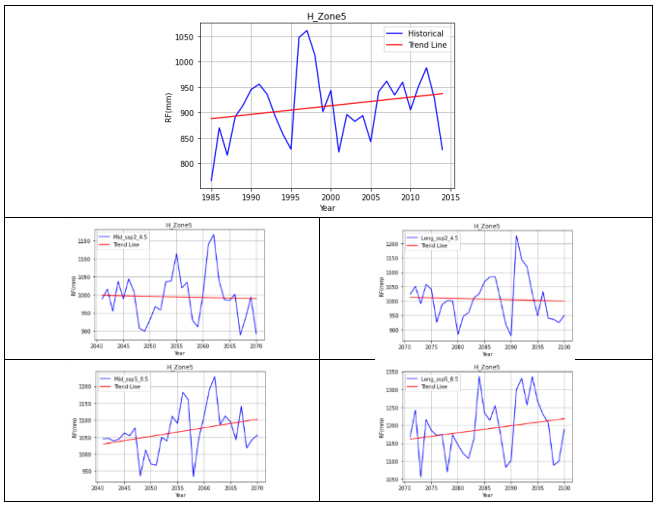

Figure 40: Ensemble model comparisons by SSP2_4.5 and SSP5_8.5 climate scenarios with historical (1985-2014) based on mid and long-term periods over homogeneity zone five

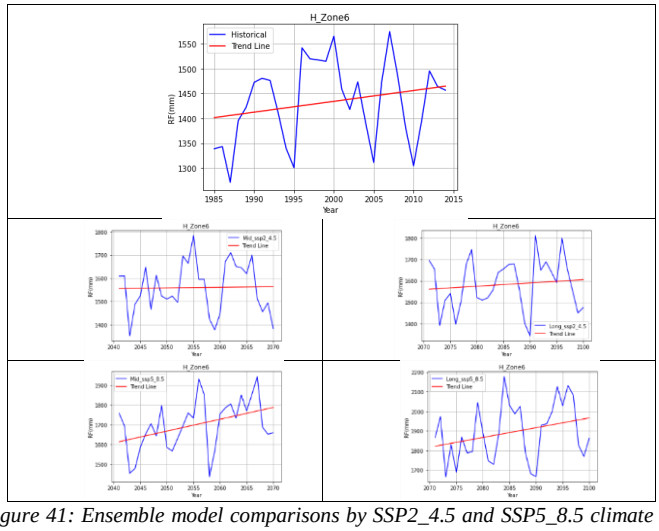

Figure 41: Ensemble model comparisons by SSP2_4.5 and SSP5_8.5 climate scenarios with historical (1985-2014) based on mid and long-term periods over homogeneity zone six

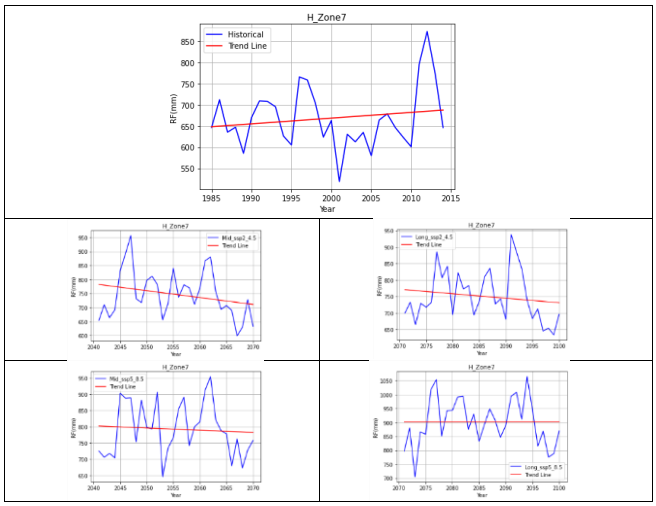

Figure 42: Ensemble model comparisons by SSP2_4.5 and SSP5_8.5 climate scenarios with historical (1985-2014) based on mid and long-term periods over homogeneity zone seven

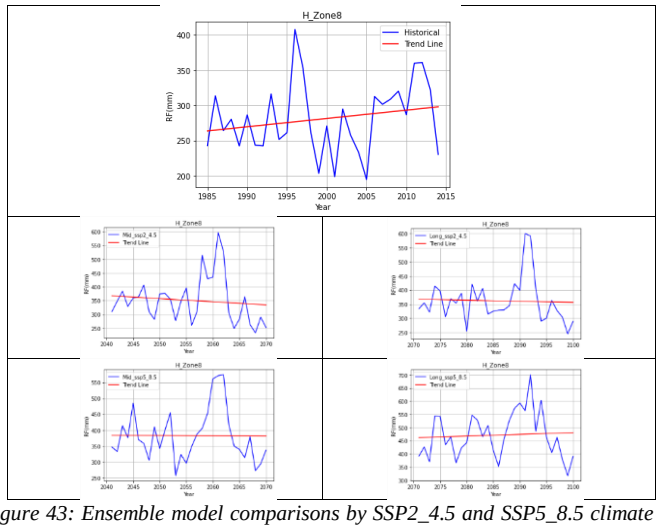

Figure 43: Ensemble model comparisons by SSP2_4.5 and SSP5_8.5 climate scenarios with historical (1985-2014) based on mid and long-term periods over homogeneity zone eight

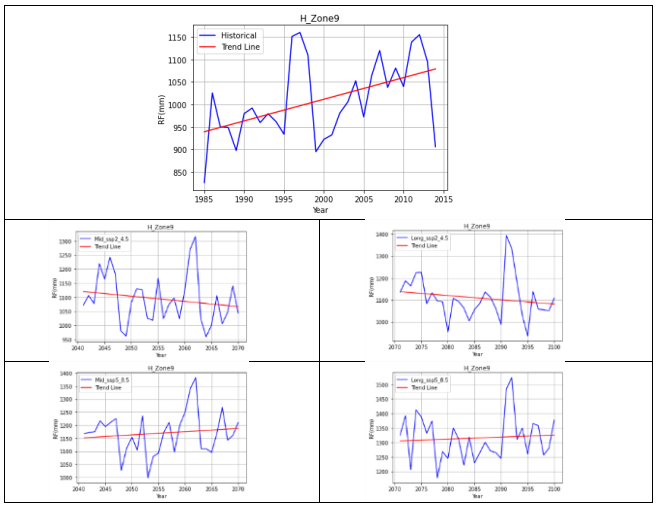

Figure 44: Ensemble model comparisons by SSP2_4.5 and SSP5_8.5 climate scenarios with historical (1985-2014) based on mid and long-term periods over homogeneity zone nine

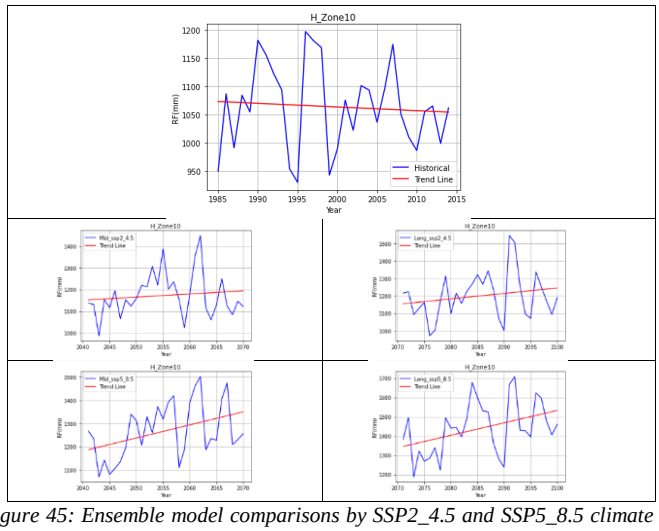

Figure 45: Ensemble model comparisons by SSP2_4.5 and SSP5_8.5 climate scenarios with historical (1985-2014) based on mid and long-term periods over homogeneity zone ten

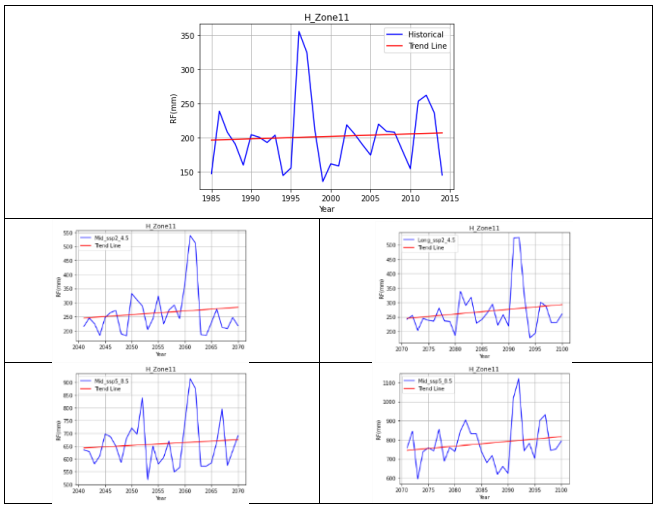

Figure 46: Ensemble model comparisons by SSP2_4.5 and SSP5_8.5 climate scenarios with historical (1985-2014) based on mid and long-term periods over homogeneity zone eleven

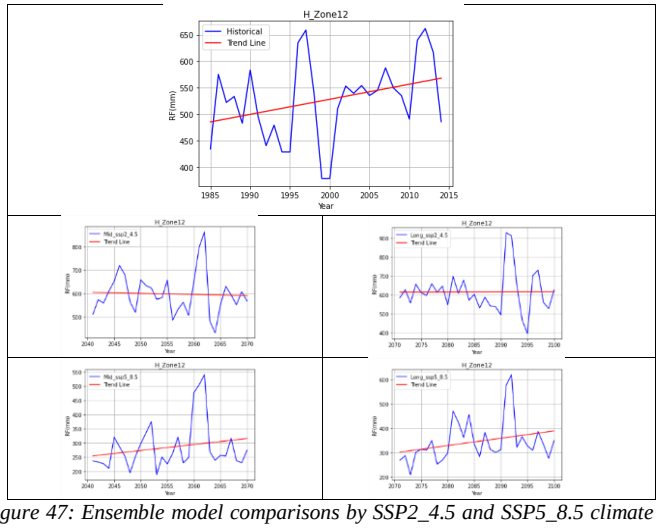

Figure 47: Ensemble model comparisons by SSP2_4.5 and SSP5_8.5 climate scenarios with historical (1985-2014) based on mid and long-term periods over homogeneity zone twelve

Annual and seasonal Mid-term rainfall anomalies (2041-2070)

Annual rainfall anomalies

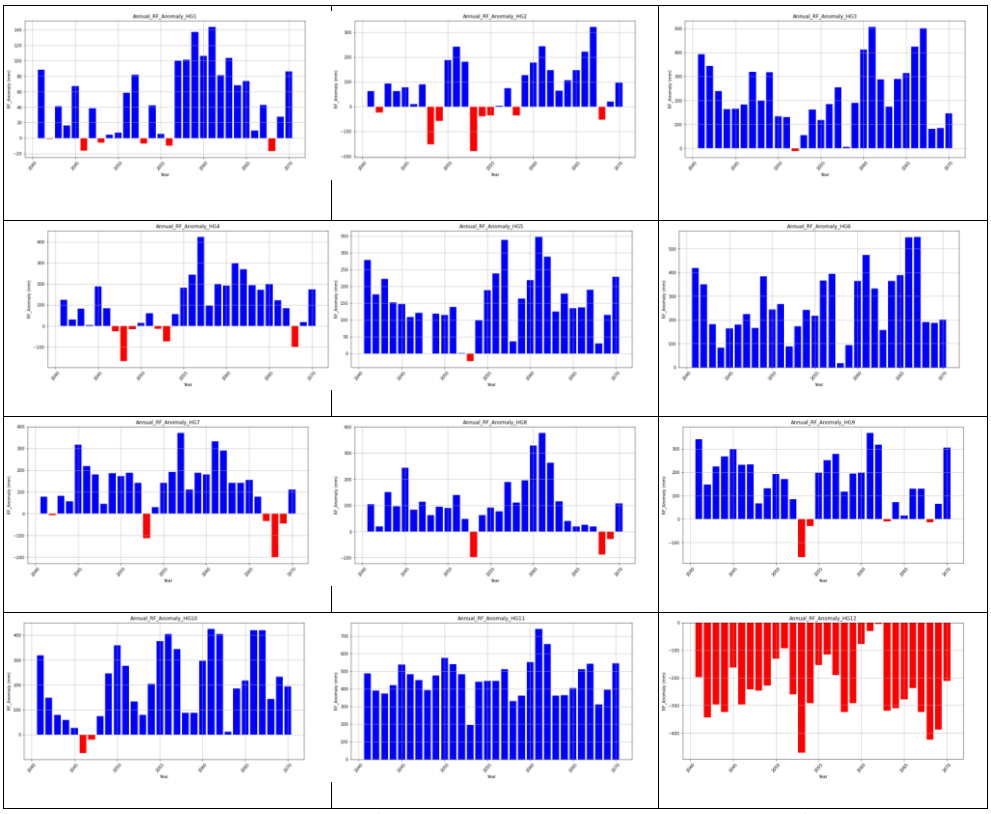

Figure 48: Future projection Annual rainfall anomalies under SSP2_4.5 climate scenarios for mid-term period

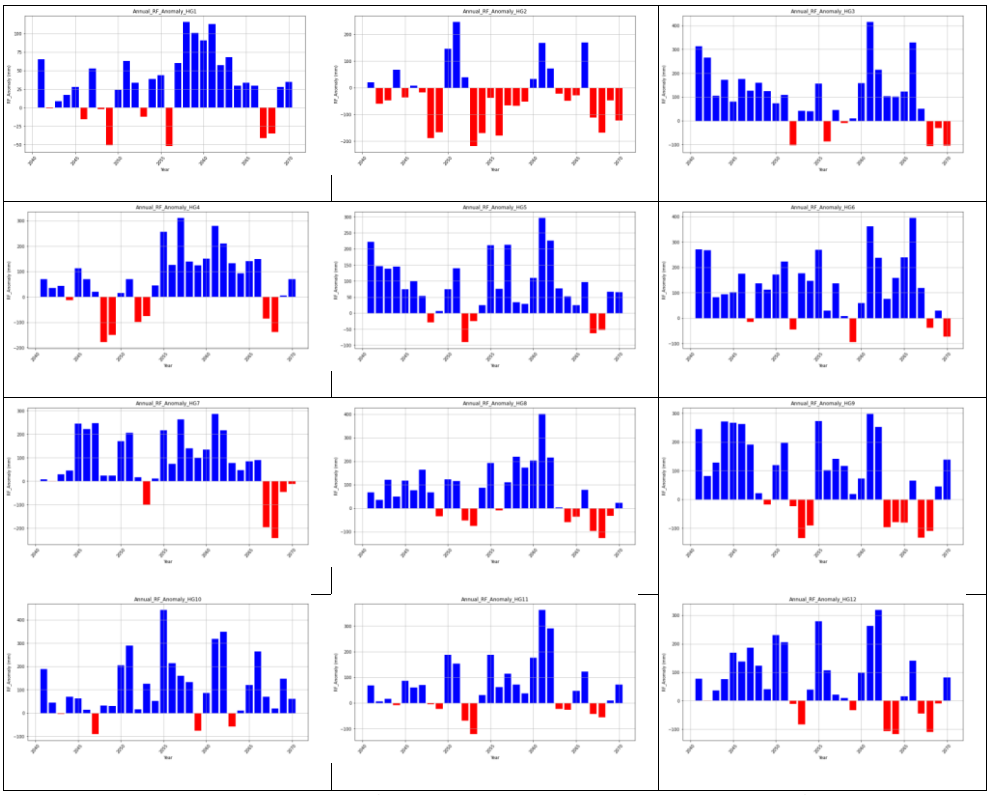

Figure 49: Future projection Annual rainfall anomalies under SSP5_8.5 climate scenarios for mid-term period

Belg (FMAM) rainfall anomalies

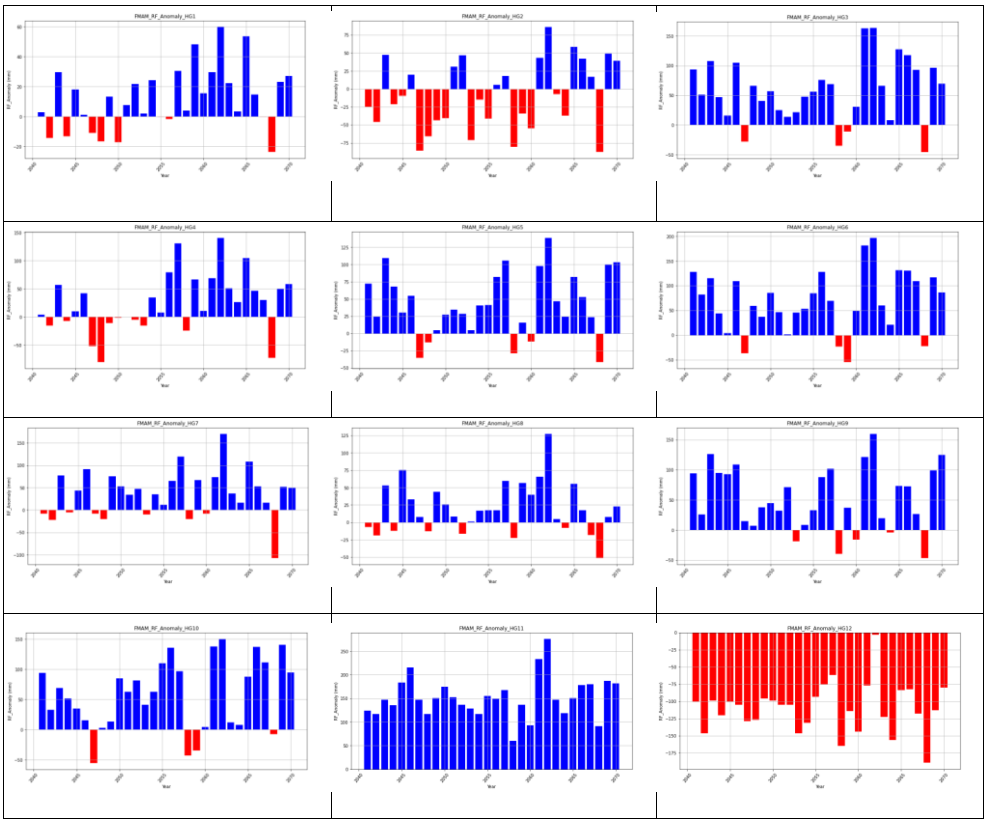

Figure 50: Future projection Belg season rainfall anomalies under SSP2_4.5 climate scenarios for mid-term period

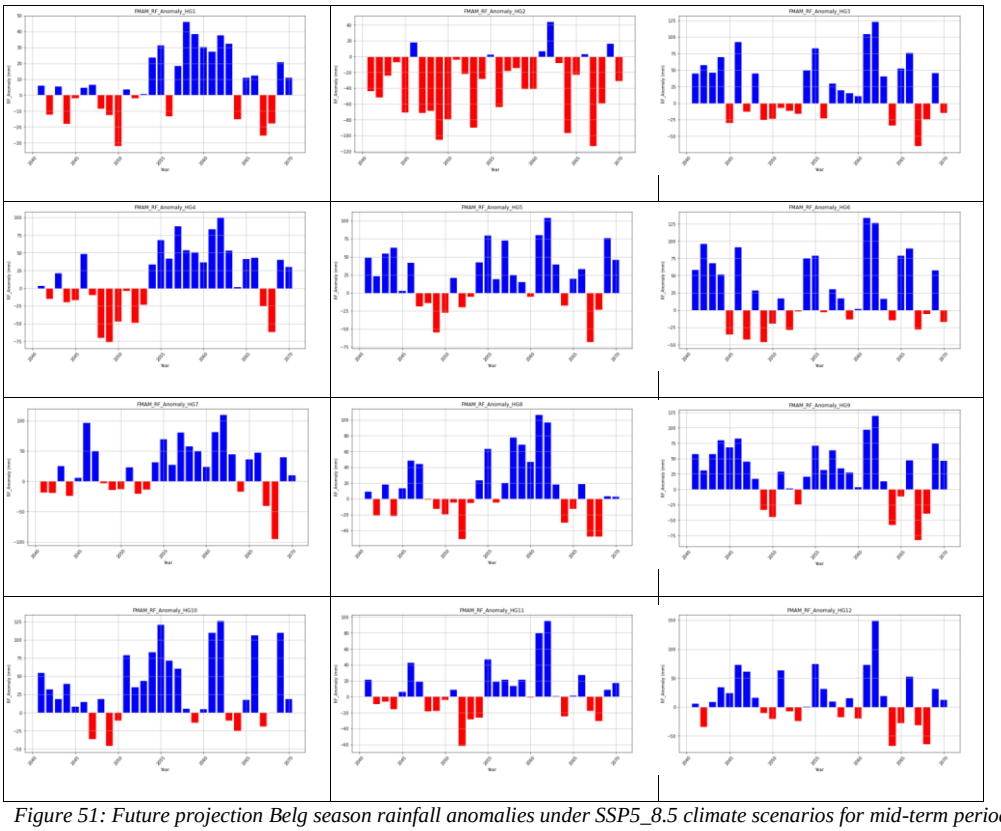

Figure 51: Future projection Belg season rainfall anomalies under SSP5_8.5 climate scenarios for mid-term period

Kiremt (JJAS) rainfall anomalies

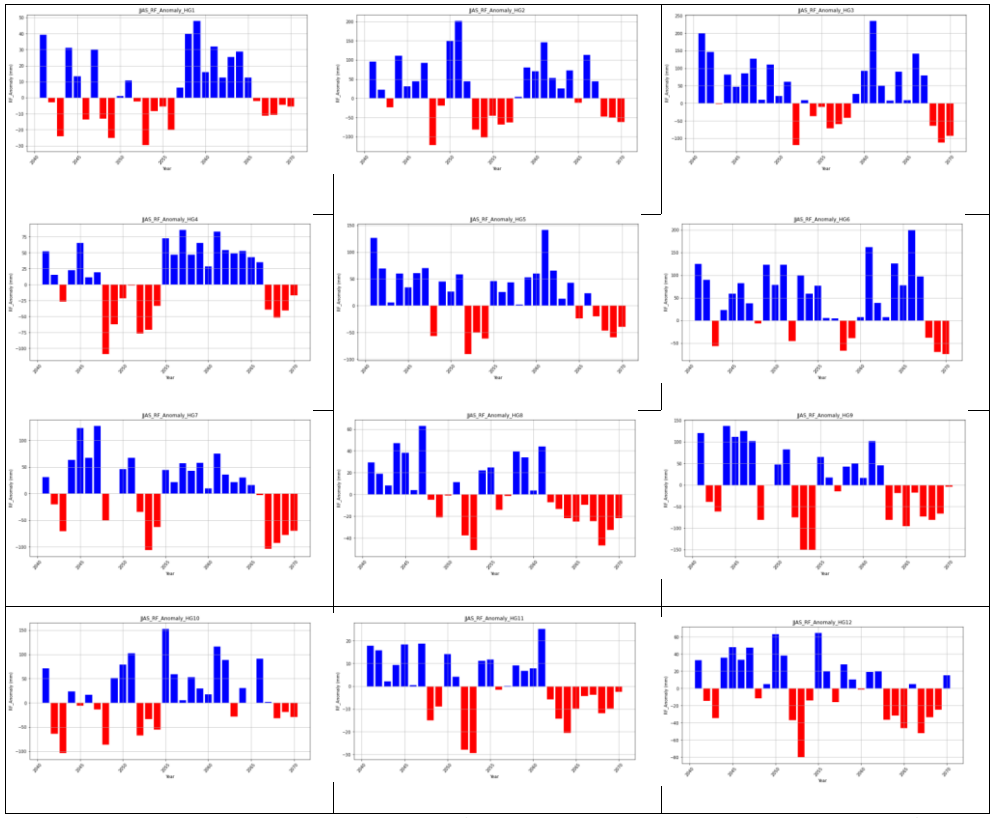

Figure 52: Future projection Kiremt season rainfall anomalies under SSP2_4.5 climate scenarios for mid-term period

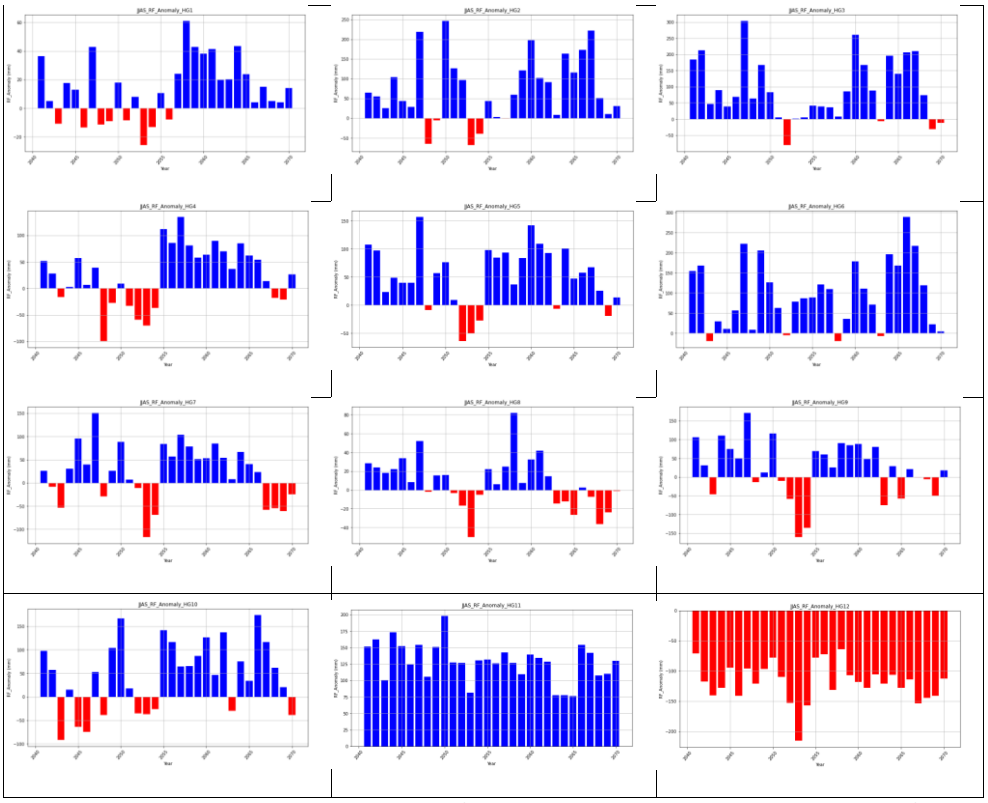

Figure 53: Future projection Kiremt season rainfall anomalies under SSP5_8.5 climate scenarios for mid-term period

Bega (ONDJ) rainfall anomalies

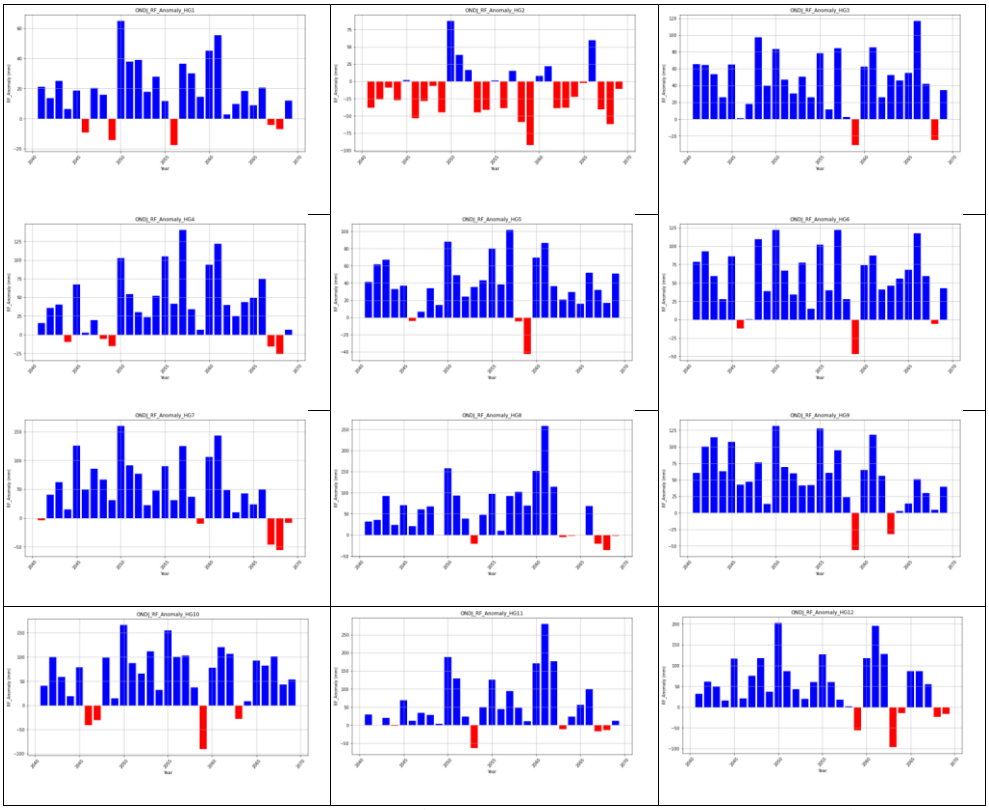

Figure 54: Future projection Bega season rainfall anomalies under SSP2_4.5 climate scenarios for mid-term period

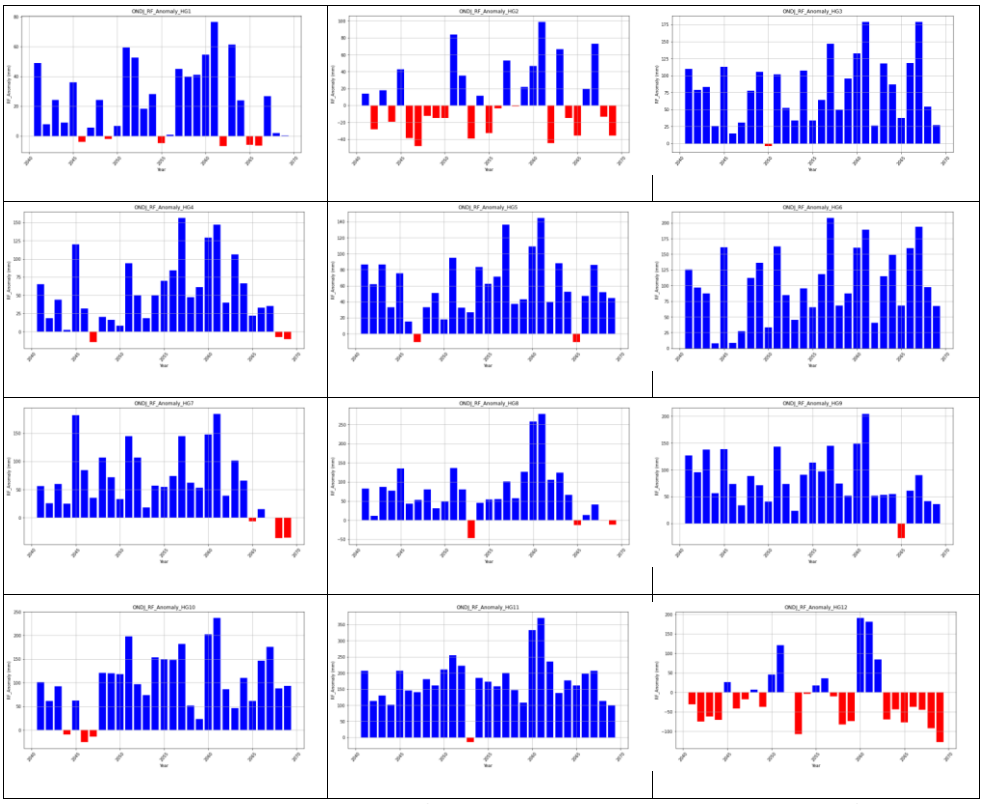

Figure 55: Future projection Bega season rainfall anomalies under SSP5_8.5 climate scenarios for mid-term period

Annual and seasonal long-term rainfall anomalies (2071-2100)

Annual rainfall anomalies

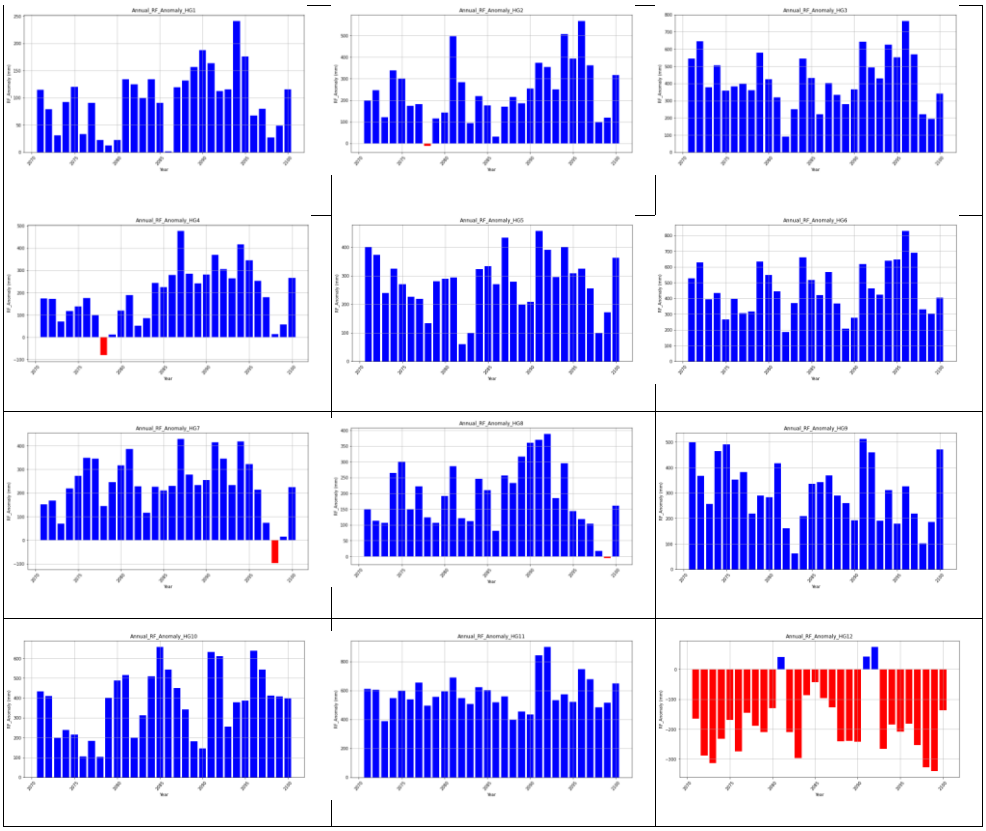

Figure 56: Future projection Annual rainfall anomalies under SSP2_4.5 climate scenarios for long-term period

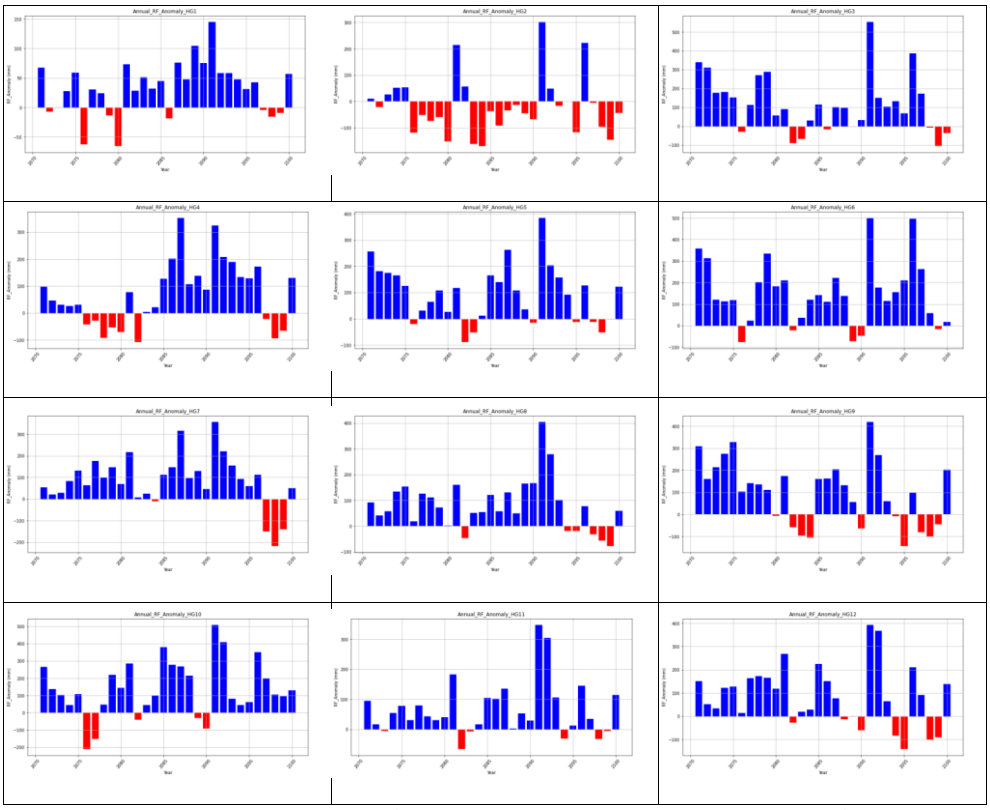

Figure 57: Future projection Annual rainfall anomalies under SSP5_8.5 climate scenarios for long-term period

Belg (FMAM) season rainfall anomalies

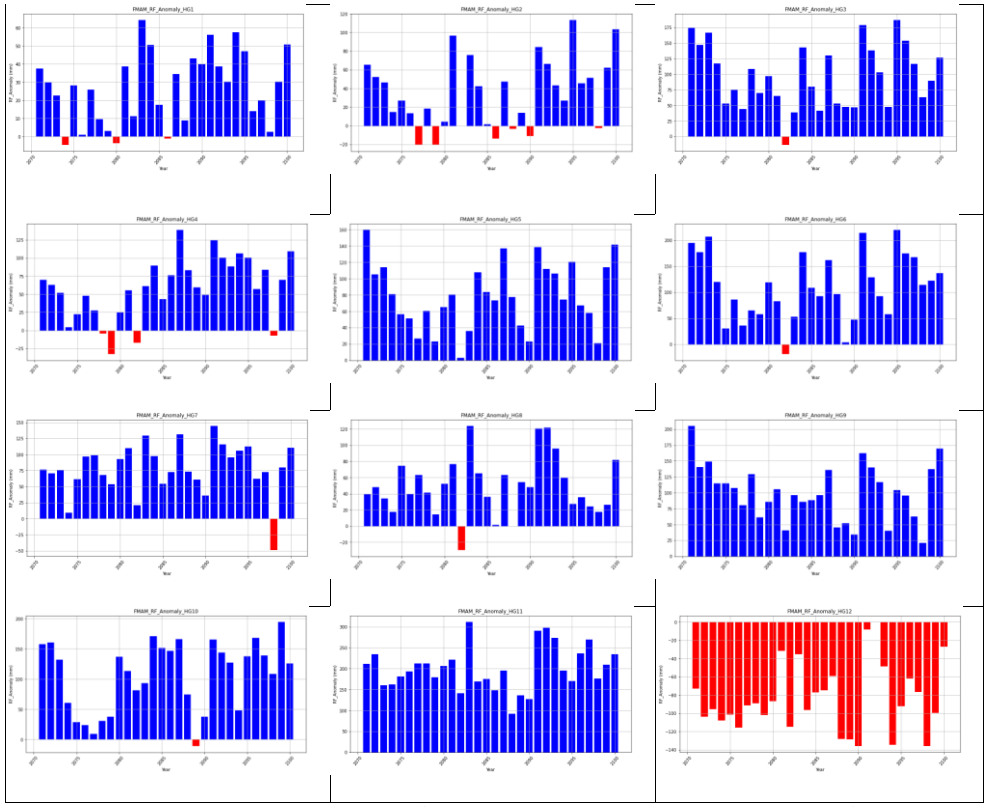

Figure 58: Future projection Belg season rainfall anomalies under SSP2_4.5 climate scenarios for long-term period

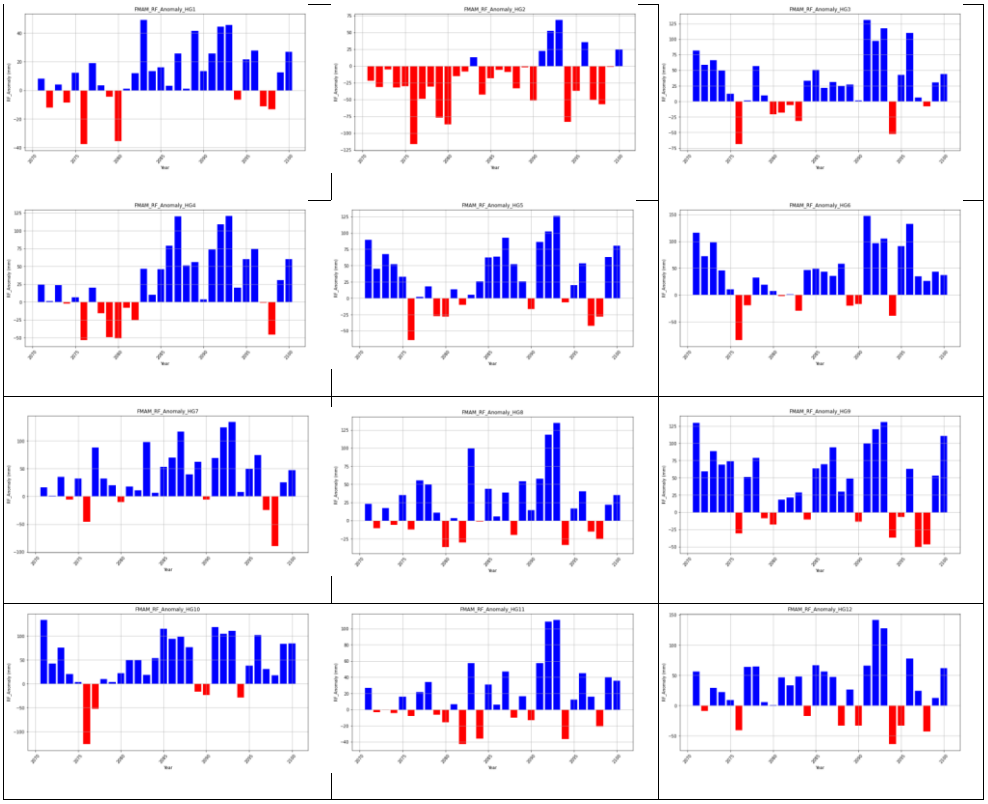

Figure 59: Future projection Belg season rainfall anomalies under SSP5_8.5 climate scenarios for long-term period

Kiremt (JJAS) season rainfall anomalies

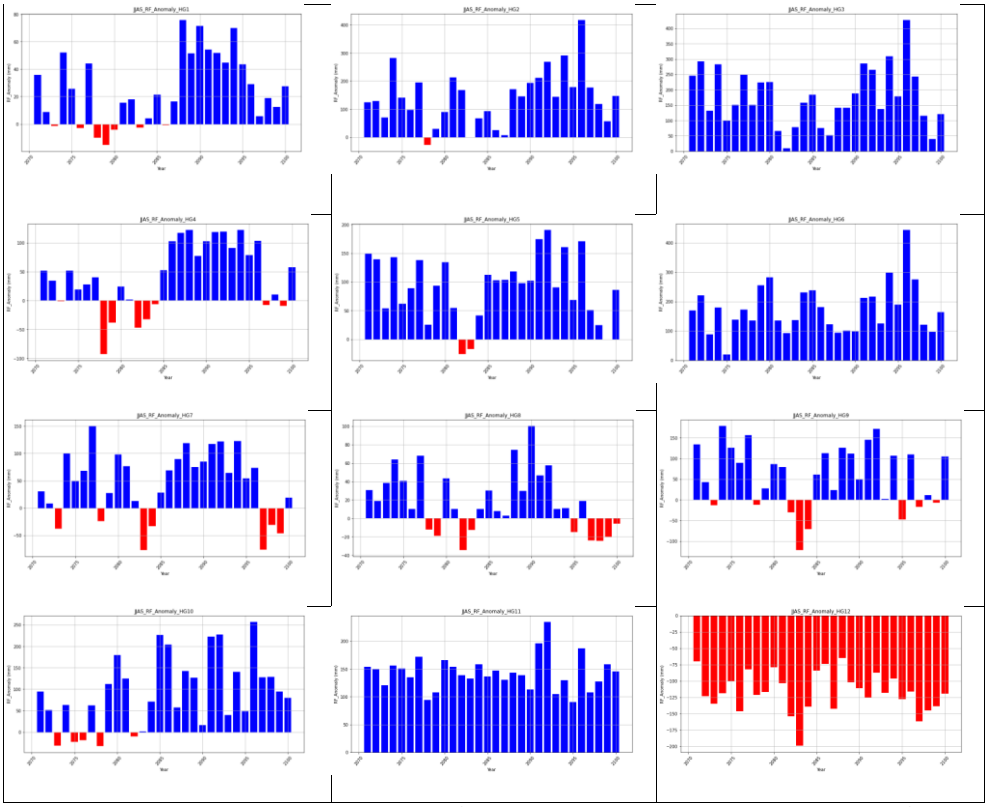

Figure 60: Future projection Kiremt season rainfall anomalies under SSP2_4.5 climate scenarios for long-term period

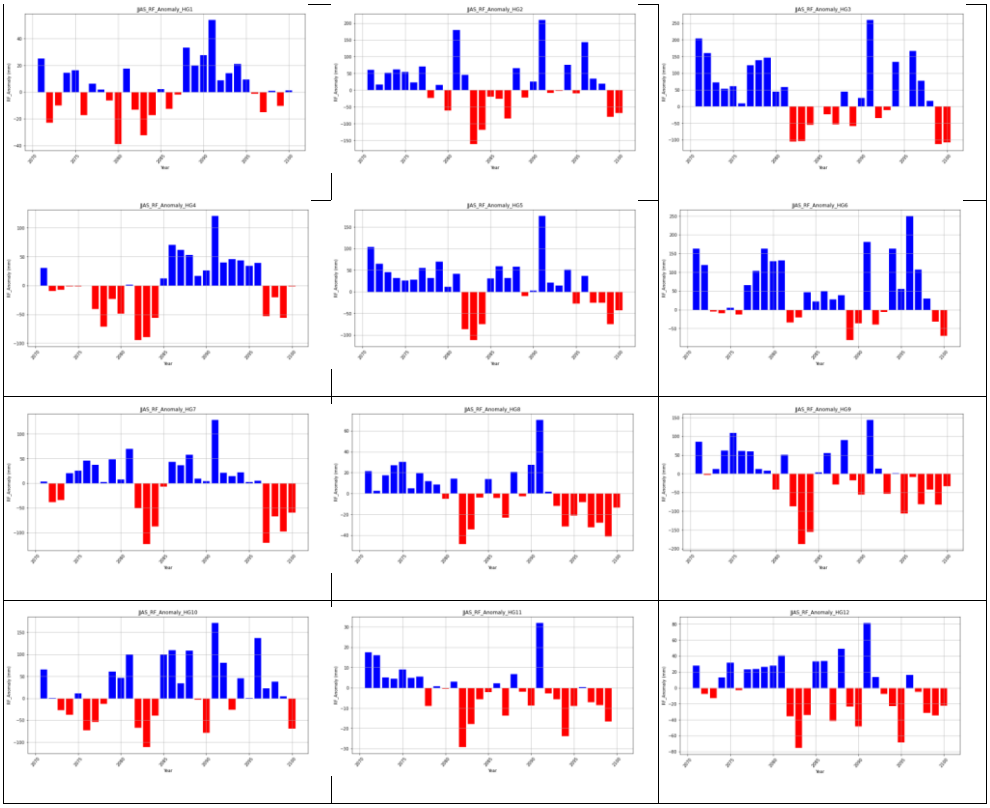

Figure 61: Future projection Kiremt season rainfall anomalies under SSP5_8.5 climate scenarios for long-term period

Bega (ONDJ) season rainfall anomalies

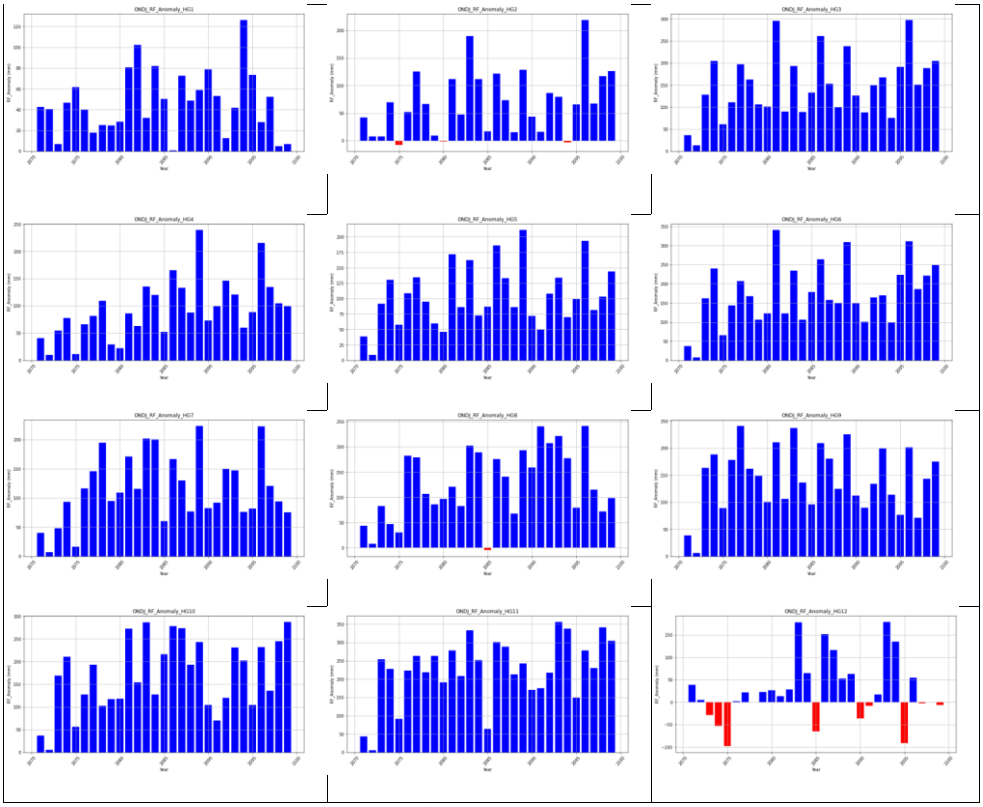

Figure 62: Future projection Bega season rainfall anomalies under SSP2_4.5 climate scenarios for long-term period

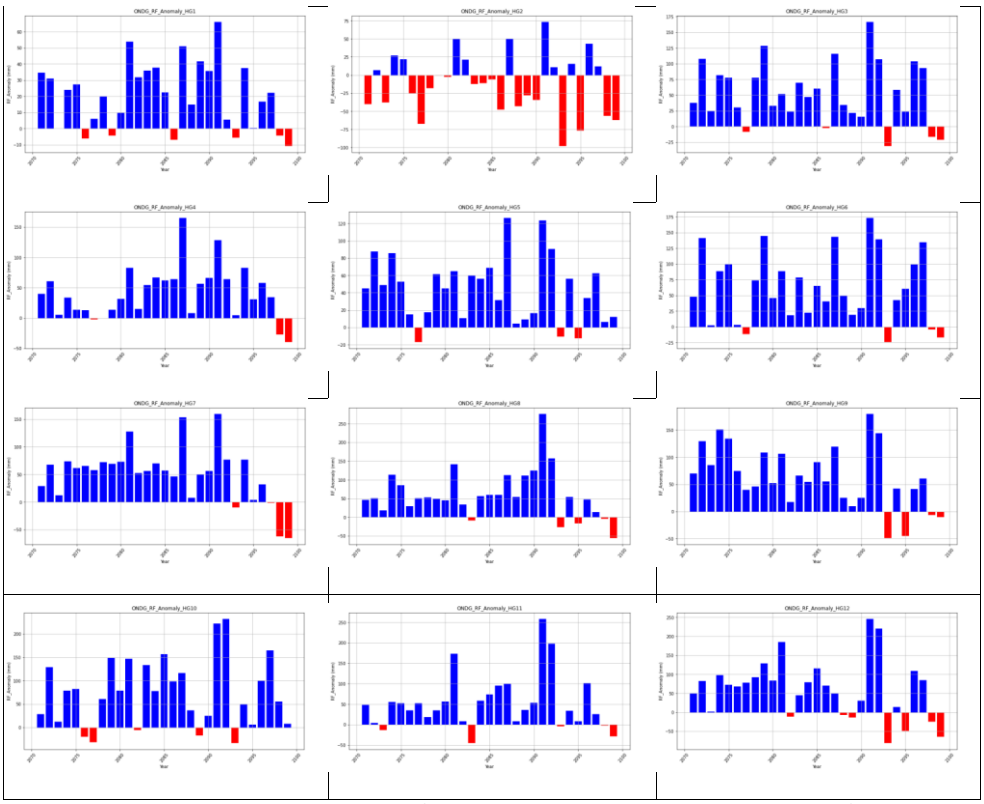

Figure 63: Future projection Bega season rainfall anomalies under SSP5_8.5 climate scenarios for long-term period